

WCTE 2016

World Conference on
Timber Engineering

August 22-25, 2016 | Vienna, Austria

RESEARCH OUTCOMES

A contribution to the timber building development

Research Projects Partner



CNR-IVALSA
TREES AND TIMBER INSTITUTE



UNIVERSITY OF TRENTO - Italy
Department of Civil, Environmental
and Mechanical Engineering



 **rothoblaas**



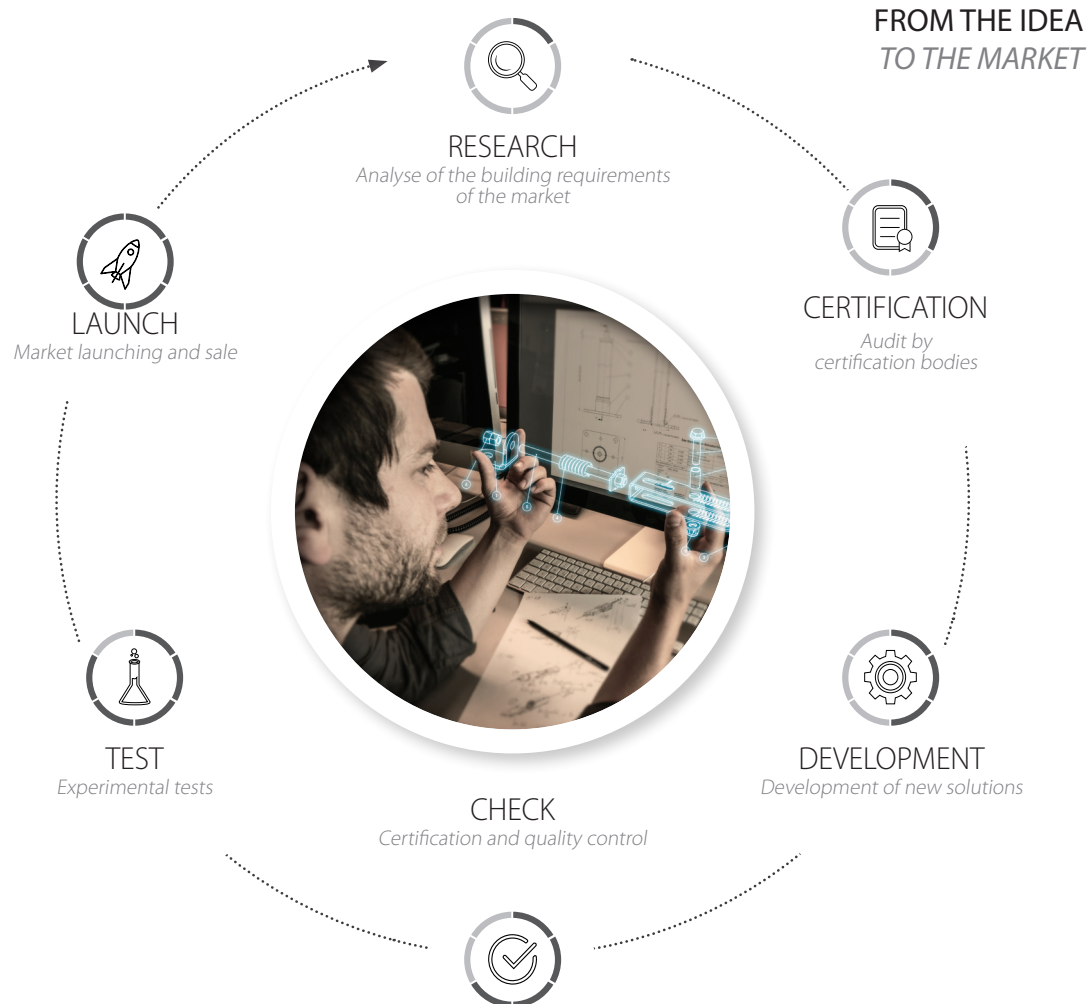
ALPINE HEART

INTERNATIONAL SPIRIT



Italy - Cortaccia (Bolzano)

France - Austria - Spain - Russia - Argentina - Brazil
Colombia - Ecuador - Chile - Australia - Canada



OUR OFFER

AT YOUR SERVICE



FASTENING

18 rothoschool courses



Airtightness and
WATERPROOFING

200 technical details
in .dxf format



SOUNDPROOFING

10000 consultings



FALL PROTECTION

540 different types of connections
calculable with MYPROJECT



TOOLS AND MACHINES

1600 technical documents
to download

1991 *Foundation in Bolzano*

2003 *Rothoblaas becomes a producer of fixing systems*

2005 *Beginning of the export activity*

WCTE 2006 *A new ductile approach design of joints assembled with screw connectors
Portland, USA*

2007 *Waterproofing and fall protection systems*

WCTE 2010 *Refurbishment of traditional timber floors by means of wood-wood composite
structures assembled with inclined screw connectors _Riva del Garda, IT*

2011 *Opening of new affiliate companies*

WCTE 2014 *Structural characterization of multi-storey buildings with clt cores
Quebec, Canada*

WCTE 2016 *Experimental analysis of flanking transmission of different
connection systems for clt panels
Experimental campaign for the mechanical characterization of connection
systems in the seismic design of timber buildings
Mechanical characterization of an innovative connection system
for clt structures
Structural analysis of clt multi-storey buildings assembled with the innovative
x-rad connection system: case-study of a tall-building
Clt buildings laterally braced with core and perimeter walls
System solutions for point-supported wooden flat slabs*

2020 *Rothoblaas is a leader in the building sector, strictly for timber constructions*



EXPERIMENTAL ANALYSIS OF FLANKING TRANSMISSION OF DIFFERENT CONNECTION SYSTEMS FOR CLT PANELS

Alice Speranza¹, Luca Barbaresi², Federica Morandi³

ABSTRACT: This paper presents the first results of the *flanksound* project, a study promoted by Rotho Blaas srl regarding flanking transmission between CLT panels jointed with different connection systems. The vibration reduction index K_{ij} is evaluated according to the EN ISO 10848 standard by measuring the velocity level difference between CLT panels. The performance of the X-RAD connection system is compared to the performance of a traditional connection system made of shear angle bracket and hold-down, both the configurations being tested with and without a resilient material placed between the construction elements. Concerning the traditional system, the influence of the difference sizes and types of fasteners - including the method of nailing or screwing - was also evaluated. The results of the measurements exposed in this work will hopefully contribute to the development of the acoustic design of timber buildings by providing a solid database of K_{ij} values, which can be used to forecast the acoustic performance of the building according to the prediction models proposed in EN 12354-1.

KEYWORDS: acoustic characterization, flanking transmission, innovative connection system, CLT constructions, experimental tests, vibration reduction index K_{ij} , X-RAD connection system, soundproofing profiles, *flanksound* project

1 INTRODUCTION

CLT structures have become widely employed for multi-storey buildings and are often characterized by the presence of many different typologies of connection systems. As far as it concerns static properties and technology development, CLT constructions have reached very encouraging levels of detail, providing countless solutions and refined calculation methods. On the other side, the acoustic properties of such structures are being investigated only recently [1-3]. Timber constructions, as all lightweight structures, tend to show insulation problems at low frequencies, in particular as it concerns impact sounds and the structural transmission of the vibration of the construction elements. The *flanksound* project, promoted by Rotho Blaas srl in collaboration with the University of Bologna, involved a measurement campaign aimed at investigating the flanking transmission of different connection systems for CLT panels. This work presents a detailed description of the measurement setup and the first results achieved.

2 THE TEST CONFIGURATIONS: JUNCTIONS AND PRODUCTS

The measurement campaign involved the test of CLT panels from seven suppliers. Two different connection systems were tested: the X-RAD and the traditional connection system. X-RAD is a novel solution patented by Rotho Blaas srl consisting of a point-to-point mechanical connection system fixed to the corners of the CLT panels (Fig. 1). Given the peculiarity of the fixing system, the acoustic transmission of vibration and the radiation properties of the panels depend on the installation of the X-RAD.

The traditional connection systems (Fig. 2), made of shear angle bracket and hold-down, were investigated by changing the kind and number of screws, using or not resilient profiles at the wall-ceiling interface and testing different number of plates. Not all test configurations could be performed on all kinds of CLT, nevertheless some configurations were kept constant to test the variability of the K_{ij} values which occur due to the differences among CLT panels and to the installation tolerances with the same nominal fastening systems.

Two resilient materials are tested: Xylofon and Aladin Stripe. Xylofon (35 Sh) is an extruded polyurethane supplied in the thickness of 6 mm. Aladin Stripe Soft is a EPDM rubber stripe with a tooth profile. In order to determine the differences between the screws, fully threaded structural screws (type VGZ) and partially threaded carpenter screws (type HBS) were compared. The horizontal partition was fixed through hold down WHT 440 and shear angle bracket Titan TTN 240.

¹ Alice Speranza, Product Engineer, Rotho Blaas srl, via dell'Adige 2/1 39040 Cortaccia (BZ) Italy.

E-mail: alice.speranza@rothoblaas.com

² Luca Barbaresi, Senior Researcher, CIRI - Building and Construction Unit, Department of Industrial Engineering, University of Bologna, via Terracini 34, 40131 Bologna, Italy.

E-mail: luca.barbaresi@unibo.it

³ Federica Morandi, Research Fellow, Department of Industrial Engineering, University of Bologna, via Terracini 34, 40131 Bologna, Italy.

E-mail: federica.morandi6@unibo.it

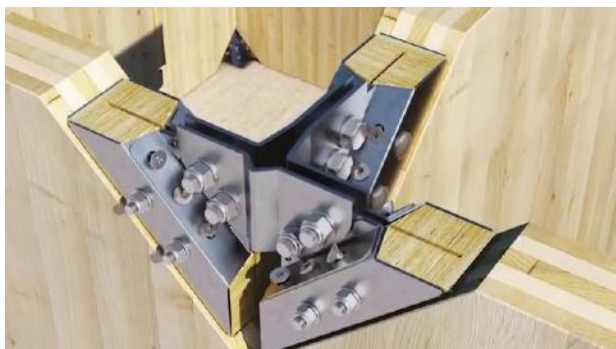


Figure 1: The X-RAD connection system: X-ONE elements are the ones connected to each CLT panel while X-PLATE is the system of plates to which the X-ONE elements converge



Figure 2: Fixing connection realized with angle bracket for shear loads TITAN with sound insulating profile ALADIN STRIPE

3 MEASUREMENT SETUP

The flanking transmission measurements were performed inside the headquarters of Rotho Blaas in Cortaccia (BZ). The measurements, conducted in accordance to the standard ISO 10848 [4], provided the vibration reduction indices K_{ij} which can be used to predict the apparent sound insulation index according to EN 12354 [5].

Vertical and horizontal junctions were tested. The vertical junctions have been tested in close accordance to the prescription of the standard in the “T” and “X” configurations. The horizontal junctions have been tested partially notwithstanding the prescriptions of the standard due to installation and handling constraints.

Vertical panels of thickness 100 mm (3 or 5 layers) were provided with dimensions 2,3x3,5 m and 2,3x4 m respectively. The horizontal partition (3,5x4 m) is supplied in a 160 mm panel (5 layers) divided into two pieces. This choice, required by the ease of management, has offered the opportunity to investigate the different propagation between the horizontal junction between panels, for which each supplier provides a distinct solution. The panels are fixed to the ground by means of concrete blocks of thickness 100 mm and are fixed to them through hold downs (two per panel). The blocks laid on the industrial floor of the Rotho Blaas warehouse. The accelerometers are fixed to the panels using magnets. Eyelets are screwed to the panels with screws

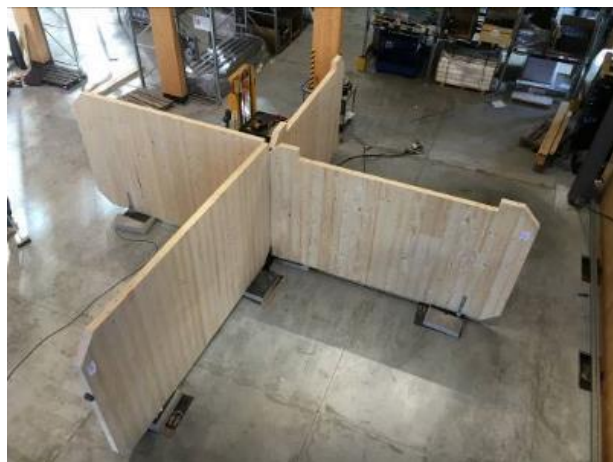


Figure 3: The test setup for a “X” node vertical transmission: perspective view of the measurement setup (top) and zoom on the shaker connected to a vertical panel (bottom)

whose length depended on the thickness of the panel, in order to reach its innermost stratigraphy. During the measurements, temperature and humidity of the environment were monitored: the average temperature varied between 14 and 15°C and the relative humidity varied between 40 and 50%. The humidity of the panels ranged around 9%.

The excitation and measurement points were chosen according to the ISO 10848 [4] standard. The source consisted of a shaker with sinusoidal peak force of 200 N, which was fixed to the panel using a plate (see Fig. 3). A pink noise filtered at 30 Hz was fed to the shaker and velocity levels were acquired using 4 accelerometers at a time. The structural reverberation time has been extracted from IR measurements, which were measured in the number of four measurement positions per each source. ESS signals were used, which showed to have a better performance than MLS signals, displaying SNR up to 50 dB. The structural reverberation time T_{15} was extracted using the *pre-processed energy detection method* [6, 7] implementing a reverse filter.

To test the measurement setup, an entire configuration has been tested using the both the measurement equipment described above and the hammer, used both to measure the vibration level difference and to record impulse responses. All “impact source” measurements were conducted with three different tips (rubber, Teflon and steel). The results, presented in national proceedings [8], showed that no appreciable different is found

between the measurement setups. Moreover, no difference was found at all in the use of the different tips: each hit on the CLT panels in fact caused a mechanical deformation of the surface, whose entity depended on the distance of the cut of each board from the heartwood. Thus, while for elements with infinite stiffness the different tips excite vibrational behaviors of the structure in different frequency ranges, CLT panels display a more homogenous response.

4 EXPERIMENTAL RESULTS

The results presented in this contributions will refer to some significant results accomplished within a subset of the measurement campaign, in particular:

1. X-RAD vs traditional connection systems
2. Transmission paths hierarchy in the vertical “X” junction
3. Resilient profiles at the wall-wall interface
4. Resilient profiles at the wall-ceiling interface
5. The incidence of the kind and number of screws on a vertical “L” test configuration
6. The incidence of connections on a “T” vertical junction

The K_{ij} are expressed as average values or plotted versus frequency depending analysis that the authors wished to accomplish. Though acquisitions were performed in the frequency range 50-5000 Hz, the results presented here are reported within the range 100-3150 Hz and/or expressed in terms of an average between 125 and 2000 Hz.

4.1 X-RAD VS TRADITIONAL CONNECTION SYSTEMS

The comparison between the traditional fastening system and the X-RAD might result critical due to the variability in the installation related to both construction systems. The tolerance in the laying of the X-RAD is not easily predictable: one transmission path may have panels in contact one with the other while a transmission path nominally symmetrical might have panels not in direct contact. The sound energy distributed by the X-PLATE element is very different in the two cases. Moreover, though the junction length is the same in the two configurations, the geometrical junction of the panels is totally different.

Table 1: Vertical “X” junction: X-RAD versus traditional connection systems

	Path	K_{ij} X-RAD (dB)	K_{ij} Trad (dB)
T vert junction	1-4	5.3	7.0
	1-2	11.1	13.0
X vert junction	1-3	13.6	10.9
	2-3	15.2	17.8
	1-2	9.7	12.2
	2-4	11.5	21.2
X hor junction	4-5 (1-5)	11.3	8.4

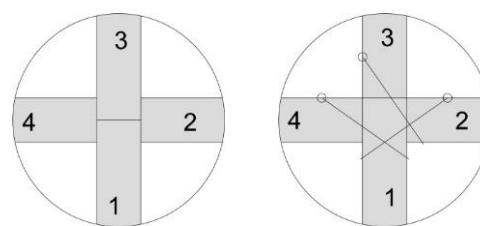


Figure 4: Test configuration to compare the X-RAD (left) and the traditional connection system (right).

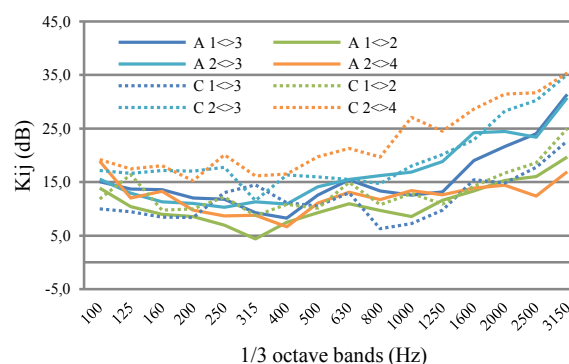


Figure 5: Vertical X junction: X-RAD (solid line) versus traditional connection systems (dotted line)

A certain amount of variability is also ingrained in the traditional fastening systems. Structural and carpenter’s screws offer a very different behaviour in terms of sound transmission; while the second tend to bring the panels close, the first tend to depart the panels, despite the use of tensioners.

With these premises, the K_{ij} averaged over the octave bands ranging from 125 to 2000 Hz are presented in Tab. 1, while the hierarchy of the panels is reported in Fig. 4. For the X-RAD configuration the panels were fixed only by the X-PLATE element while in the traditional connection configuration the panel are fixed with 4 HBS screws $\varnothing 8 \times 240$ mm fixed with an angle of 30-35° compliant to the assembly instructions.

The results show no significant discrepancies between the two construction systems, both for vertical and horizontal junctions. The differences found for different transmission paths is greater for “T” junctions for the X-RAD connection, while the “X” vertical junction provides a more uniform energy distribution.

The traditional system tends to provide greater K_{ij} values, with a difference of about 2 dB, i.e. complying with the uncertainties assumed relative to the K_{ij} [7]. An exception is represented by the transmission path 2-4, the one which involves panels in line with no direct contact.

With the traditional system the sound transmission is very low because the panels are not in direct contact and because the disposition of the screws does not provide privileged transmission paths and thus the panels are weakly connected. For the X-RAD, the connection between the panels is strengthened by the X-PLATE element, which allows a greater amount of energy to be transmitted between the panels.

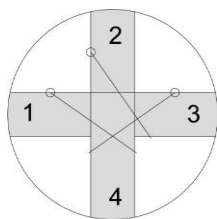


Figure 6: Test configuration used for the traditional connection systems.

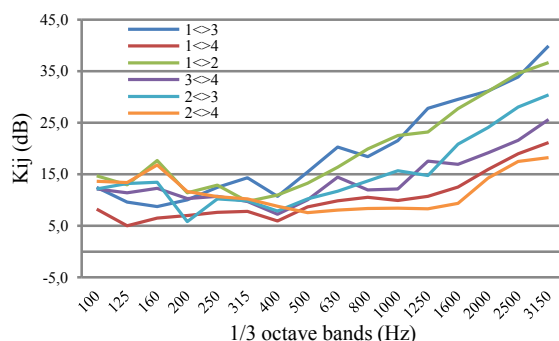


Figure 7: K_{ij} measured in a vertical “X” junction between the panels

4.2 THE HYERARCHY OF THE TRANSMISSION PATHS IN THE VERTICAL “X” JUNCTION

Since the energy distribution among the different transmission paths showed to be strongly dependent on the hierarchy of the panels, Fig. 5 reports the K_{ij} values measured on a “X” vertical junction plotted versus frequency. The measurements labelled “A” refer to the X-RAD construction system, while those labelled “C” use traditional solutions. The hierarchy of the panels within the junction is critical also for X-RAD as the trend of K_{ij} in frequency depends strongly on the transmission path. For all the transmission path there is a good match between the two construction systems. The trends superimpose for almost all connections with the exception of the transmission path 2-4, where the X-RAD displays higher transmission because a significant amount of energy is transmitted through the X-PLATE element.

The analysis on both X-RAD and traditional connection systems showed that the hierarchy of the connection between panels have a great incidence on the vibration reduction index versus frequency. This was also confirmed by the analysis on the test configuration D, reported in Fig. 6: the number and kind of screws was the same used for configuration C but the CLT supplier was different. In Fig. 7 the results of the 6 transmission paths are reported vs frequency. The results show that, for this kind of junction, the use of the vibration reduction index in terms of frequency-dependent values requires a detailed knowledge of the junctions. The mostly attenuated transmission paths are 1-3, i.e. panels in line and not in contact, and 1-2. The transmission path 1-2 and 2-3 are nominally identical and should provide similar results. In fact, measurements on this and other configurations showed that the screws fixed in panel 2

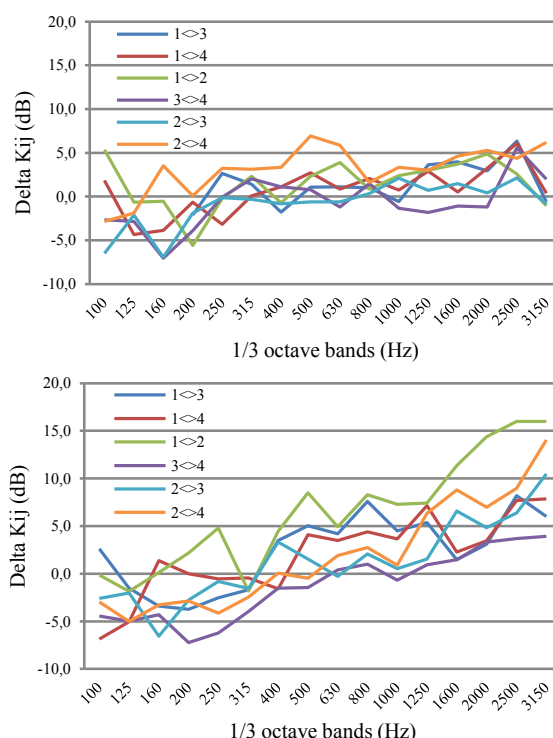


Figure 8: Increase in K_{ij} due to the use of EPDM rubber between the panels. Panels fixed with HBS screws (top) and with VGZ screws (bottom)

reach panel 3, providing a stronger connection between these two panels compared to the 2-1 transmission path.

4.3 THE USE OF RESILIENT PROFILES BETWEEN VERTICAL PANELS

Some measurements were conducted aimed at investigating the possibility to reduce sound transmission by interposing a resilient material between the vertical panels. The material chosen is the Construction Sealing, an EPDM rubber stripe originally used to provide airtight connections. Fig. 8 reports the differences in K_{ij} for the different transmission paths between standard installation of walls and the installation of the same walls laying Construction Sealing between the panels. The transmission paths indicated refer to the scheme provided in Fig. 6. The delta reported in the two graphs are the differences between the K_{ij} measured with and without EPDM when panels are fixed by 4 HBS Ø 8 x 240 mm screws (on the top) and the K_{ij} measured with and without EPDM when panels are fixed by 4 VGZ Ø 7 x 260 mm screws. For panels fixed with HBS screws the delta is always positive but assesses to small values. The difference is greater when panels are fixed with VGZ screws. The CLT suppliers are different in the 4 measurement setups, thus these results may be considered valid only if future work will prove the analogue behaviour of CLT panels which have nominal equivalent mechanical characteristics. Given the variation which was found due to different screwing conditions, this aspect might be critical. Moreover, the feasibility of laying the EPDM rubber stripe between the

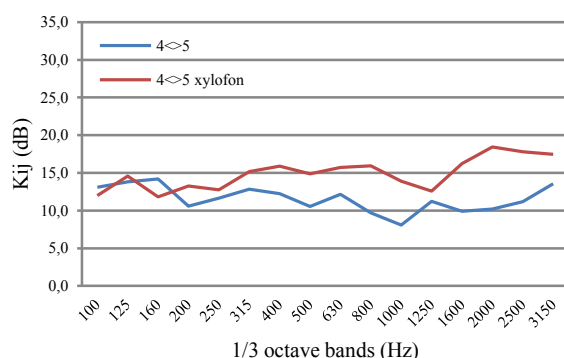


Figure 9: The improvement in K_{ij} related to the use of Xylofon with the X-RAD connection system

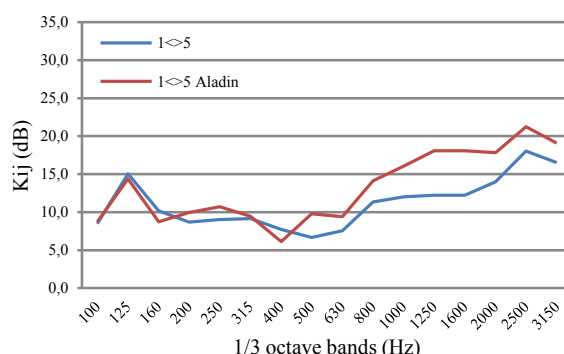


Figure 10: The improvement in K_{ij} related to the use of Aladin Stripe Soft with the traditional connection system

panels in the construction process should be defined.

4.4 THE USE OF RESILIENT PROFILES AT THE WALL-CEILING JUNCTION

A set of results is reported to qualify the vibration transmission between horizontal and vertical partitions in the two construction systems X-RAD and traditional in order to assess the effectiveness related to the use of resilient materials. In the following, Xylofon (35 Sh) is used on the X-RAD connection system while Aladin Stripe Soft is used in the traditional connection system. In both configurations the panels were fixed using the same number and kind of screws, angle brackets and hold-down.

Figure 9 and 10 show the increase in K_{ij} achievable by positioning a resilient material at the wall-ceiling junction. In each graph measurements were conducted using the same CLT panels, so that the delta between the two configurations can be considered independent from the CLT panels characteristics and the only uncertainty is related to the installation. For both configurations, since the static load was not sufficient to make the mass-spring-mass work as due, no effect at low frequencies is quantifiable.

Fig. 9 reports the vibration reduction indices K_{ij} measured between a vertical panel and the slab with and without the use of the Xylofon (35 Sh) profile. The difference between the two tests shows benefits starting from 400 Hz; the difference increases with increasing

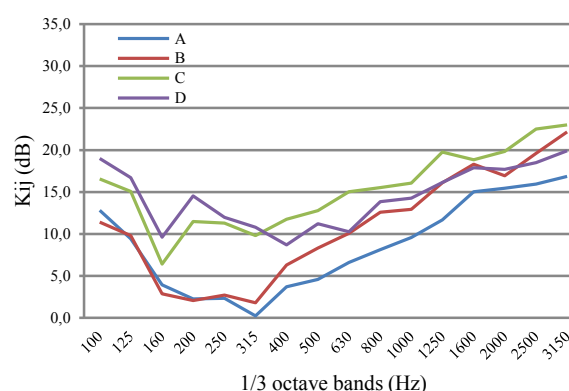


Figure 11: The K_{ij} measurement on a “L” test configuration varying the number and kind of screws.

frequency and reaches up to 8 dB in the 1/3 octave band centred at 2000 Hz.

Fig. 10 shows the results provided by the use of the Aladin Stripe Soft profile when the horizontal partition is fixed with a traditional fastening system. The effectiveness of the Aladin profile in this configuration is evident from 800 Hz on, while at lower frequencies no significant improvement is found.

In the X-RAD connection system the slab is connected to the X-PLATE element and the vertical partitions have a notch for housing the slab. Thus the constrain conditions and the load distributions are very different with respect to traditional connection systems, where the slab simply leans on the walls and is fixed with screws, hold down and plates. These features might explain the different K_{ij} values displayed in Fig. 9 and 10 in the “bare” configuration.

4.5 THE INCIDENCE OF THE KIND AND NUMBER OF SCREWS ON A VERTICAL “L” JUNCTION

To test the incidence in sound transmission varying the kind and number of screws, a “L” junction was tested whose panels were connected in 4 configurations:

- A. 8 HBS Ø 8 x 240 mm
- B. 4 HBS Ø 8 x 240 mm
- C. 3x2 VGZ Ø 7 x 260 mm
- D. 4x2 VGZ Ø 9 x 400 mm

The results are reported in Fig. 11. As previously pointed out, HBS and VGZ screws provide different connections among the panels: HBS screws bring the panels to a closer contact and thus provide the lowest K_{ij} values. Halving the number of screws (configuration B) results in a 3 to 5 dB increase in K_{ij} starting from the 400 Hz octave band. This is also confirmed in the analysis of the VGZ screws, varied in number and in length of the screw. Configuration D provided attenuation values smaller than configuration C as expected. It is very interesting to notice the vibration reduction index measured with HBS-screwed panels displays a dip between 160 and 315 Hz, which is not present when panels are fixed with VGZ screws, i.e. when panels vibrate “independently” one from the other, or at least less constrained.

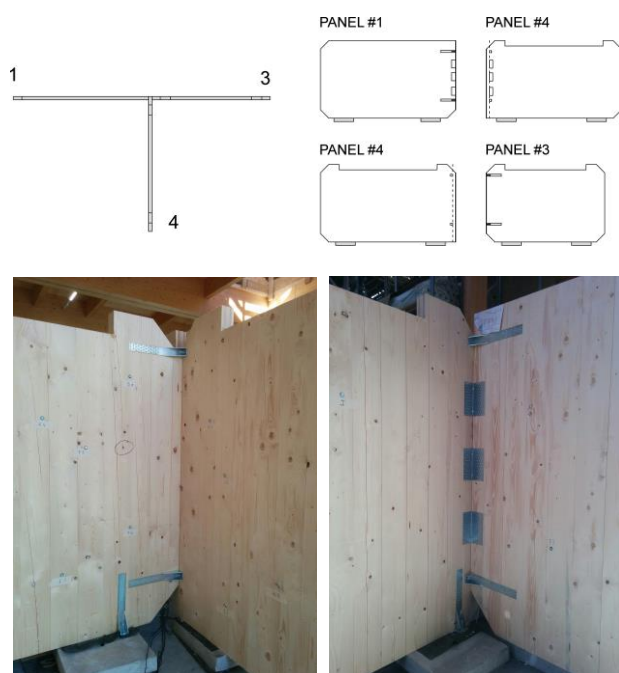


Figure 12: Test setup of for measurements with and without plates on a T vertical junction. Transmission paths 3-4 (left) and 1-4 (right).

4.6 THE INCIDENCE OF CONNECTIONS ON A “T” VERTICAL JUNCTION

In order to test the influence of the connection system on flanking transmission, additional measurements have been conducted on a vertical “T” junction. On the same junction, measurements have been done with panels connected by HBS screws or VGZ screws. After testing the junction with only screws, 3 TTN240 angle brackets and 2 WHT440 hold-down were added to both measurement setups and flanking transmission measurements were repeated. A scheme of the setup and some pictures of the connections are reported in Fig. 12. It is to notice that this test configuration is not related to any real application on the construction site and was only tested to check the influence of the connection on a junction.

The measured K_{ij} are reported for junctions with HBS or VGZ screws respectively in Figs. 13 and 14. In both configurations, the transmission path 1-4 is the angular transmission path, which is most strongly influenced by the addition of other connection systems. Dashed lines represent connections with only screws while solid lines represent values measured with plates and hold-down. The measured values show strong differences among the different configurations. The transmission path which is mostly involved by the addition of the plates is 1-3, i.e. between panels aligned but not directly in contact. Here, K_{ij} displays a significant decrease starting from mid frequencies. This difference is more marked for panels connected with VGZ screws since, as discussed above, the connection with this kind of screws provides higher attenuation since the panels are not brought in close contact. The connection between panels 1 and 4, directly

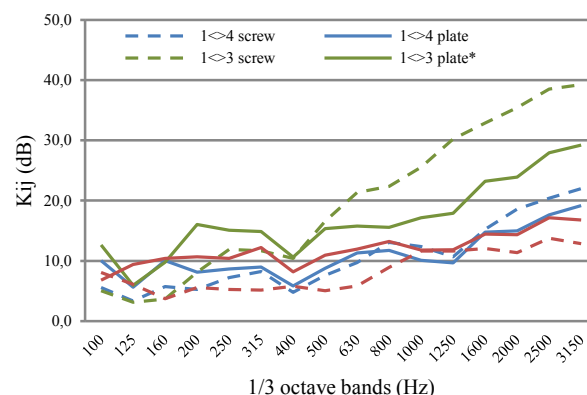


Figure 13: Vertical T junction with base HBS screws and with the addition of plates and hold-down

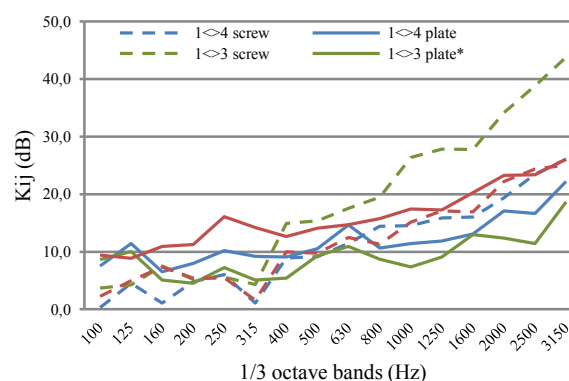


Figure 14: Vertical T junction with base VGZ screws and with the addition of plates and hold-down

involved in the addition of plates, is not strongly marked: there is a slight increase in sound transmission, again more marked for the VGZ connected panels. As far as it concerns panels 3 and 4, whose connection is incremented only through the laying of hold-down, the results show an increase in K_{ij} which appears to be higher at lower frequencies.

5 CONCLUDING REMARKS

This paper reports the results of flanking transmission measurements performed on CLT panels jointed with different construction systems and connectors.

Two construction systems are analysed: the X-RAD, a novel system patented by Rotho Blaas, and the traditional solutions, with panels connected by screws, hold-down and shear angle brackets.

In order to provide a clear exposition of the results, the measurement sessions are grouped by affinity; here the main results achieved from each measurement setup are reported briefly.

The comparison between the X-RAD and the traditional connection system show that the discrepancies between the two systems are not critical except for the transmission path relative to panels in line with no direct contact. The X-RAD, which provide a more homogeneous energy distribution thanks to the X-PLATE element, provides in this case lower attenuation.

Then the transmission paths were analysed for both X-RAD and traditional connection systems on a vertical “X” junction. The results showed that the hierarchy of the connection between panels have a great incidence on the vibration reduction index versus frequency, with differences that range up to 15 dB at mid-high frequencies.

Another test setup saw the laying of Construction Sealing, an EPDM rubber stripe, between vertical panels, and measurements were conducted on junctions connected with HBS and VGZ screws. The results, reported as differences with respect to the configuration without resilient stripe, showed that for panels fixed with HBS screws the delta is always positive but assesses to small values. The difference is greater when panels are fixed with VGZ screws. This comparison is based on the hypothesis that the four CLT qualities tested provide similar results, assumption which will be tested in the near future.

The effectiveness related to the use of resilient stripes at the wall-ceiling junction has been tested on a horizontal junction for X-RAD and traditional connection systems. The X-RAD junction was tested with the soundproofing stripe Xylofon, an extruded polyurethane profile. Benefits show starting from 400 Hz; the difference increases with increasing frequency and reaches up to 8 dB in the 1/3 octave band centred at 2000 Hz. The traditional connection system was tested with the Aladin Stripe Soft, an EPDM rubber profile, providing attenuation from 800 Hz on, while at lower frequencies no significant improvement is found. The effectiveness of the stripe at low frequencies is to be related to the static load to which the stripes were subject, which did not allow a proper mass-spring-mass behaviour of the system.

A “L” test junction was used to verify the incidence in kind and number of screws in the connection. The results are very interesting proving that halving the number of screws the vibration reduction index could reach values higher up to 5 dB. The comparison of carpenter screws HBS and structural screws VGZ also showed that the second ones provide higher attenuation due to the fact that, notwithstanding the use of tensioners, the panels are not brought in contact closely. It was also noticed that the vibration reduction index measured with HBS-screwed panels displays a dip between 160 and 315 Hz, which is not present when panels are fixed with VGZ screws.

The final analysis was aimed at investigating the effect of adding plates to a vertical junction. A vertical “T” junction fixed with HBS or VGZ screws was tested and then plates and hold-down were added to test how the sound transmission would change. It is to notice that this configuration is not related to any real application on the construction site. The results show a significant increase in transmission among the panels in line not directly in contact, and an increase in transmission between the panels angled at 90° not directly fixed through plates. The propagation between panels kept in contact is not critical.

The availability of these data allows the complete characterization of the structural nodes according to the

forecast method proposed in the EN 12354-1 [5] standard and finally will give a powerful tool to the engineers and architects to evaluate the best solution to use in order to achieve the desired sound insulation.

These results are the first data published regarding the measurement campaign and the data analysis is still in progress. Still, from the first results it is possible to draw some possible lines of development. In particular, a special attention will be posed into the analysis of similar configurations with different CLT panels, to check the tolerances due to the installation and in case to try to identify the sound transmission related to the radiation characteristics of the panel and its damping.

The study of sound energy distribution in the X-RAD deserves a more detailed analysis. Finally it will be interesting to check the consistency of the floor-floor junction provided by different CLT suppliers.

Hopefully the availability of in-situ measurements of finished lightweight CLT buildings will help to contribute to the definition of prediction models specifically tailored for CLT structures.

ACKNOWLEDGEMENTS

The measurement campaign was promoted and funded by Rotho Blaas srl to which the authors wish to express their gratitude.

REFERENCES

- [1] COST Action FP0702 Net-Acoustics for Timber based lightweight buildings and elements.
- [2] Schoenwald S.: Comparison of proposed methods to include lightweight framed structures in EN 12354 prediction model. NRC Publication Archive, 2012.
- [3] Guigou-Carter C., Villot M.: Junction characteristics for predicting acoustic performance of lightweight wood-based buildings. Proc. of InterNoise, San Francisco, 2015.
- [4] EN ISO 10848-1:2006. Acoustics - Measurement of the flanking transmission of airborne and impact sound between adjoining rooms. CEN, Brussels, 2006.
- [5] EN 12354-1:2015. Building acoustics – Estimation of acoustic performance of buildings from the performance of element. Part 1: Airborne sound insulation between rooms. CEN, Brussels, 2015.
- [6] D’Orazio D., De Cesaris S., Garai M.: Measuring reverberation time using preprocessed energy detection”, Proc. of InterNoise 2012, New York 2012.
- [7] De Cesaris S., D’Orazio D., Morandi F., Garai M.: Extraction of the envelope from impulse responses using pre-processed energy detection for early decay estimations. J. Acoust. Soc. Am. **138** (4), 2015.
- [8] Morandi F., De Cesaris S., D’Orazio D., Guidorzi P., Barbaresi L.: La misura della trasmissione laterale nelle strutture in legno: problematiche e

metodologie a confronto. Proc. of AIA National Conference, Alghero, 2016 (in Italian).

- [9] Wittstock V., Scholl W.: Determination of the uncertainty of predicted values in building acoustics. Proc. of NAG/DAGA09, Rotterdam, 2009.



CLT BUILDINGS Laterally Braced with Core and Perimeter Walls

Andrea Polastri¹, Cristiano Loss², Luca Pozza³, Ian Smith⁴

ABSTRACT: In this work the behaviour of hybrid multi-storey buildings braced with Cross-Laminated-Timber (CLT) cores and shear-walls is studied based on numerical analyses. Two procedures for calibrating numerical models are adopted and compared to test data and application of provisions in current design codes. The paper presents calibration of parameters characterising connections used to interconnect adjacent CLT panels and building cores, and attach shear-walls to foundations or floors that act as elevated diaphragms. Different case studies are analysed comparing the structural responses of buildings assembled with ‘standard’ fastening systems (e.g. hold-downs and angle-brackets), or using a special X-RAD connection system. The aim is to characterize behaviours of connections in ways that reflect how they perform as parts of completed multi-storey superstructure systems, rather than when isolated from such systems or their substructures. Results from various analyses are presented in terms of principal elastic periods, base shear forces, and uplift forces in buildings. Discussion addresses key issues associated with engineering analysis and design of buildings having around five or more storeys.

KEYWORDS: CLT core, experimental tests, innovative connectors, seismic response, shear-walls, timber buildings

1 INTRODUCTION

Except for low-rise houses traditional timber buildings typically employ so-called heavy-timber post-and-beam arrangements to resist effects of gravity loads. In such cases timber cross-bracing elements, non-timber frame-infill materials or masonry walls are used to resist effects of lateral loads (e.g. earthquake or wind) [1, 2]. Some modern timber-based construction technologies are similar, but others emerging approaches employ Cross-Laminated-Timber (CLT) shear-walls located in building cores or

elsewhere in superstructures to resist effects of lateral loads. Such systems having CLT shear-walls that work in conjunction with timber columns supporting gravity loads have been built already. This reflects that they are structurally efficient, and if overloaded fail in predictable benign stable ways [1]. Other advantages include ability to create large open interior spaces, reduced construction costs, shortened on-site construction periods, and increased quality control compared to alternative typologies created from timber and other materials. However, at present there remain gaps in technical understanding of how to optimize structural behaviors of buildings having CLT shear-walls.

It is not yet, for example, fully clear which structural configurations of CLT shear-walls are most efficient from technical performance or cost perspectives. This not having clearly defined what practical (as opposed to hypothetical) ranges should be for the number of storeys or spans of elevated floors should be. Similarly it is not clear what are the trade-offs between in reducing or increasing respective numbers of shear-walls or columns in systems where both those types of element work together with others (e.g. beams, floor slabs) to create an entire building superstructure. The missing knowledge can be gleaned from experimental studies and practical experience, but those are resource and time consuming methods. The most comprehensive relevant experimental investigations to date addressed seismic performances of complete multi-storey

¹Andrea Polastri, Research Associate, Trees and Timber Institute of the National Research Council of Italy (CNR -IVALSA), Via Biasi 75, 38010 San Michele all’Adige, Italy.

E-mail: polastri@ivalsa.cnr.it

²Cristiano Loss, Research Fellow, Department of Civil, Environmental and Mechanical Engineering, University of Trento, via Mesiano 77, 38123 Trento, Italy

E-mail: cristiano.loss@unitn.it

³Luca Pozza, Ph.D., Department of Civil, Environmental and Architectural Engineering, University of Padova, via Marzolo 9, 35131 Padova, Italy

E-mail: luca.pozza@dicea.unipd.it

⁴Ian Smith, Professor, Faculty of Forestry & Environmental Management, University of New Brunswick, Canada

E-mail: ismith@unb.ca

buildings having CLT walls that resisted effects of all gravity and lateral loads. Those tests were undertaken by the Italian research organization CNR–IVALSA under the SOFIE Project [3][4]. Other important investigations have been conducted at the University of Trento in Italy [5]. The industry led R&D organization FPInnovations in Canada has undertaken tests to determine structural properties and seismic resistance of CLT shear-walls based investigation of reduced-scale three-dimensional structures [6]. These mentioned and other studies [6] have enabled characterisation of failure mechanisms in shear-wall systems having horizontally interconnected vertically CLT sub-plates and one or several storeys typical of what is known as platform construction [7]. An in-depth experimental study on shear and tension forces in CLT connectors is ongoing at the Buildings and Construction Laboratory (CIRI) of the University of Bologna [8].

Innovative connection methods that can create discrete CLT panel-to-CLT panel, or CLT panel -other material joints have been developed in Italy [9] for prefabricated construction of mid-rise and high-rise buildings. This method results in point-to-point mechanical connections that only connect corners of individual CLT panels in ways that fulfil hold-down and lateral shear resistance functions associated with resisting effects of lateral loads on buildings [9]. The particular or similar systems have the advantage of making load-paths within superstructures unambiguous, which is crucial to effective seismic design of buildings. Tests have determined the best ways to make point-to-point connections between CLT panels and steel elements [10].

A 2014 World Conference on Timber Engineering paper by Polastri et al [11] examined the global response of entire multi-storey superstructures braced with CLT shear-walls located in building cores and additional locations, based on three-dimensional numerical analyses of various arrangements. They adopted two ways of calibrating numerical models, with those ways being to use design code or experimental test data to characterize how connection systems within superstructures will behave. The numerical analyses addressed seismic behaviour of tall buildings constructed with new technologies or hybrid steel-timber construction systems [12, 13].

Overall the literature on buildings constructed with CLT shear-walls reveals crucial structural design issues to be those pertinent to vertical continuity between storeys, connections between elevated floors and building core elements, and core-to-foundation and shear-wall-to-foundation connections. Calls have been made for development of standardized procedure leading to reliable seismic design of superstructures containing CLT walls, based on validated modal response spectrum analyses covering a range of building configurations [14, 15]. This includes issues related to in-plane behaviour of elevated floors that act as diaphragms which will retain their shape to a level that ensures proper functioning of complete

buildings during seismic (or strong wind) events. Also to note is current seismic codes do not provide guidance on the most crucial aspects of designing hybrid structural systems that combine post-and-beam frameworks with CLT cores and/or shear-walls. The primary issue is that those codes do not address estimation of fundamental elastic vibration periods (T_1) of buildings and estimation of force flows within superstructure systems. Compounding this is uncertainty that engineers may have about how to represent elements when carrying out design analyses that support seismic or other structural performance related aspects of design. Apart from estimation of T_1 , engineers need to be able to estimate inter-storey drift accurately [15].

This work presented and discussed here is aimed primarily at providing design guidance for evaluating T_1 which is central to ability to design structures that combine CLT shear-walls and post-and-beam substructures.

2 EXPERIMENTAL ANALYSES

Test data collected to characterize, stiffness, strength and hysteretic behaviour of connections is a primary basis of numerical models of building superstructures. This reflects that when CLT plates or other structural elements are used, use of appropriate connections is the most viable way of ensuring proper behaviour of those systems during seismic or other extreme loading events. Development of models discussed below is predicated on connections being ductile control elements and kinetic energy sinks, while CLT elements respond elastically. In the present study connection test data used was collected to characterize connection stiffness according to ‘method b’ specified by EN 12512 [16]. Such data measures elastic and post-elastic range responses of connections and enables determination of characteristic load-carrying capacities $F_{v,Rk}$ and slip moduli k_{ser} calculated consistent with provisions in Eurocode 5 [17].

2.1 MECHANICAL CHARACTERIZATION OF TRADITIONAL CONNECTORS

The mechanical behaviour of connection systems for CLT structures that employ thin metal elements fastened to panels with nails or other slender metal fasteners is well known [4], [19]. The behaviour of such connectors is determined largely by the elasto-plastic response of the fasteners, and to a lesser extent by the response of the steel elements. Stiffness values assumed in the numerical models described in Section 4 were calculated directly from experimental data. The experimental results presented below refer to tests carried out at CNR-IVALSA [4], and the University of Trento [5]. Both sets of tests were conducted according to the EN 12512 [16] loading protocol, which employs a load-path characterized by cycles of increasing displacement amplitude. The protocol applies to structures in seismic regions. As suggested by the standard, a preliminary monotonic test were undertaken

to estimate suitable amplitudes of cyclic load excursions (Figure 1).

Although initial stiffness values were calculated according to ‘method b’ specified by EN 12512 [16], as this paper deals with Linear Dynamics Analysis of superstructure systems only parameters characterizing the elastic properties (k_{test}) and maximum load at failure (F_{max}) are reported here (Table 1). The numerical (Finite Element, FE) models presented in Section 4 implement Rothoblaas WHT 620 hold-down anchors [19] and TITAN TTF200 angle-brackets [21] connectors joined to CLT panels manufactured from wood boards of strength class C24 and using 32 4x60 or 30 4x60 Anker nails.

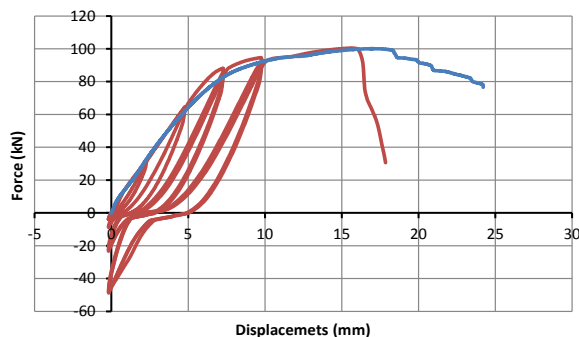


Figure 1: Typical test results on hold-down connector, monotonic (blue line) and cyclic test (red line)

The initial stiffness of connectors was calculated taking into account the stiffness of the steel-to-timber nailed connections. Deformation of steel parts within the connections are very small, compared to deformation of nails, and was therefore neglected.

Table 1: Experimental and code derived connection properties

Connection type	Elastic stiff. (kN/mm)		Capacity (kN)	
	Test (k_{test})	EC5* (k_{ser})	Test (F_{max})	EC5* ($F_{v,Rk}$)
TITANTTF200	8.2	23.1	70.1	35.5
WHT 620	12.1	24.8	100.1	85.2

* k_{ser} and $F_{v,Rk}$ indicate the stiffness and capacity calculated according to Eurocode 5 [17]

2.2 MECHANICAL CHARACTERIZATION OF X-RAD CONNECTOR

The innovative X-RAD connection that create discrete panel-to-panel, or panel-to-other material joints structural response data and parameters are reported in the literature [9, 22, 23]. Section 4 includes a case study using X-RAD connectors.

Different experimental campaigns X-RAD connectors have been performed at University of Trento, CNR-IVALSA and the TU Graz [24] in order to characterize their mechanical behavior. Figure 2 illustrates a typical connectors installed on a CLT plate.

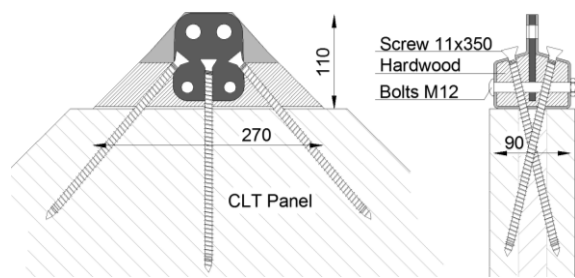


Figure 2: Geometrical characterization of X-RAD connector

X-RAD connectors have a steel box element and hardwood side pieces that makes it possible to attach them to CLT elements using 6 fully-threaded self-tapping VGS screws (11mm x 350mm) [25] inserted into predrilled holes in the hardwood side pieces that anchor into softwood layers within CLT (Figures 2 and 3). Some of the results of conducted tests are given in Table 2. Capacity and initial stiffness data was obtained from a large number of cyclic and monotonic load tests conducted by CNR-IVALSA at its laboratory in San Michele all’Adige, Italy.

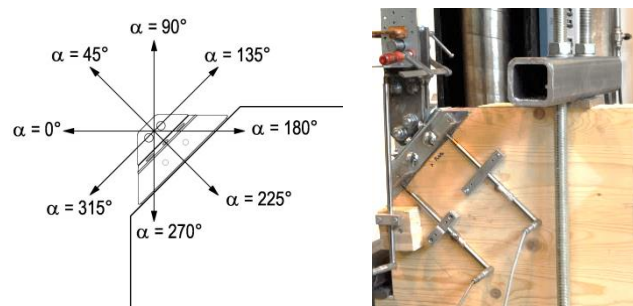


Figure 3: Studied load configurations (left) and typical test on the connector (right).

Figure 4 presents a typical force-displacement response of the connector loaded monotonically in tension or cyclically at 45° to edges of a CLT plate. X-RAD tests adopted the EN 12512 approach already discussed in Section 2. Equivalent viscous damping and strength impairment were calculated at displacement levels of 2, 4 and 6 times the yield displacement.

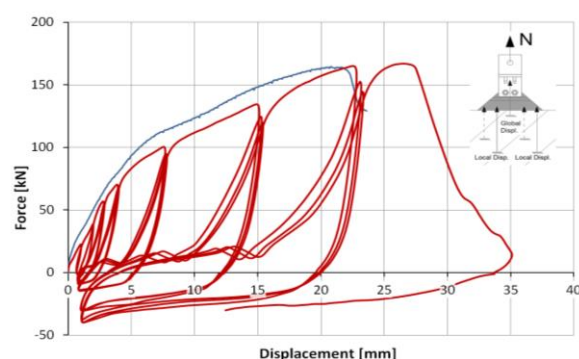


Figure 4: Test results of tension configuration: F-v monotonic (blue line) and cyclic (red line curves)

Regarding the tension configuration (Figure 4), after a third repetitive load cycle the ductility ratio was found 6 and the strength less than 20% compared with the strength during the first load cycle. This means that the X-RAD connector can be considered as a dissipative zone within building superstructures. Energy dissipation (mean equivalent damping ratio) was about 18% at the first cycle and 10% at the third cycle during repetitive loading. This resulted from plastic deformation of the steel box element at low displacement amplitudes. Further information about the post-elastic response in shear configurations (135° in Figure 3) is given elsewhere [24]. Table 2 summarizes the results. Ability to transfer large forces and achieve high stiffness is to be noted. For example, the load-carrying capacity in the tensile load configuration (45°) was 171kN and the initial elastic stiffness 23.6kN/mm. The tests results are used in the FE analyses reported in Section 4.

Table 2: X-RAD mechanical properties

Angle *	Test	F_{mean} [kN]	k_{mean} [kN/mm]
45°	Cyclic	171,15	23.63
135°	Cyclic	108,95	9.00
0°	Monotonic	128,95	11.80
180°	Monotonic	185,88	13.40
225°	Monotonic	289,66**	23.01

* Reported angle correspond to load configuration in Figure 3.

** Tests reached the limit capacity of testing machine

3 STANDARD CONNECTOR HYBRID-BUILDING CASE STUDIES

This section presents information on seismic responses of buildings containing CLT shear-wall elements interconnected or connected to other parts superstructure systems using standard connectors (i.e. hold-down anchors and angle-brackets) to create Seismic Force Resisting Systems (SFRS). The authors reported a preliminary FE model studies on the behaviour of similar buildings [14][15]. This paper presents improved analyses that eliminate effect of previous model simplifications.

3.1 GEOMETRICAL CHARACTERIZATION OF STUDIED BUILDINGS

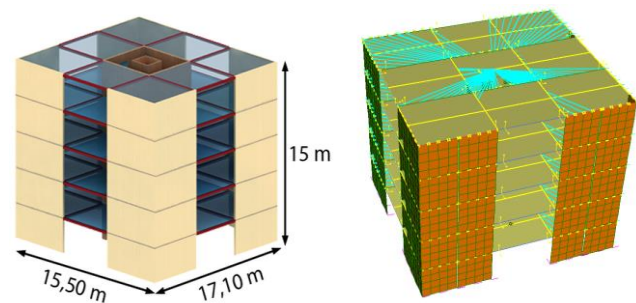


Figure 5: Geometry of 5-storey case study (left) and related FE model (right)

Examined case study building superstructures have footprint dimensions of 17.1m by 15.5m. Their SFRS incorporate a building core that is 5.5m by 5.5m on plan and partial perimeter CLT shear-walls each 6m long. The example case of a 5 building is shown in Figure 5. Perimeter wall segments are placed at plan corners of buildings to maximize their modal stiffness characteristics associated with torsional lateral motions. The main aim of analyses is to characterize how variations in design parameters alter the behaviour of buildings having 3, 5 or 8 storeys. This range of storeys encompasses traditional heights of timber buildings and the likely maximum heights of future buildings (of the particular type). Apart from building height effects of construction methodology for CLT shear-walls were examined by altering the number of CLT plate elements within a wall and altering the regularity of connectors interconnecting attaching them to the SFRS. Figure 6 summarizes shear-wall element and connection configurations studied.

Case study ID	3(5-8) A R	3(5-8) A I	3(5-8) B R	3(5-8) B I	3(5-8) C R
Graphical schematization of building cores (ex. 3-storey case)					
Panel assembly	Joint free wall panels		Jointed wall panels		Joint free wall panels
Elev. regularity	Regular	Irregular	Regular	Irregular	Regular
Constr. method	Platform System				-

Figure 6: Shear-wall and connection configurations studied

3.2 DESIGN AND MODELLING

The earthquake action for the case study buildings was calculated according to Eurocode 8 [25] adopting the design spectra and other relevant seismic design parameters in Table 3.

Table 3: Design parameters for standard connector case studies

	3 storey	5 storey	8 storey
Soil type	C		
PGA (peak ground acceleration)	0.35 g		
H (building height)	9.0m	15.0m	24.0m
$T_1 = 0.05 H^{3/4}$	0.26 s	0.38 s	0.54 s
M (global mass)	276 t	482 t	800 t
$S_{d,el}(T_1)$	0.82 g	0.82 g	0.78 g
q_0 (behaviour factor)	2		
$S_d(T_1)^*$	0.42 g	0.42 g	0.39 g

*For non-regular config. $S_d(T_1)$ is multiplied by $k_r=0.8$

Starting from the estimation of the elastic periods reported in Table 3, and following the iterative design procedure explained by Polastri et al [15] it is possible to define the connection pattern appropriate for different building configurations. The applied procedure starts with a

preliminary definition of the external force induced in each CLT wall element by the design earthquake according to the well-known equivalent static force linear analysis method. This in turn allows estimation of the connection stiffness, and then realistic preliminary estimation of T_1 . Afterward T_1 is used in modal analyses to calculate the forces induced in connections by design earthquakes. Obtained estimates of connection forces may or may not be compatible with the way connection strengths are determined. If there is inconsistency it is necessary to redesign the connections, which enables subsequent precise iterative convergent solution of T_1 values and final design of connections.

In this section the numerical models of the investigated building were realized using the commercial FE software Strand 7 [26]. Resulting FE models uses linear elastic shell elements to represent CLT plates and link elements to simulate the elastic stiffnesses of connectors. Beam elements with pinned-end conditions were used to represent beam members interconnecting perimeter shear-walls and shear-walls within the building cores at the tops of storeys.

In total 15 building configurations were analyzed to represent possible combinations of variables in Table 3 and Figure 6. Natural frequency and modal response spectrum analyses were performed with the models. To note is within the models interactions between the orthogonal walls and the out-of-plane stiffness provided by the floor slabs were neglected. Consequently model outputs represent the maximum possible deformability of the SFRS.

3.3 RESULTS: BUILDINGS WITH STANDARD CONNECTIONS

Results given here are the fundamental elastic periods (T_1) summarized in Figure 7; peak base shear forces (v) on angle-brackets at the Ultimate Limit State (ULS) summarized in Figure 8; and peak uplift forces on base hold-down anchors at the ULS (N) summarized in Figure 9. Within Figures 7 to 9 the alternative values in each case represent effects of taking connection stiffnesses (k_{conn}) equal to values derived from design code information (k_{ser}) versus values derived from experimental data (k_{test}). The alternative estimates (k_{ser} , k_{test}) are those given in Table 1. Also in the case of Figure 7, estimates are given of values determined by the approximate equation suggested in Eurocode 8 [26].

From Figure 7 it is evident that using test-based connection stiffnesses ($k_{conn} = k_{test}$) leads to much higher T_1 values than are predicted based on connection stiffnesses derived from code information ($k_{conn} = k_{ser}$). Similarly, using the simple formula given by Eurocode 8 leads to low estimates of T_1 values.

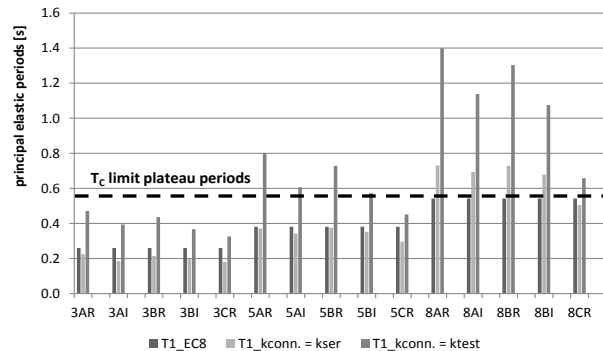


Figure 7: Predicted principal elastic periods, T_1

Interestingly use of code based estimates of k_{conn} results in estimates of T_1 relatively close to those obtained using the Eurocode 8 formula. However, this is believed to be purely coincidental. What the comparisons show in an overall sense is neither use of code based estimates of k_{conn} nor the Eurocode 8 formula are reliable as the basis of estimating fundamental elastic periods of SFRS of hybrid-buildings that contain CLT shear-wall connected using standard connectors. Relevant to this is to note how obtained values T_1 compare with the limit periods T_C of the plateaus of the design spectra for the building (depicted in Figure 7 with by the heavy dashed horizontal line). Based on this comparison 3-storey building configurations all have T_1 values that fall within the plateau range regardless the assigned connection stiffness. In contrast for 5- and 8-storey building configurations the connection stiffness induce elastic periods estimates can be either greater or less than T_C , especially if k_{conn} properties are assigned based on test data. This effect has significant implications for susceptibility of structural systems to damage during seismic events.

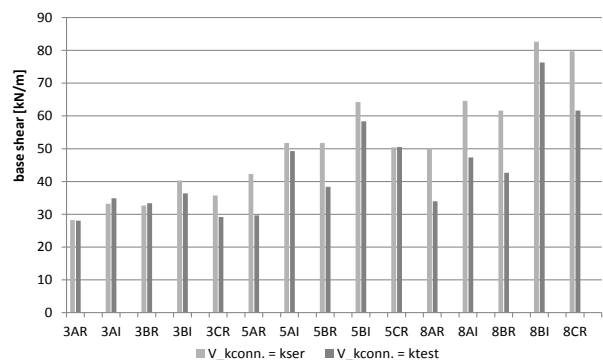


Figure 8: Peak base shear forces on angle-brackets

It also demonstrates that effects of adopting simplified engineering design practices are not uniform for buildings of different height. Given that in the present studies building height (number of storeys) is a surrogate for slenderness of superstructures, the implication is that what might be traditionally acceptable design practice for low-rise timber buildings is not of necessity suitable practice for design of medium- or high-rise timber buildings. This finding supports recommendations given elsewhere [28].

Additional consequential discrepancies associated with the way k_{conn} values are estimated are effects on v and N .

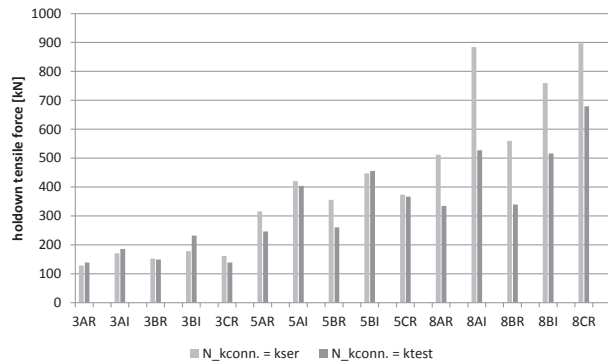


Figure 9: Peak base uplift forces on hold-down

In general, results in Figure 8 and 9 show that the way connection stiffnesses are estimated significantly alters design forces that then determine element selection and dimensioning decisions. Practical results can include undersizing or oversizing elements in SFRS that might alter the structural design strategy in unintended ways.

4 X-RAD CONNECTOR HYBRID-BUILDING CASE STUDIES

This section presents information about seismic responses of buildings containing CLT shear-wall elements that are connected to other parts superstructure systems using innovative connectors. Studied configurations are the same multi-storey CLT building configurations A3, A5 and A8, but with X-RAD connectors (Figure 2) substituted for standard connections at appropriate location. In terms of structural action this makes point-to-point mechanical connections, which, as was previously mentioned, is important eliminate ambiguity in load-paths within the SFRS. During construction of buildings prefabricated sections of the system are assembled in a manner that requires only standard connections to be made on-site (Figures 10 and 11). As Figure 11 shows X-RAD connectors are used at junctions between CLT plates segment elements where those segments lie in the same plane, or where segments in vertically or horizontally orthogonal planes intersect.

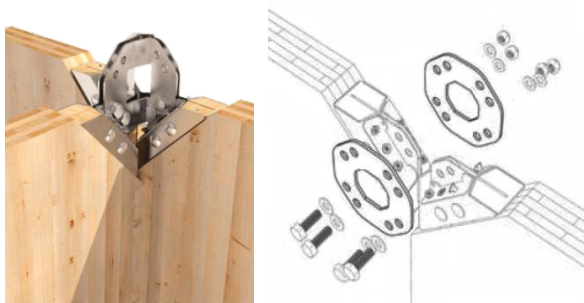


Figure 10: CLT panel-to-panel three-way connection (left) and assembly of a simple X-RAD connection

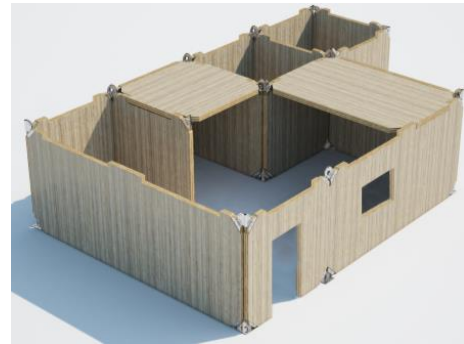


Figure 11: Schematic example of a simple CLT plate structure with X-RAD connections

4.1 FEM MODELS

FE numerical models of each configuration were implemented based on details reported in Table 3. X-RAD connections were included within shear-walls, at their junctions with building foundations, and at their junctions with floors. The numerical models were realized using the commercial FE software SAP 2000 [29]. Incorporation of X-RAD devices allowed simplified modelling of SFRS because CLT plate segments were are connected at their vertices corresponding to physical point-to-point junction locations in load-paths. Consequently FE models were composed of two-dimensional plate elements representing CLT plate elements interconnected at relevant nodes by specifically calibrated elements representing X-RAD connections. Behaviour of the X-RAD connection were simulated by introducing two orthogonal uniaxial springs accounting for stiffnesses in vertical and horizontal direction that were derived from experimental results listed in Table 2. Figure 12 and 13 show an example of FE modelling of a CLT plate with X-RAD connection at its vertices.

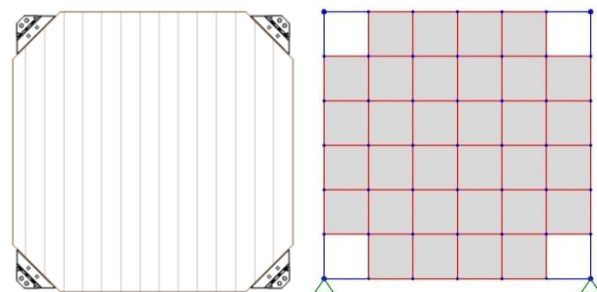


Figure 12: CLT plate segment with X-RAD connectors (left) and corresponding FEM representation (right)

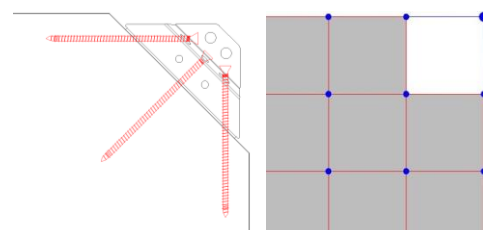


Figure 13: X-RAD connector (left) and associated FEM implementation (right)

Apart from CLT shear-walls and X-RAD elements the FE models contained floor diaphragms that could be rigid or deformable, with adopted rigidities based on using traditional connection elements within those substructures (Figure 14). Unlike for buildings having standard connections there is no need in the case of those employing X-RAD connectors to iteratively adjust component sizes (and properties), then refine estimates of T_1 and peak internal force flows until a design analysis is sufficiently accurate.

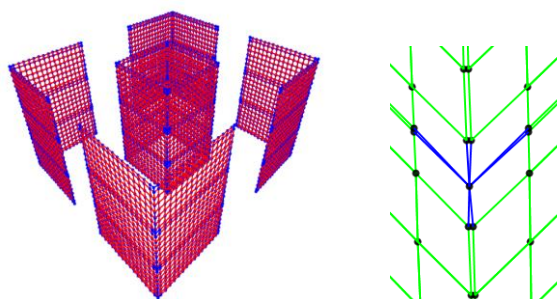


Figure 14: FE model of 3-storey shear-wall configuration: global view (left) and details of corner connections (right)

Based on analyses it was determined that only 3-storey buildings were viable with X-RAD connectors because in 5- and 8-storey buildings the load carrying capacities of the connectors were insufficient to resist effects of predicted peak force flows during design level seismic events. Therefore for the taller buildings (> 3 storeys) a new structural approach was adopted. That new approach was to incorporate continuous vertical structural steel profiles that connect CLT shear-wall elements directly to the building foundation. Those steel profiles were placed at the corners of the building and were connected to X-RAD connectors by means of bolts (Figure 15 to 17). As a result the tensile force acting on individual X-RAD connectors flowed directly to the foundation. This demonstrates that in practical circumstances engineers will tend to utilize CLT elements, special connection hardware and other types of structural components that do not lend themselves to simple classification with the spectrum of hybrid-construction options. It also suggests the notion of ‘all timber’ solutions for creation of taller timber building is unlikely to be viable.

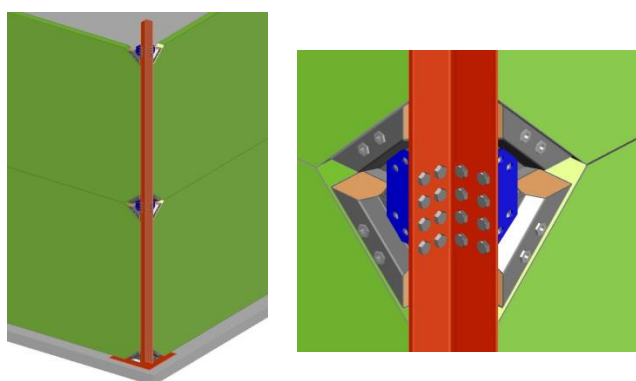


Figure 15: Detail of steel profiles at the corners of buildings

4.2 RESULTS: 3-STOREY BUILDING WITH X-RAD CONNECTIONS

Table 4 summarizes T_1 , total base shear force (V_{tot}), and maximum shear force (v_{max}) and maximum uplift force (N_{max}) on an X-RAD connector. That table also shows corresponding results for the matched building with standard connectors.

Table 4: Results of 3-storey FE model: X-RAD connection and standard connection (case study AR Section 3)

	X-RAD connect. ($k_{conn} = k_{test}$)	Standard connect. ($k_{conn} = k_{test}$)
T_1	0.49s	0.47s
V_{tot}	855.7kN	892.4kN
v_{max}	69.1kN	28.1kN/m
N_{max}	163.1kN	128.3kN

Results show that the for 3-storey buildings considered T_1 and V_{tot} are not very sensitive to alterations in the shear-wall connection methods. This is consistent with results shown in Figure 7 where there is a similar relative lack of influences of connection stiffnesses on the fundamental modal stiffness of the SFRS. However, the qualification is required that this comparability depends on how connection stiffnesses were estimated (i.e. $k_{conn} = k_{tes}$ in shown instances). Also, as the tabulated comparison shows, it should not be supposed that v_{max} and N_{max} will exhibit matched sensitivity or insensitive to alterations in the connection methods.

4.3 RESULTS 5- AND 8-STOREY BUILDINGS WITH X-RAD CONNECTIONS

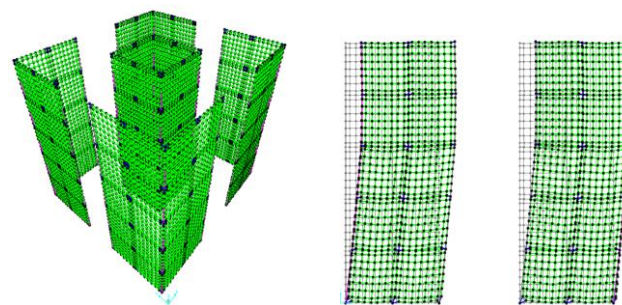


Figure 16: FE model of hybrid-building (left) and the first vibration mode -entire façade- (right)

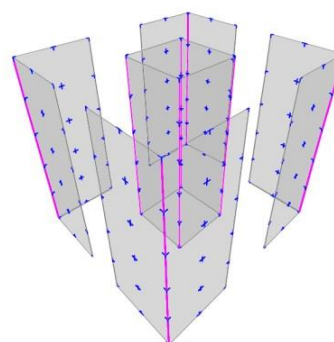


Figure 17: FE model of hybrid-building with steel vertical profile

Tables 5 and 6 contain FE results for 5- and 8-storey buildings respectively having X-RAD connectors. Those tables also show corresponding results and compare them with corresponding results for systems with standard connectors (systems 5B-R and 8B-R). Figure 16 (right) shows the first order mode shape for the 5-storey building with X-RAD connectors. As might be expected a sway mode is strongly influenced by shear deformation within the shear-walls in the building core and facades.

Table 5: Results of 5-storey FE model: X-RAD connection + steel profile and standard connection (case study BI Section 3)

	X-RAD connect. ($k_{conn} = k_{test}$)	Standard connect. ($k_{conn} = k_{test}$)
T_1	0.46s	0.73s
V_{tot}	1722 kN	1853kN
v_{max}	70.1kN	38.4kN/m
$N_{max_free\ edge}$	91.2kN (X-RAD)	253.4kN
	154.4kN (steel profile)	
$N_{max_corner_}$	76.9kN (X-RAD)	260.1kN
	135.6kN (steel profile)	

Table 6: Results of 8-storey FE model: X-RAD connection + steel profile and standard connection (case study BR Section 3)

	X-RAD connect. ($k_{conn} = k_{test}$)	Standard connect. ($k_{conn} = k_{test}$)
T_1	0.66s	1.14s
V_{tot}	2112kN	2265kN
v_{max}	91.7kN	47.4kN/m
$N_{max_free\ edge}$	142.7kN (X-RAD)	339.5kN
	250.3kN (steel profile)	
$N_{max_corner_}$	108.3kN (X-RAD)	379.4kN
	156.3kN (steel profile)	

Comparing the fundamental elastic periods (T_1 values) in Tables 5 and 6 it is clear that for buildings with five or eight storeys that altering the connection system and adding the steel profile anchor elements at building corners significantly alters modal stiffnesses of SFRS. There will of course be related effects on mode shapes and modal mass but the dominant influence is that the systems with X-RAD connectors and steel profiles have the greatest stiffnesses. In general it is reliable to conclude that the taller buildings are the more sensitive their fundamental vibration periods are to structural detailing decisions. Choosing the type(s) of connection methods to employ is a particularly important detailing decision. However to note is that except for the 8-storey building with standard connections the T_1 values are either within or reasonably close to the plateau range of the design spectra (Section 3). Practical implications of this is that quite simple structural detailing decisions are an effective way of creating taller SFRS that will behave in ways that push the modal frequencies well outside the range where those frequencies would make buildings highly susceptible to seismic damage. Also to note is intrinsic ductility capabilities of X-RAD connectors make them suitable for benign

redistribution of forces if some are damaged during an earthquake.

Other results presented in Tables 5 and 6 (V_{tot} , v_{max} , N_{max}) exhibit strong sensitivities to connection method decisions, as should be expected.

5 GENERAL DISCUSSION

The FE analyses presented here reveal very strong influences of construction detailing decisions related to choice of connection methods for SFRS on performance and vulnerabilities of buildings having CLT shear-walls during earthquakes. Allied with careful choices of the structural configurations that place shear-walls in locations that maximise their contributions to system level modal stiffnesses, this gives designers a powerful tool for ensuring buildings are safe and economic to construct. The current study shows that employing relatively new construction products (e.g. CLT plates and X-RAD connectors) in conjunction with realistic numerical models of SFRS permits designers to create tall timber superstructures that will behave in predictable and desirable ways during extreme events. Although the discussion is contextualized relative to seismic design load analyses the same general conclusion can be expected for wind and other design load scenarios. As has been discussed elsewhere [28], accurate and reliable knowledge (at the design stage) of likely lateral vibration periods of buildings is also important for control of motions that occur during strong wind events. Similarly knowing vibration periods of buildings can help with serviceability performance issues like buildings being shaken by ground motions caused by vehicular traffic [28]. It is not an exaggeration to say it is incumbent on designers to use relatively refined structural analysis methods like detailed FE models if they desire to use timber in ways that maximise its potential as a construction material.

Comparison between predicted characteristics of buildings assembled with standard connectors (hold-down anchors, angle-brackets) and those assembled X-RAD connectors allows it to be stated:

- *For 3-storey buildings:* Fundamental elastic vibration periods (T_1) are not strongly sensitive to the choice of connection methods.

- *For 5-storey buildings:* Building height and slenderness are still not sufficient to make T_1 strongly sensitive to the choice of connection methods. However, for the system with X-RAD connectors those components used alone were not sufficiently strong to resist uplift forces generated by earthquake design loads. Use of reinforcing vertical steel profiles is an efficient method of solving that inadequacy.

- *For 8-storey buildings:* In this instance T_1 was strongly sensitive to the choice of connection methods. Values for systems with standard connectors were in some instances

well above, and that for the system, with X-RAD connectors and vertical steel elements, about 0.6s. Values of T_1 about 0.6s correspond roughly to the plateau region of the Eurocode 8 design spectrum. As already discussed in Section 4, this means that choice of the connection methods for SFRS can strongly influence vulnerability of relatively tall and slender buildings to seismic damage.

Results of all the analyses make clear effectiveness of correctly selecting a combination structural configuration and choose suitable matching connection hardware is not to be taken as sufficient in itself. Decisions must be supported by accurate predictions of T_1 and other response parameters that drive the engineering design decisions. It follows that any suggestions or assertions that using, for example, one connection hardware instead of another will always result in reduced possibilities of building sustaining damage during particular types of events are very suspect. It also follows that prescriptive design practices are inherently unreliable except in the case of low-rise buildings in terms of expected seismic performance.

6 CONCLUSIONS AND FUTURE DEVELOPMENTS

Work presented here demonstrates unambiguously that maximize structural potential of modern timber products, and related connection technologies, equates to basing design on accurate analyses methods. Appropriate accurate analytical methods are ones that use accurate information about stiffness and strengths characteristics of employed materials and connection hardware. Relying on information gleaned from generic timber design codes (e.g. fastener stiffness information in Eurocode 5) as model input will often prove inadequate. Using information gathered via test campaigns specific to products should be strongly favoured. Similarly practices such as using approximate formulas to estimate fundamental elastic vibration periods of buildings (e.g. formula in Eurocode 8) are not a sufficiently accurate or reliable underpinnings to design practice.

Trends toward greater use of timber as a construction material for medium- and high-rise buildings makes use of refined structural analysis models increasingly important. This is because tall and slender buildings are those most likely to be poorly designed if models inaccurately predict characteristics like elastic modal frequencies. Poor design will result in buildings that perform poorly under normal or abnormal service load conditions. Combining structural configuration and construction detailing decisions (especially choice of connection methods) is crucial to minimizing material utilization and costs, and maximizing structural performance characteristics of buildings. Debate has existed in timber engineering circles for a long time about adequacy of approximate structural design methods. There was some validity in arguments that simple approaches were adequate when timber was only used to

construct low-rise buildings. When engineers design relatively tall buildings any such validity vanishes.

Although not addressed directly here, related work has created reliable and cost effective ways of ensuring tall timber buildings have good fire and durability performances characteristics. Hence, there is no substantive impediment to timber playing a primary role as an advanced construction material for normal or exotic buildings. As case studies here demonstrate, this can be in the form of massive timber elements that form primary elements of hybrid-structures with those elements interconnected and anchored by innovative connection devices.

Ongoing studies by the authors and collaborators are further developing analytical methods discussed here, creating new construction methods and technologies that exploit new and emerging structural timber products, and contributing to development of next generation design code provisions specific to timber. A number of building have already been constructed employing ideas presented. Hopefully this will be part of a wave creating buildings that are safer, more serviceable, more economic to construct and maintain, and more durable than traditional ones.

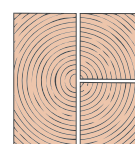
7 ACKNOWLEDGMENTS

The authors wish to thank Rothoblaas company for X-RAD experimental data, and Stefano Pacchioli for the contribution in the implementation of the FE models.

REFERENCES

- [1] Smith T., Fragiaco M., Pampanin S. and Buchanan A. H. (2009): Construction time and cost for post-tensioned timber buildings. Proceedings of the Institution of Civil Engineers: Construction Materials, 162:141-149.
- [2] Bhat P (2013): Experimental investigation of connection for the FFTT timber-steel hybrid system. MASc thesis, University of British Columbia, Vancouver, Canada.
- [3] Ceccotti A., Sandhaas C., Okabe M., Yasumura M., Minowa C. and Kawai, N. (2013): SOFIE project – 3D shaking table test on a seven-storey full-scale cross-laminated timber building. Earthquake EngStruct. Dyn., 42: 2003-2021.
- [4] Gavric I, Ceccotti A, Fragiaco M (2011) Experimental cyclic tests on cross-laminated timber panels and typical connections. Proc, ANIDIS, Bari, Italy
- [5] Tomasi R. and Smith I. (2015): Experimental characterization of monotonic and cyclic loading responses of CLT panel-to-foundation and angle bracket connections, Journal of Materials in Civil Engineering, 27(6), 04014189.

- [6] Popovski M., Pei S., van de Lindt J.W. and Karacabeyli E.: Force Modification Factors for CLT Structures for NBCC. Materials and Joints in Timber Structures, RILEM Bookseries 9:543-553, 2014.
- [6] Flatscher G. Schickhofer G. 2015. Shaking-table test of a cross-laminated timber structure. Proceedings of the Institution of Civil Engineers / Structures and buildings. Vol. 168 Issue: 11 Pag. 878–888.
- [7] Pozza L., Trutalli D., Polastri A. and Ceccotti A., (2013): Seismic design of CLT Buildings: Definition of the suitable q-factor by numerical and experimental procedures, Proceedings 2nd International conference on Structures and architecture, Guimarães, Portugal: 90 – 97.
- [8] Pozza L., Massari M., Ferracuti B., Savoia M. (2016): Experimental campaign of mechanical CLT connections subjected to a combination of shear and tension forces. Accepted for publication in Proceedings of International conference on Structures and architecture, Guimarães, Portugal - 2016
- [9] Polastri A. and Angeli A. (2014): An innovative connection system for CL T structures: experimental - numerical analysis, 13th World Conference on Timber Engineering 2014, WCTE 2014, Quebec City, Canada.
- [10] Loss C., Piazza M. and Zandonini A. (2014): Experimental tests of cross-laminated timber Floors to be used in Timber-Steel Hybrid Structures, Proceedings 13th World Conference on Timber Engineering, Quebec City, Canada.
- [11] Polastri A., Pozza L., Trutalli D., Scotta R., Smith I., (2014): Structural characterization of multistorey buildings with CLT cores. Proceedings 13th World Conference on Timber Engineering, Quebec City, Canada.
- [12] Ashtari S., Haukaas T. and Lam F. (2014): In-plane stiffness of cross-laminated timber floors. Proceedings 13th World Conference on Timber Engineering, Quebec City, Canada.
- [13] Liu J. and Lam F. (2014): Numerical simulation for the seismic behaviour of mid-rise clt shear walls with coupling beams. Proceedings 13th World Conference on Timber Engineering, Quebec City, Canada.
- [14] Polastri A., Pozza L., Loss C., Smith I., (2015): Structural characterization of multi-storey CLT buildings braced with cores and additional shear walls. Proceedings of International Network on Timber Engineering Research (INTER), meeting 48, 24-27 August 2015, Šibenik, Croatia. Paper INTER/48-15-5. ISSN 2199-9740.
- [15] Polastri A. and Pozza L. (2016): Proposal for a standardized design and modeling procedure of tall CLT buildings. Accepted for publication in International Journal for Quality Research.
- [16] European Committee for Standardization (CEN) (2006) EN 12512 - Timber structures – Test methods – cyclic testing of joints made with mechanical fasteners. Brussels, Belgium
- [17] European Committee for Standardization (CEN) (2009) EN 1995 - Eurocode 5 - design of timber structures, Part 1-1, General - Common rules and rules for buildings. Brussels, Belgium
- [18] Gavric I., Fragiocomo M. and Ceccotti A.: Capacity seismic design of x-lam wall systems based on connection mechanical properties. In: Proceeding of the meeting 46 of the Working Commission W18-Timber Structures, CIB. Vancouver, Canada, paper CIB-W18/46-15-2, 2013.
- [19] Piazza M., Polastri A., Tomasi R., (2011), Ductility of Joints in Timber Structures, Special Issue in Timber Engineering, Proceedings of the Institution of Civil Engineers: Structures and Buildings, 164 (2) PP. 79-90, doi: 10.1680/stbu.10.00017
- [20] European Organisation for Technical Assessment (EOTA) (2011), Rotho Blaas WHT hold-downs, European Technical Approval ETA-11/0086, Charlottenlund, Denmark.
- [21] European Organisation for Technical Assessment (EOTA) (2011), Rotho Blaas TITAN Angle Brackets, European Technical Approval ETA-11/0496, Charlottenlund, Denmark.
- [22] Loss, C., M. Piazza and R. Zandonini (2015a). "Connections for steel-timber hybrid prefabricated build-ings. Part I: Experimental tests." Construction and Building Materials. 10.1016/j.conbuildmat.2015.12.002.
- [23] Loss, C., M. Piazza and R. Zandonini (2015b). "Connections for steel-timber hybrid prefabricated build-ings. Part II: Innovative modular structures." Construction and Building Materials. 10.1016/j.conbuildmat.2015.12.001.
- [24] Polastri A., Brandner R., Casagrande D., (2016), Experimental analysis of a new connection system for CLT structures. Structures and Architecture: Concepts, Applications and Challenges - Proceedings of the 3rd International Conference on Structures and Architecture, ICSA 2016
- [25] Angeli A., Polastri A., Callegari E., Chiodega M., (2016), Mechanical characterization of an innovative connection system for CLT structures, 14th WCTE World Conference on Timber Engineering 2016, Vienna, Austria
- [26] Comité Européen de Normalisation (CEN) (2013): Eurocode 8 - design of structures for earthquake resistance, part 1: General rules, seismic actions and rules, CEN Brussels, Belgium
- [27] Strand 7 (2005): Theoretical Manual – Theoretical background to the Strand 7 finite element analysis system, http://www.strand7.com/html/docu_theoretical.htm
- [28] Smith I. and Frangi A. (2014): Structural use of timber in tall multi-storey buildings, Structural Eng. Doc. 13, Int. Asso. Bridge and Struct. Eng., Zurich, Switzerland
- [29] SAP 2000, version 17. Computers and Structures, Inc. 2015.



STRUCTURAL ANALYSIS OF CLT MULTI-STOREY BUILDINGS ASSEMBLED WITH THE INNOVATIVE X-RAD CONNECTION SYSTEM: CASE-STUDY OF A TALL-BUILDING

Andrea Polastri¹, Ivan Giongo², Stefano Pacchioli³ Maurizio Piazza⁴

ABSTRACT: The cross laminated timber (CLT) technology is nowadays a well-known construction system, which that can be applied to several typologies of residential and commercial buildings. However some critical issues exist which limit the full development of the CLT construction technology: problems in handling, difficulty in assembling and inadequate connection systems. The connectors that are usually adopted in CLT structures, derive from the light timber frame technology and consequently might prove inadequate when employed in tall buildings (over 6 floors). The structural design of CLT structures is also problematic because of the complexity in verifying the connectors and in defining the actual load path within/between the panels. The various connection systems, e.g. hold-downs, screwed-in elements and metal brackets are all to be nailed onsite, with ensuing uncertainties related to the use of different connection systems and to the “hard-to-verify” quality of the onsite instalment operations. An innovative connection system specifically designed for CLT structures, such as X-RAD, was analysed. The X-RAD system is characterized by a single standard connector to be placed at the corners of the CLT panels. The connector is formed by a metal box containing a pre-drilled hardwood insert that allows attaching the connector to the panel with fully threaded screws inserted at different angles. A case study of a multi-storey building was selected in order to investigate the structural behaviour of the X-RAD system and to exploit the potential of this system applied for assembling tall timber buildings.

KEYWORDS: CLT tall buildings, prefabrication, innovative connection system, structural behaviour

1 INTRODUCTION ¹²³

The versatile nature of Cross Laminated Timber (CLT) as a structural product has certainly helped the diffusion of CLT buildings. CLT panels in fact, guarantee to timber structures a high strength in both loading directions, in-plane or out-of-plane (wall/diaphragm configuration). In addition, when loaded edgewise, they also offer an extremely stiff response. The CLT technology is characterized by a high level of prefabrication: the panels are manufactured in modern factories equipped with computer numerical control (CNC) systems [1]. The critical point of the whole CLT construction method can be identified in the mechanical

connections. In the traditional CLT assembling system, single panels are connected to the foundation and to the panels of the upper floor through hold-down elements and angle brackets which are nailed to the panels. These connectors, originally designed for other construction technologies (e.g. platform frame), have been adopted for CLT structures with little or no modifications. As a result, the building capacity is limited by the strength of the connectors, which also show ultimate deformations not compatible with the CLT panel stiffness ([2],[3],[4]). Hence, in order to comply with the most recent and most advanced Standards it is fundamental to develop new and more efficient connection systems.

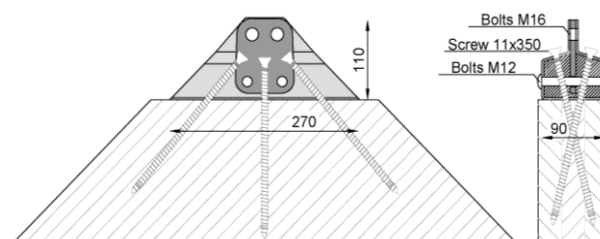


Figure 1: Geometric characteristics of the innovative connector

The innovative solution proposed [5], named X-RAD, consists of a point-to-point mechanical connection

¹ Andrea Polastri, Research Associate, Trees and Timber Institute - National Research Council of Italy (CNR IVALSA), San Michele all'Adige, Italy. E-mail: polastri@ivalsa.cnr.it

² Ivan Giongo, Research Fellow, Department of Civil, Environmental and Mechanical Engineering, University of Trento, Italy. E-mail: ivan.giongo@unitn.it

³ Stefano Pacchioli, Student, Department of Civil, Environmental and Mechanical Engineering, University of Trento, Italy. E-mail: stefano.pacchioli@studenti.unitn.it

⁴ Maurizio Piazza, Professor, Department of Civil, Environmental and Mechanical Engineering, University of Trento, Italy. E-mail: maurizio.piazza@unitn.it

system, fixed to the corners of the CLT panels [6]. This connection, designed to be prefabricated, comprises a metal wrapping and an inner hard wood element which are fastened to the panel by means of full-threaded self-tapping screws ([7],[8]). Such system permits to assemble two or more panels or to connect the panels to the foundation by the use of standard steel plates and steel bolts.

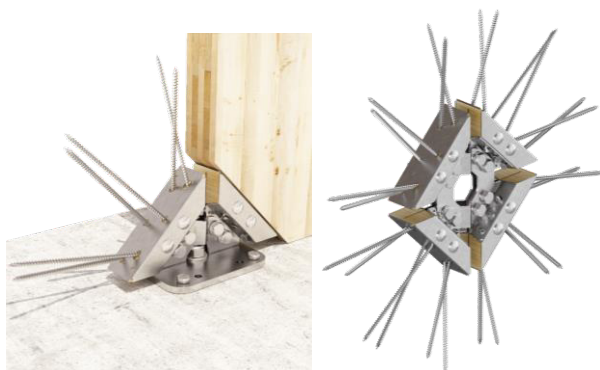


Figure 2: X-RAD units connected with steel plates and bolts

In the traditional CLT assembling system, the CLT walls are connected to the foundation by using hold-downs and angle brackets [9]. The same type of fasteners are also employed to connect the wall panels to the floor/roof panels. As a result, the wall panels at a (i)th level rest directly onto the floor panels of the i-th level, which are sitting on top of the wall panels of the (i-1)th level. Horizontal panels are therefore subjected to compression perpendicular to the grain. Another consequence of having interposed floor panels (which interrupt the continuity of vertical walls), is that a great number of connectors is required to transfer the uplift forces and the horizontal forces from one level to the next (Figure 3 left).

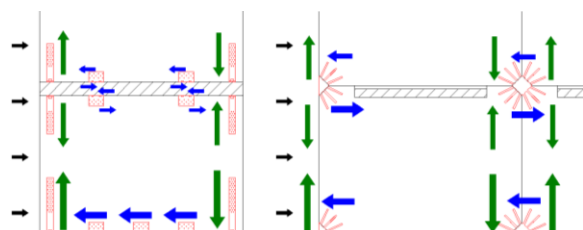


Figure 3: Load path in CLT buildings; comparison between the traditional connection system (left) and the X-RAD system (right)

Considering that the X-RAD connecting system is located at the corners of the panels it is possible to create slots where to insert the panels constituting the floor diaphragms. By doing this, the vertical loads can be transferred to the foundations through the direct contact between the vertical walls. The floor panels can be connected to the vertical skeleton by fixing them, directly with screws, to the aforementioned slots created into the CLT wall (Figure 3 right). In case of particularly high horizontal design loads, vertical steel rods may be used to link each connection to the next one (placed on the upper/lower level) so as to transfer directly to the

foundation the forces generated by the external horizontal loads.

2 EXPERIMENTAL ANALYSIS

The research and the development that led to the final version of X-RAD was marked by several testing phases throughout the entire process [5]. Experimental campaigns were carried out at the CNR-IVALSA institute of San Michele all'Adige, at TU-Graz and at the University of Trento. In particular, the tests were aimed at characterizing:

- the all-threaded fasteners in the in-use configuration (hardwood insert wrapped by a metallic box, [5]);
- X-RAD connector under different loading conditions [10];
- the wall system, where the CLT panels are fixed to each other or to the foundation by using X-RAD connectors.

2.1 TESTS ON THE X-RAD CONNECTOR

In 2014 an extensive experimental campaign was focused exclusively on the X-RAD connector [10]. 50 specimens were tested both in “tension” and “shear”. Monotonic and cyclic loading protocols were selected in accordance with EN 26891:1991 [11] e EN12512:2006 [12] respectively.

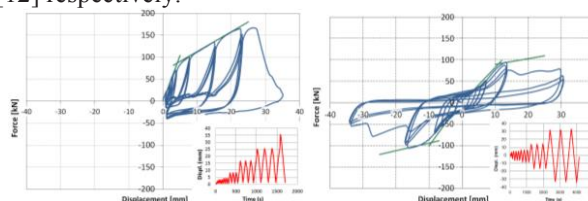


Figure 4: Experimental results, F-v curve: tension (left) and shear (right) configurations

Further testing, to determine the connector performance under different loading configurations, is in progress (Figure 5).

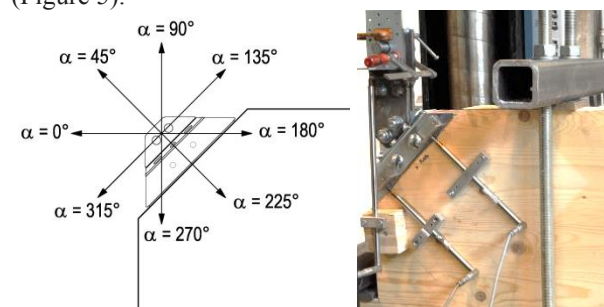


Figure 5: Configurations being studied (left) and typical test setup (right)

From the analysis of the experimental data [13] it was possible to identify the connector elastic properties (stiffness k , and yielding capacity f_y), the failure conditions (ultimate displacement v_u and ultimate capacity F_u), the energy dissipation (equivalent viscous damping v_{eq}) and the ductility (D) [10].

Table 1 gives the mechanical properties (i.e. connection stiffness k_{mean} and connection capacity F_{mean}) that were

used for the static analyses which will be described in chapter 3.

Table 1: Test results for different load configurations

Angle [°]	Test	n°	F _{mean} [kN]	k _{mean} [kN/mm]
45°	Cyclic	15	171,15	23.63
135°	Cyclic	15	108,95	9.00
0°	Monotonic	6	128,95	11.80
180°	Monotonic	6	185,88	13.40
225°	Monotonic	3	289,66*	23.01

* Tests in load configurations 225° reached the limit capacity of testing machine

2.2 TESTS ON CLT WALLS CONNECTED WITH X-RAD

Below, the description of the tests performed at the University of Trento on wall systems assembled with X-RAD is reported. Two tests, one monotonic and one cyclic were conducted on a 2.5 m × 2.5 m CLT panel connected to the steel base by means of n. 2 X-RAD connectors (Figure 6). A cyclic test on 4-panel system (each panel size was 1.25 m × 1.25 m) with multiple X-RADs completed the experimental campaign (Figure 7).

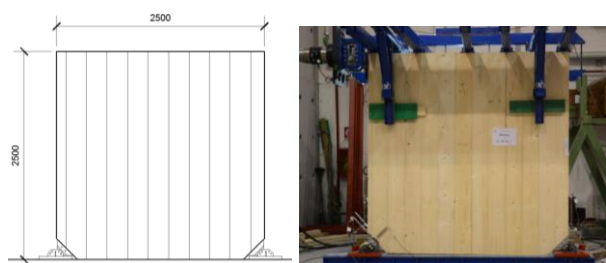


Figure 6: Test on CLT wall connected to the foundation with X-RAD

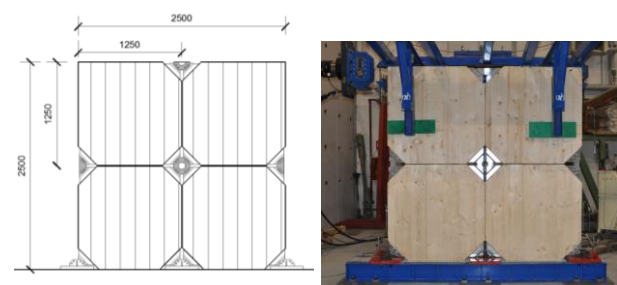


Figure 7: Test on composite CLT wall system connected with X-RAD

The test results in terms of *applied force versus storey drift* are given in Figure 8. It is interesting to note how the cyclic test backbone curve closely matches the curve from the monotonic test. This evidences a reliable response from X-RAD connections under different loading histories.

By comparing the curves resulted from the two cyclic tests (single panel, 4-panel system) it can be observed that despite an obvious reduction in global stiffness when moving from the single panel to the composite wall system, there was no capacity decrease.

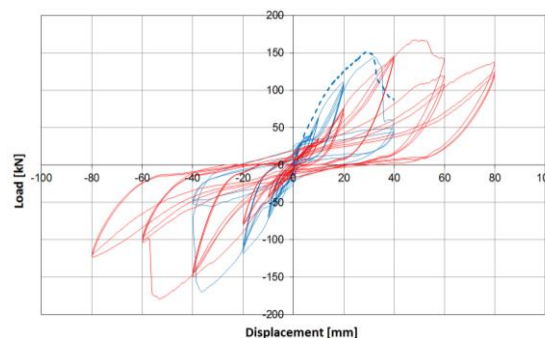


Figure 8: Results from tests on simple CLT wall, monotonic test (dashed blue) and cyclic test (solid blue). Composite wall system cyclic test (red)

As will be better explained in section 4.2, the X-RAD system implies that a structural systems is analysed by referring not to “vertical strips of pier elements” (typical of traditional connection systems) but to the “façade”, assuming that the entire 2D system is resisting the horizontal forces. The resisting mechanism in fact, involves all the CLT panels and forces are exchanged between adjacent vertical strips of panels. Such interaction does not take place when hold-downs and angular brackets are employed.

3 FE ANALYSIS OF CLT PANELS CONNECTED WITH X-RAD

3.1 FE MODELLING OF X-RAD CONNECTORS

Figure 9 schematizes one of the possible solutions that can be adopted to model X-RAD with finite element (FE) software packages. The elastic properties of the connectors are simulated by 3 elastic springs that reproduce the response under different loading configurations. The spring stiffness does not correspond to just the all-threaded screw stiffness but represents the stiffness of the whole connection, deformability of the X-RAD unit included.

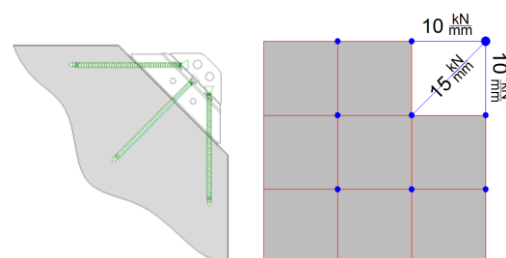


Figure 9: The X-RAD connector (left) and the 3 associated links implemented into the FE model (right)

Such modelling approach, proved to have adequate refinement as it provided results extremely close to the experimental response. However, when modelling complex building structures, the adoption of the schematization shown in Figure 10 is preferable. The use of 2 link elements instead of 3, permits to improve the computational efficiency while maintaining an

acceptable level of global accuracy. The stiffness of the 2 elastic rods in Figure 10 is identical (25 kN/mm) and was derived from the experimental results presented in section 2 for the 45° and 225° loading directions.

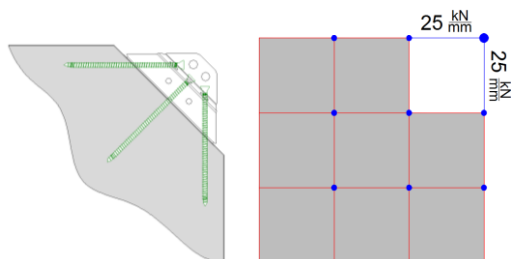


Figure 10: The X-RAD connector (left) and the 2 associated links implemented into the FE model (right)

The simplification introduced by the 2-link model, is inevitably reflected in the different ability of the two approaches of matching the experimental behaviour at the connector level. From Table 2, it can be appreciated how the 3-link model can reproduce the experimental stiffness in every loading direction, while the 2-link model falls short of accuracy for the “shear” loading configuration (angle of load inclination = 135°).

Table 2: Comparison between experimental and FE models stiffness of X-RAD connector in different load configurations

Angle [°]	k_{exp} [kN/mm]	k_{3links} [kN/mm]	k_{2links} [kN/mm]
45°	23,63	25,00	25,00
135°	9,00	10,00	25,00
0°	11,80	15,00	25,00
180°	13,40	15,00	25,00
225°	23,01	25,00	25,00

Despite the large approximation error shown for the 135° loading direction, the 2-link approach was adopted for modelling the case study building that will be presented in section 4. This because of the smaller computational effort and also because the 2 links directly provide the horizontal and vertical components of the force acting on the X-RAD connectors. *Gap* elements (SAP2000 [14]) were also introduced in the model to simulate contact between panels. Being such elements *compression only*, they require nonlinear solution methods.

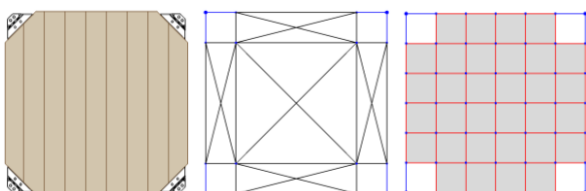


Figure 11: CLT panel with X-RAD connectors (left) and related FE schematization, “frame” model (middle) and “shell” model (right)

For the determination of the modal frequencies via linear dynamic analyses, the gap elements were removed from model of the case-study building Chapter 6 and [15].

Alternative approaches where the panel is modelled with equivalent truss elements are possible (see Figure 11).

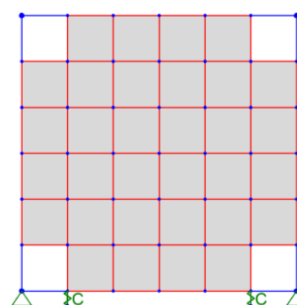


Figure 12: FEM of a CLT panel with X-RAD connectors, “shell” model with compression-only links

3.2 FE MODEL OF CLT PANELS CONNECTED WITH X-RAD

The FE model of a complex wall system, where multiple CLT panels are connected to each other and to the foundation by using X-RAD, can be implemented as visible in Figure 13. The wall panels, modelled with linear elastic 2D shell elements, are connected at their corner joints where the link elements representing the X-RAD connectors replace the shell elements. At the interface between adjacent panels, gap elements are also inserted.

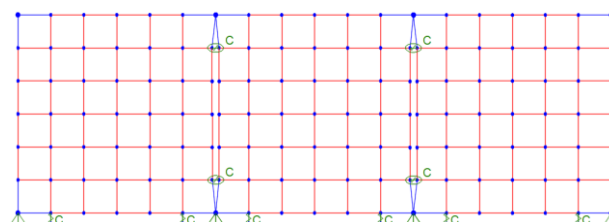


Figure 13: FE model of assembled CLT walls

3.3 VALIDATION OF FE MODEL ON THE EXPERIMENTAL TEST DATA

Both the 2-link and 3-link modelling approaches were validated on the results from the experimental testing on single panel walls and composite walls carried out at the University of Trento (refer to section 2.2).

As already mentioned, being the models based on linear elastic material properties (except for the gap elements), the comparison with the tests was made within the elastic threshold of the experimental response, at a lateral force of 100 kN. Nonlinear models able to simulate the post-elastic behaviour of the X-RAD wall system were also developed, the results of which will be published in the near future.

Table 3: Comparison between experimental and numerical results in terms of displacement at the top of the tested walls

Test	V_{test} [mm]	$V_{FEM,3links}$ [mm]	$V_{FEM,2links}$ [mm]
Simple wall°	16,5	16,2	13,1
Composite wall	26,2	24,7	19,2

As can be noted from the values shown in Table 3, the 3-link model matches the experimental results with sufficient accuracy for both the single panel wall and 4-panel wall system, while the 2-link model overestimates the stiffness of approximately 25%.

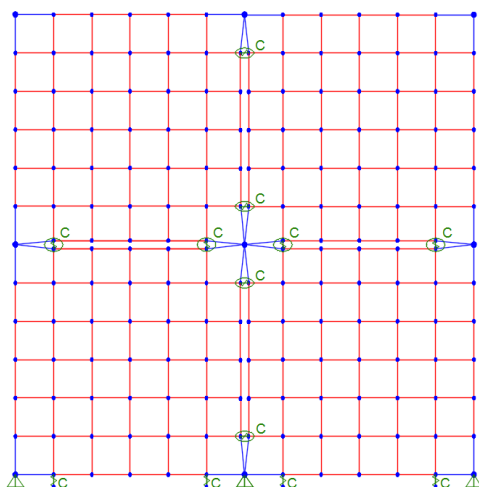


Figure 14: FE model of the composite wall specimen tested at UNITN

4 TALL BUILDING CASE STUDY

A case study of a multi-storey building assembled with the X-RAD connectors was analysed under different loading conditions. Also a variation of the number of storey was considered. In particular 5-storey and 8-storey case scenarios were studied. Both wind and seismic action were accounted for. Areas in Italy where wind and earthquake are most severe (Trieste and L'Aquila respectively) were chosen as construction site for the case study building. For sake of completeness also a low seismic area like is Trento, was included.

4.1 DESCRIPTION OF THE CASE STUDY

The case study is representative of a multi-family residential building. Typical example of structure destined to social housing, the floor plan consists of 4 living units, each one of them being 75 m² in size (Figure 15). A staircase and an elevator permit the access to the upper floors.

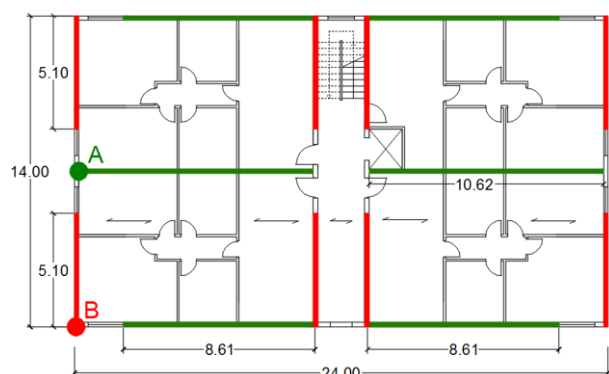


Figure 15: Case study – Floor plan layout: structural walls in X direction (green) and Y direction (red)

By looking at the floor plant and at the elevation drawings it is evident that the geometrical aspect ratios are such that the building appears as “slender” in Y direction and “squat” in X direction. Despite that, the arrangement of the openings together with the floor layout (floor load is transferred to the walls oriented along the Y axis) makes it not surprising that the magnitude of the uplift phenomena in the two directions was observed to be comparable (see section 5).

The design loads assumed for the analyses were: 2.5 kN/m² for diaphragm dead loads (CLT floor panel weight included); 0.7 kN/m² to account for CLT wall panels; 2.0 kN/m² for live loads. The load combinations varied according to the horizontal action (wind or earthquake) considered in the analysis. For the first three levels from the ground, the thickness of the CLT wall panels was 140 mm while for the upper levels a thickness of 100 mm was selected.

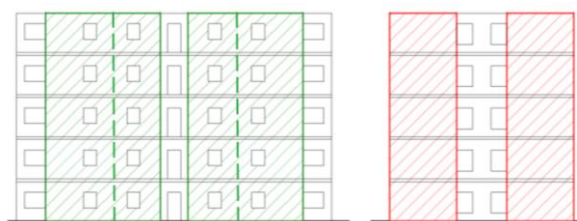


Figure 16: Case study - structural elevation, X façade (green) and Y façade (red)

4.2 STRUCTURAL ANALYSIS

To better understand the peculiarity of X-RAD system, some remarks on the common analysis methods that are used for CLT buildings realized with the traditional connection systems are due. The presence of numerous intersecting walls induces in CLT buildings a box-like behaviour that is normally neglected by both the numerical models and the analytical procedures. The connection between orthogonal walls, usually ensured by screw fasteners, is considered a “construction detail” and is generally neither designed nor verified.

It is therefore quite complex to define the 3D behaviour of a CLT structure. Taking into account the box-like response of a CLT building requires refined analysis procedures and advanced modelling skills: only few research works have presented 3D models that can effectively reproduce the interaction between orthogonal walls in CLT structures ([16], [17], [18], [19]). Further source of complexity can be found in the sheer number of connection types that need to be implemented (e.g. hold-downs, angular brackets, various types of screws in different configurations), despite the mechanical behaviour of some of which has not been fully characterized yet. All these aspects result in excessive computational complexity and a significant level of uncertainty [20].

As already mentioned, practitioners inevitably turn to extremely simplified assumptions which cannot take into account the box-like behaviour and the interactions between orthogonal walls. The structure is therefore schematized with a series of cantilevers (Figure 17)

connected to each other by inextensible rods placed at the floor levels. The diaphragms are assumed as rigid and the horizontal load is distributed among the cantilevered walls proportionally to the wall shear stiffness.

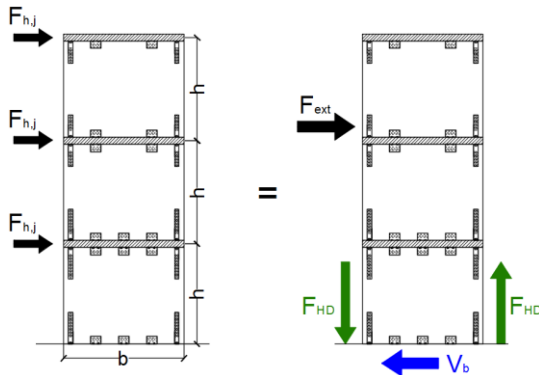


Figure 17: Simplified design method commonly adopted by practitioners

Thanks to X-RAD system the CLT structure can be analyzed by referring not to “vertical strips of pier elements” (typical of traditional connection systems) but to the “façade”, assuming that the entire 2D system is resisting the horizontal forces.

The use of X-RAD connections, means that the wall panels are connected to each other not only vertically (panel i to panel $i+1$, Figure 18) but also laterally (panel i to panel j , Figure 18). The resisting mechanism involves all the CLT panels and ensures a force transfer exchanged between adjacent vertical strips of panels.

4.3 FE MODELLING OF A 3D STRUCTURE

In section 3, details about how to model via finite elements both single-panel walls and multiple adjacent walls assembled with X-RAD are given. However, to analyse a full building, a step forward is required and the 2-link / 3-link wall models need to interact with each other in a 3D space.

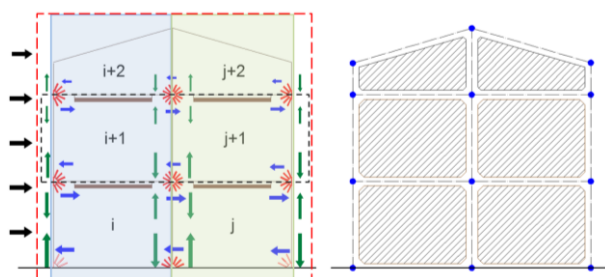


Figure 18: CLT structure assembled with X-RAD (left) and its structural schematization (right)

Being all X-RAD connectors identical (same mechanical behaviour) no matter what the wall arrangements are, it becomes straightforward to model the structure by using a series of 2D wall macro-components (meshed with linear elastic membrane elements) located on independent orthogonal planes but connected at their

corner nodes with the link elements described in section 3.1.

The numerical tool used for modelling the case study presented in subsection 4.1 was SAP2000 [14]. Figure 19 shows the FE model for the 5-storey version of the building.

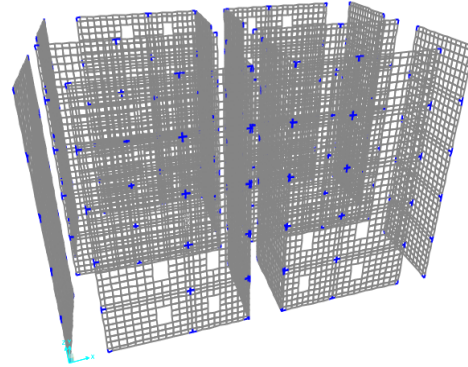


Figure 19: 5-storey FE Model (without vertical tie elements), shell elements (grey) and X-RAD frame elements (blue)

5 STRUCTURAL ANALYSIS OF A CASE STUDY

A case study of a multi-storey building assembled with the X-RAD connectors was analysed under different loading conditions, taking into account both wind and seismic actions. Numerical models specifically developed for the X-RAD system and provisions from current Standards documents were used. Finite element (FE) models were implemented in order to study the mechanical behaviour of the whole structure. Particular care was adopted when determining the load paths and the actions on the X-RAD connectors for the different load combinations.

5.1 CASE STUDY VARIATIONS

As pointed out by research works available in literature ([16],[17],[20]), the most stressed structural elements in tall buildings are the connectors that transfer the uplift forces to the ground. Typically this role is taken on by the hold-downs while in buildings assembled with the X-RAD system are the X-RAD connectors that come into play. They can resist uplift forces up to 150 kN and consequently can be considered adequate for most applications. However, in areas characterized by “extreme seismicity”, vertical tie elements that span from the foundation level to the roof can be employed to help tie the building to the ground. Such elements are placed to either side of the wall systems.

The tie elements are constituted by steel plates (for the 5-storey case a cross section of 140 mm × 10 mm was adopted) that can be fixed to the X-RAD connections by means of bolts.

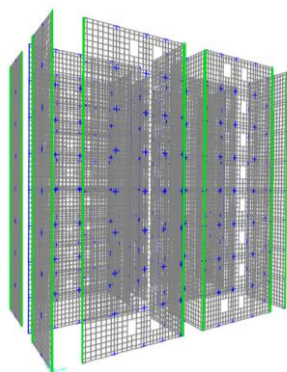


Figure 20: 8-storey case study, shell elements (grey), X-RAD frame elements (blue) and tie frame elements (green)

The list of the analysed case scenarios includes:

- 5 storeys, low seismicity;
- 5 storeys, wind action;
- 5 storeys (vertical tie elements), high seismicity;
- 8 storeys (vertical tie elements), low seismicity;
- 8 storeys (vertical tie elements), wind action;
- 8 storeys (vertical tie elements), high seismicity.

5.2 SEISMIC ANALYSIS

The earthquake action for the various case scenarios was calculated according to Eurocode 8 [21] and the associated Italian regulation code [22].

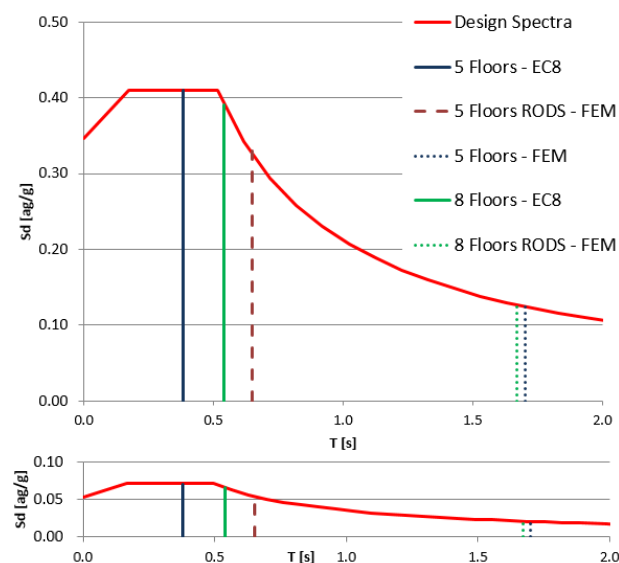


Figure 21: Design spectra for high seismic areas (above) and low seismic areas (below).

Design response spectra for ground type C were selected. The PGA was taken equal to 0.26g (corresponding to the PGA of L'Aquila city that is characterized by one of the highest values in Italy). A building importance factor $\lambda = 0.85$ was assumed. The seismic action was calculated by applying an initial reduction factor q of 2 to the elastic spectra [21]. The k_r coefficient was taken equal to 1.0, as for regular structures. Figure 21 shows the adopted design spectra,

the T_1 values obtained from the simplified formula suggested by Eurocode 8 and the T_1 values given by the FE models discussed in section 6.

5.3 FEM ANALYSIS RESULTS

Equivalent static analyses were performed using the FE model described in Section 3. For the “wind” load case scenario, distributed pressure was applied to the walls to simulate wind forces, while the vertical load on the floors was taken so as to maximize the effects of the horizontal action [22]. As concerns the seismic analyses, the earthquake force was introduced into the models at the floor levels as suggested by [21] and [22] for regular structures (simplified procedure). The combination coefficient for vertical loads was that corresponding to the seismic load combination.

Thanks to the model relative simplicity, the evaluation of the internal forces for the various structural elements is straightforward:

- Because the CLT panels are modelled by shell elements, the panel verification can be done by referring to the stress values of the most stressed element;
- Being X-RAD connectors schematized by 2 orthogonal frame elements (elastic rods), the force level on such rods provides the input for a direct comparison with the failure surface described in [24];
- Vertical ties can be verified in accordance with [25] by reading the force components on the frame elements representing them.

The 5-story version of the case study building without tie elements, satisfied the standard requirements for the “low seismicity” and wind loading conditions [Table 4]. At present X-RAD connectors come in one-size only. Therefore, to guarantee that the connection system is adequate, just the most loaded joints need to be verified. Not surprisingly, the highest force level was registered for the connectors located at the ground level (Figure 22 on the left). The connector in position A (Figure 15) was the most severely loaded when the seismic action acted along the X axis, while the one in position B (Figure 15) was the most stressed by an earthquake parallel to the Y axis.

Table 4: Results of 5-storey tall building FE analysis

Load case	Vb XRAD	Uplift XRAD	Uplift Tie El.	Vb XRAD	Uplift XRAD	Uplift Tie El.
	[kN]	[kN]	[kN]	[kN]	[kN]	[kN]
	X direction			Y direction		
Wind	18.7	91.5	-	24.3	2.6	-
Low s.	12.6	27.7	-	21.0	94.6	-
High s.	45.8	99.6	271.2	68.4	78.8	181.1

From figure 22 (on the right), the interaction between two adjacent strips of panels due to X-RAD coupling effect can be appreciated. The two vertical strips in fact, thanks to the shear forces exchanged at the interface by

the X-RAD connectors, behave as a single cantilever fixed at its base. The maximum uplift force measured on the central connectors at the base of the wall was 41.3 kN, significantly smaller than the 96.4 kN registered for the lateral connectors. This is an indicator of the coupled response from the two strips.

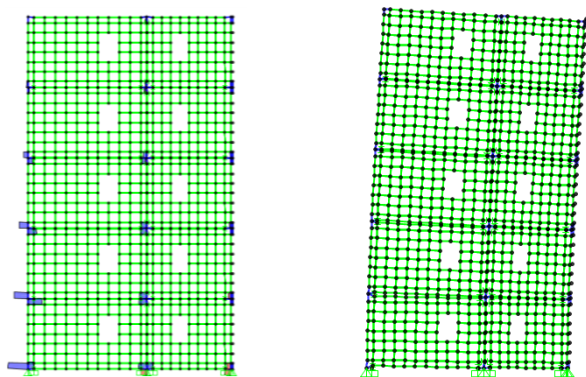


Figure 22: 5-storey building without tie elements (wind loading), uplift forces on the connectors (left) and deformed shape (right)

As already mentioned, for the “high seismicity” case scenario, vertical tie elements were introduced into the model to help transfer the uplift forces to the foundation. The ties were connected to the X-RAD connectors at each storey level (Figure 23).

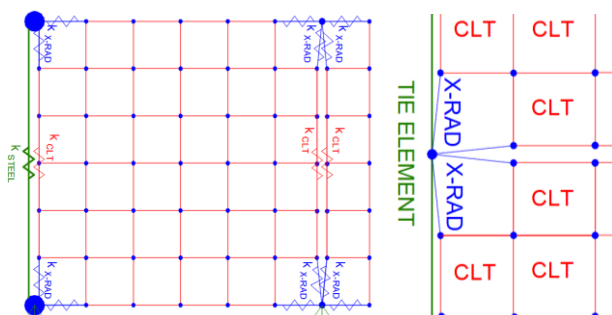


Figure 23: Schematization of different resisting systems (left) and a close-up on the finite elements at the connection node

As regards uplift forces, two different resisting systems can therefore be identified (Figure 23):

1. Vertical tie elements;
2. CLT panels + X-RAD connectors.

The two systems work in parallel and consequently a higher quota of the uplift force is absorbed by the most stiff system of the two: the ties (Table 4 and Table 5).

An example of the force distribution registered for the vertical ties is reported in Figure 24. The tensile force in the ties increases from one level to the next below. Such regular “staircase” distribution is not always to be expected, for example when multiple structural systems (with different stiffness distributions over the building height) are responsible for the lateral load carrying capacity [15].

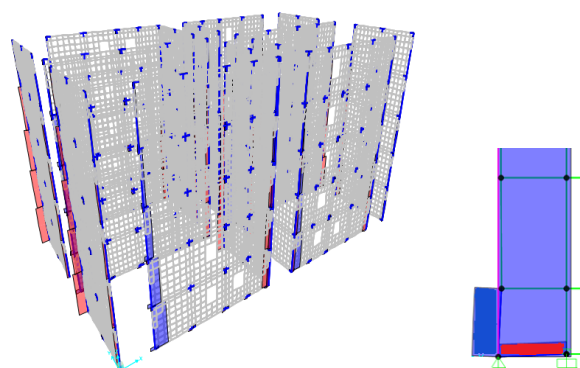


Figure 24: Resultant forces in the tie and X-RAD elements (left) and a close-up on forces at the foundation node. X-RAD shear stress is in “red”, X-RAD uplift is in “blue”, tie uplift is in “light blue” (right)

Table 5 gives the forces obtained from the analyses on the 8-storey building (with ties) for X-RAD connectors and tie elements: in case of severe earthquakes (highly seismic areas), the element capacity is exceeded and the building safety is not guaranteed.

Table 5: Results of 8-storey tall building FE analysis

Load case	Vb XRAD	Uplift XRAD	Uplift Tie El.	Vb XRAD	Uplift XRAD	Uplift Tie El.
	[kN]	[kN]	[kN]	[kN]	[kN]	[kN]
	X direction			Y direction		
Wind	19.9	26.4	127.4	45.4	-12.2	-63.3
Low s.	29.2	52.2	350.2	42.9	7.3	13.6
High s.	83.2	198.7	1011	126.3	164.8	866.3

The simplified static analysis procedure contained in [21], provides a T_1 value close to the values corresponding to the plateau of the spectrum, resulting in extremely high inertial forces. The period value derived from the numerical model (Figure 21) suggests that the use of the simplified formula might lead to an overestimation of the seismic force. However, additional investigation (e.g. on different layouts and even higher buildings) is required to further validate such outcome.

6 DISCUSSION

The numerical results shown in the previous section indicate that the X-RAD connectors proved to be adequate in all the case scenarios except for an 8-storey building placed in a highly seismic area.

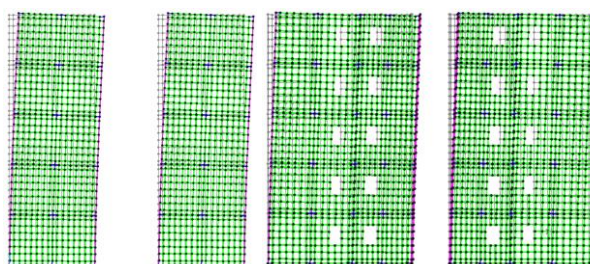


Figure 25: 5-storey building with tie elements (high seismicity), first vibration mode – Y façade – $T_1=0.65$ s, 75% Y mass, second vibration mode – X façade – $T_2=0.47$ s, 80% X mass.

With a minor modification of the model (i.e. removing the “compression only” spring elements [15]), linear dynamic analyses were performed in addition to the “static” analyses presented so far. Linear dynamic analysis was used to control if the first vibrational modes were actually “translational” as requested by standards when adopting equivalent static procedure (torsional modes are admitted for the higher modes only).

In Figure 21 the natural periods calculated for the 5-storey and 8-storey building according to the simplified formula provided by [21] are reported together with the numerical results. The formula appears to largely underestimate the period of vibration of tall buildings characterized by slender lateral-load resisting structures. For the 5-storey building modeled with ties, the FE analysis provided a T_1 very close to the “plateau range” while for all the other cases extremely large period values were registered. It is worth noting that the models did not account for secondary effects that contribute to stiffen a real building (e.g. presence of multi-span CLT floor panels and non-structural elements).

7 CONCLUSIONS

Over the next 20 years, a strong need for rebuilding large derelict areas is expected in most of the major cities. In this scenario, timber constructions and CLT structures represent quite competitive building technologies, thanks to their assembling speed and high structural performance. Being highly prefabricated and suitable for tall buildings, the X-RAD system can surely foster the development of the CLT technology. The paper presented different case-studies of tall buildings assembled using this innovative system.

Analysis results regarding 5-storey and 8-storey buildings, subjected to horizontal loading due to seismic or wind action, were presented.

Further analysis focused on non-linear FE models is recommended for a better understanding of the mechanical behaviour of the different “X-RAD solutions” (e.g. with or without ties) studied in the paper.

8 ACKNOWLEDGMENTS

The authors wish to thank eng. Ester Sinito and eng. Ernesto Callegari. The tests presented in the paper were conducted within the framework of the research project X-REV proposed by Rothoblaas company and partially financed by the Autonomous Province of Bolzano.

REFERENCES

[1] Brandner R., Flatscher G., Ringhofer A., Schickhofer G., Thiel A., Cross laminated timber (CLT): overview and development. *European Journal of Wood and Wood Products*, 10.1007/s00107-015-0999-5.

[2] Casagrande D., Polastri A., Piazza M., Sartori T., Loss C., (2016): Experimental campaign for the

mechanical characterization of connection systems in the seismic design of timber buildings. *World Conference on Timber Engineering (WCTE)*, Vienna, Austria.

[3] Gavric I., Fragiaco M., Ceccotti A., (2015): Cyclic behaviour of typical metal connectors for cross-laminated (CLT) structures. *Materials and Structures/Materiaux et Constructions*, 48,6,1841,1857,10.1617/s11527-014-0278-7.

[4] Tomasi R., Smith I., (2015): Experimental characterization of monotonic and cyclic loading responses of CLT panel-to-foundation and angle bracket connections. *Journal of Materials in Civil Engineering*, 27(6), 04014189.

[5] Polastri A., Angeli A., (2014): An innovative connection system for CLT structures: experimental - numerical analysis, 13th World Conference on Timber Engineering 2014, Quebec City, Canada.

[6] European Organisation for Technical Assessment (EOTA) (2015): Rotho Blaas X-RAD, European Technical Approval ETA-15/0632, Vienna, Austria.

[7] Bejtka I., Blass H. J., (2002): Joints with inclined screws. *Proceeding of the meeting 35 of the Working Commission W18-Timber Structures*, CIB.Vancouver, Canada, paper CIB-W18/35-7-5.

[8] Ringhofer A., Brandner R., Schickhofer G., (2013): Withdrawal resistance of self-tapping screws in unidirectional and orthogonal layered timber products. *Materials and Structures*. DOI:10.1617/s11527-013-0244-9.

[9] Smith I., Frangi A., (2014): Use of timber in tall multi-storey buildings. *Struct. Eng. Doc. 13*, Int. Assoc. Bridge & Struct. Eng., Zurich, Switzerland.

[10] Polastri A., Brandner R., Casagrande D., (2016): An innovative connection system for CLT structures: experimental – numerical analysis. *Structures and Architecture: Concepts, Applications and Challenges - Proceedings of the 3rd International Conference on Structures and Architecture, ICSA 2016*.

[11] European Committee for Standardization, (1991), EN 26891 Timber structures – Joints made with mechanical fasteners – General principles for determination of strength and deformation characteristics. CEN, Brussels, Belgium.

[12] European Committee for Standardization (CEN) (2006): EN 12512 - Timber structures – Test methods – cyclic testing of joints made with mechanical fasteners. Brussels, Belgium

[13] Piazza M., Polastri A., Tomasi R., (2011): Ductility of Joints in Timber Structures, *Special Issue in Timber Engineering. Proceedings of the ICE: Structures and Buildings*, 164 (2): 79-90.

[14] SAP 2000, version 17. *Computers and Structures*, Inc. 2015.

[15] Polastri, A., Loss C., Pozza L., Smith I. (2016), CLT buildings laterally braced with core and perimeter walls, 14th WCTE World Conference on Timber Engineering 2016, Vienna, Austria

[16] Ceccotti A., Sandhaas C., Okabe M., Yasumura M., Minowa C., Kawai N., (2013): SOFIE project – 3D shaking table test on a seven-storey full-scale cross-

- laminated timber building. *Earthquake EngStruct. Dyn.*, 42: 2003-2021.
- [17] Rinaldin G., Poh'sie G.H., Fragiaco M., Amadio C., (2014) Non-linear modelling of the three and seven storey X-lam buildings tested within the SOFIE Project. *Proceeding of the 13th World Conference on Timber Engineering WCTE 2014*, Quebec City, Canada.
 - [18] Popovski M., and Gavric I., (2015). Performance of a 2-Story CLT House Subjected to Lateral Loads. *J. Struct. Eng.*, 10.1061/(ASCE)ST.1943-541X.0001315, E4015006.
 - [19] Fragiaco M., Dujic B., Sustersic I., (2011): Elastic and ductile design of multi-storey crosslam massive wooden buildings under seismic actions. *Engineering Structures*, Vol. 33 (11), p. 3043-3053. ISSN 0141-0296. eISSN 1873-7323
 - [20] Polastri A., Pozza L., Loss C., Smith I., (2016), Numerical analyses of high- and medium- rise CLT buildings braced with cores and additional shear walls. *Structures and Architecture: Concepts, Applications and Challenges - Proceedings of the 3rd International Conference on Structures and Architecture, ICSA 2016*.
 - [21] European Committee for Standardization (CEN) (2013): Eurocode 8 - design of structures for earthquake resistance, part 1: General rules, seismic actions and rules, CEN Brussels, Belgium.
 - [22] Ministero delle Infrastrutture e dei Trasporti (MIT) (2008): DM Infrastrutture 14 gennaio 2008 - Norme tecniche per le costruzioni - NTC (Italian national regulation for construction), MIT, Rome, Italy.
 - [23] European Committee for Standardization (CEN) (2009): EN 1995 - Eurocode 5 - design of timber structures, Part 1-1, General - Common rules and rules for buildings. Brussels, Belgium.
 - [24] Angeli A., Polastri A., Callegari E., Chiodega C., (2016), Mechanical characterization of an innovative connection system for CLT structures, 14th WCTE World Conference on Timber Engineering 2016, Vienna, Austria
 - [25] European Committee for Standardization (CEN) (2005): Eurocode 3 - Design of steel structures - Part 1-8: Design of joints, CEN, Brussels, Belgium.

MECHANICAL CHARACTERIZATION OF AN INNOVATIVE CONNECTION SYSTEM FOR CLT STRUCTURES

Albino Angeli¹, Andrea Polastri², Ernesto Callegari³, Manuela Chiodega⁴

ABSTRACT: This paper presents the numerical-experimental analysis of an innovative connector for CLT structures. The connection system, named X-RAD, has generated a new approach to CLT constructions, characterized by precision and effectiveness. Thanks to the possibility of assembling the X-RAD connectors directly within the factory, the CLT panels can be lifted during the production phases, transported to the construction site and assembled by the use of a sole element represented by the steel elements placed at the corners of the different panels. The X-RAD components in fact are meant to be pre-assembled in the factory by using all-threaded self-tapping screws, so that the system could act as a lifting point for the positioning operations. Several experimental tests are presented and analysed: tests on screws and monotonic tests on different load configurations. The test outcome lead to the mechanical characterization of the connector. X-RAD has been studied also with an analytical approach: the different load configurations have been solved “at limit” condition by the use of equilibrium. The experimental and analytical approach permitted to define respectively the experimental and the analytical capacity domains. Finally a method to verify X-RAD loaded by a generic external load is proposed.

KEYWORDS: innovative connection system, CLT constructions, experimental tests, analytical computation

1 INTRODUCTION

CLT panels have become quite widely employed to build multi-storey buildings: these structures are often characterised by the presence of many different typologies of connection system [1]. Recently innovative connection solutions have been studied [2], [3], [4] in order to create panel to panel, or panel to other material joints and represent an alternative to traditional connections made using shear and hold-down anchors. Moreover, different connectors have been tested in order to define the best way to joint CLT panels [5], [6]. From a structural design and analysis perspective point-to-point interconnection between CLT panels or point-to-point connections at their boundaries leads to less ambiguity in load paths than exists for other approaches. It also lessens the chances that structural systems will not fail in unintended ways if overloaded by force flows through superstructure elements or from superstructures

to foundations. Although buildings of the new typology have already been built there has not been full study of the structural behaviour. The innovative solution herein proposed, named X-RAD, consists of a point-to-point mechanical connection system, fixed to the corners of the CLT panels [7].

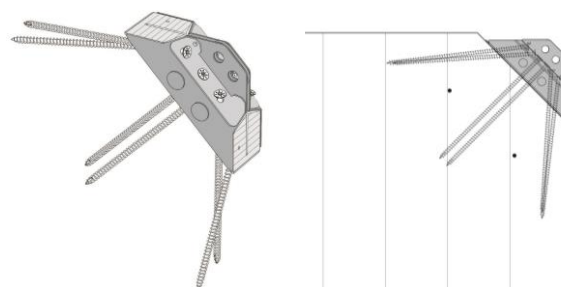


Figure 1: the innovative connector at the CLT panel

This connection, designed to be prefabricated, is comprised of a metal wrapping and an inner hard wood element which are fastened to the panel by means of all-threaded self-tapping screws. Such system permits to reduce significantly the number of bolts/fasteners required to assemble two or more panels together or to connect the panels to the foundation. In order to maximize their withdrawal strength, the all-threaded screws are installed at two different angles of inclination. This implies that the X-RAD joints, where the screws are subjected to a combination of shear and tension forces, are stronger and stiffer than the traditional joints where shear is the predominant action. Thanks to the

¹ Albino Angeli Structural Engineer, Via delle Pozze 7, Commezzadura (TN) Italy

E-mail: ing.albino.angeli@gmail.com

² Andrea Polastri, Research Associate, Trees and Timber Institute - National Research Council of Italy (CNR IVALS), San Michele all'Adige, Italy.

E-mail: polastri@ivalsa.cnr.it

³ Ernesto Callegari, Structural Engineer, DiLEGNO Studio Tecnico Associato, Via Dos Serena, 24 38019 Ville d'Anaunia, Italy.

E-mail: ernesto.callegari@gmail.com

⁴ Manuela Chiodega Pruduct Engineer, Rothoblaas srl Via dell'Adige 2/1 39040 Cortaccia (BZ) Italy

E-mail: manuela.chiodega@rothoblaas.com

characteristic crossed disposition of the fasteners, the X-RAD system is capable of developing the full capacity of both the CLT panels and the all-threaded screws.

2 X-RAD SOLUTIONS

Buildings constructed using CLT technology present a large number of panels interconnected so as to form walls and floors. The wall and floor panels are typically connected using metal elements consisting of thin metal plates fastened with nails to the wooden elements. The function of the nailed plates is to transmit the shear forces (angular brackets) or uplift actions (hold down) Figure 2. The CLT technology also requires the use of a wide range of screws used for example to interconnect the panels of the same storey, especially in the case of floor-floor connection so as to create continuous storey diaphragms. Finally, inclined screws are often used in perpendicular wall-wall connections.

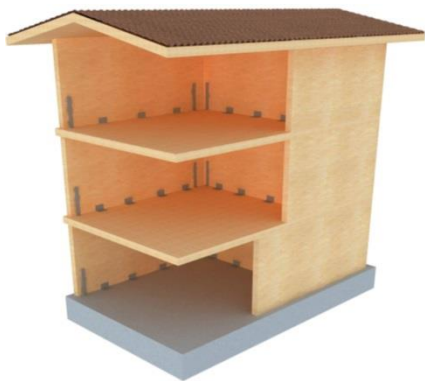


Figure 2: Example of CLT structure assembled using traditional connections (connectors are not drawn to scale)

The X-RAD connection system is a standard connector capable of reacting simultaneously to “shear” and to “uplift” actions thanks to the special 3D layout of the full-threaded screws (Figure 1), as demonstrated in the following paragraphs. Therefore, X-RAD is suitable for replacing both “angular brackets” and “hold down” elements (Figure 4). The advantage deriving from using a single connector, not only increases the amount of prefabrication, but also simplifies connector calculation and verification processes and allows the designer to acquire real control of the structure internal load paths. X-RAD can be used to assemble CLT buildings, as already illustrated by [7], or it can be used to assemble 3D modules that can be connected one to the other very quickly on site, Figure 3. In some cases, the modules can be handled directly by fastening the lifting elements to the X-RAD connection plates. The advantage gained with the use of the X-RAD is that the various modular elements can be assembled as well as disassembled, for example in the case of temporary structures, since connection is achieved using standard steel bolts.

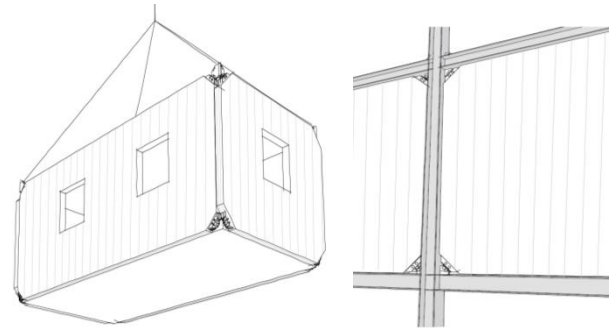


Figure 3: Different possibilities to use X-RAD connector

The X-RAD can also be easily bolted, using simple metal plates, to non-wooden structures such as concrete bracing walls. Obviously, X-RAD is especially suited for connecting CLT panels to steel elements to which it can be bolted: a steel frame with vertical CLT braces is shown in Figure 3.



Figure 4: Example of CLT structure assembled using X-RAD connections (connectors are not drawn to scale)

Figure 5 shows how two X-RAD connectors can be quite simply connected using external plates and standard M16 steel bolts. The X-RAD system uses a series of standard plates for the more common connections, such as wall-foundation or wall-wall connections (for in plane or perpendicular intersections). In the event of non-perpendicular connections between walls or of special requirements, the connection plates should be properly designed.

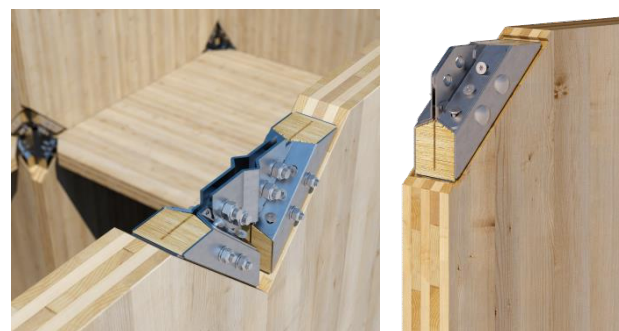


Figure 5: CLT panels connected with X-RAD and bolted steel plates (left) and X-RAD screwed at CLT panel (right)

3 EXPERIMENTAL ANALYSIS

Different extended experimental campaigns were performed in 2013-2015 at the Mechanical Testing Laboratory of CNR-IVALSA, in San Michele all'Adige, in order to characterize the mechanical behaviour of the X-RAD connector.

Tests were conducted on samples in which the X-RAD element was connected to CLT panels as shown in Figure 11. The connector consists of a steel element (external box) and an internal hardwood insert so that it is possible to screw the X-RAD to the CLT panel by means of 6 full-threaded self-tapping screws (VGS 11 mm in diameter and 350 mm in length) [8] inserted both in the predrilled hardwood insert and in the CLT softwood. The X-RAD unit [9] is shown in Figure 6 where it is possible to see the aforementioned external steel box and internal hardwood insert. The figure also shows the central steel plate that is joined to the other parts via two transversal M12 bolts.

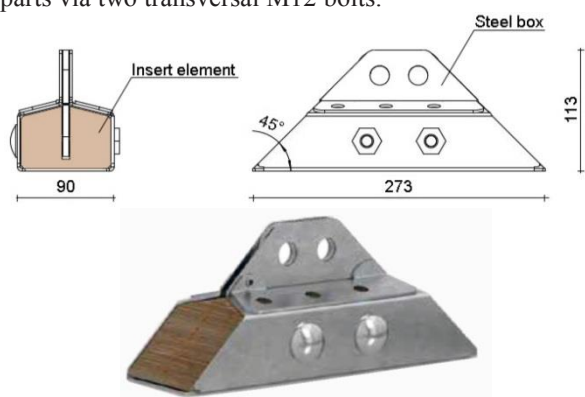


Figure 6: Schematic representation X-RAD connector

3.1 PRELIMINARY TESTS – WITHDRAWAL CAPACITY

A testing campaign was performed with particular focus on determining the maximum withdrawal capacity of different VGS screws typologies driven into different wood elements inserted into a steel tube profile [7].



Figure 7: Specimens after a typical withdrawal failure (above) and after tensile steel failure of the screw (below)

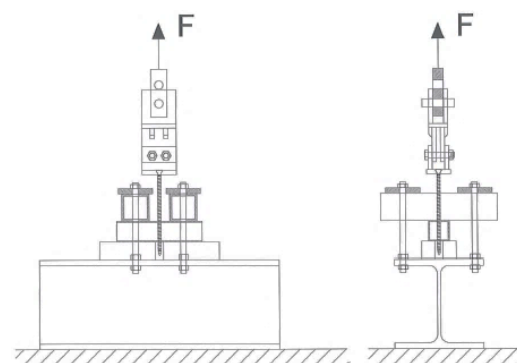


Figure 8: Setup used to test the withdrawal capacity of fasteners, schematic views

The actual insert consists of an element made of beech hardwood LVL (Laminated Veneer Lumber) with mean density greater than 680 kg/m^3 .

Tests represented by Figure 7 and Figure 8 allow to define the withdrawal resistance per length unit, that in case of VGS 11 mm diameter inserted in LVL element, is equivalent to $0,49 \text{ kN/mm}$. Mean withdrawal resistance of used screws driven into the LVL insert, with 70 mm of thread length, is therefore equivalent to 34,5 kN. Screws subjected to compression (in Figure 15 the screws in blue that tend to be expelled from the LVL insert) shall have a resistance value equivalent to the value indicated above, i.e. 34,5 kN. Conversely, screws subjected to tension, red in Figure 15, are capable of providing a resistance equivalent to the screw tensile strength, i.e. 42,0 kN, since the screw head resistance is added to the withdrawal capacity of the resistance mechanism.

3.2 MAIN TESTS – X-RAD CAPACITY

In the last 3 years, a large number of tests on the X-RAD connector have been conducted. Cyclic and monotonic tests were conducted, in particular, at CNR-IVALSA.

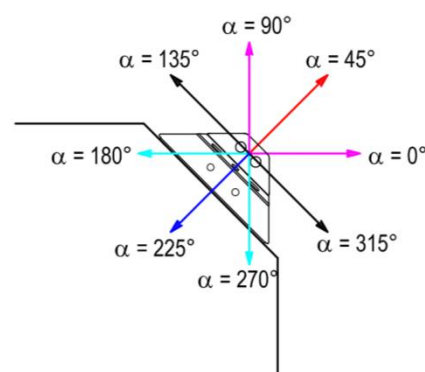


Figure 9: Loading configurations and adopted reference system

The CLT panel used for testing was a typical 3-layer panel with a thickness equal to 100 mm for 45° and $135^\circ/315^\circ$ load configurations while, for load configuration $180^\circ/270^\circ$ and $0^\circ/90^\circ$, 100 mm thick 5-layer CLT panels were used.

The connection system was tested in 5 different loading configurations, see Figure 9; as an example, one of the adopted test setup configurations is shown in Figure 11.

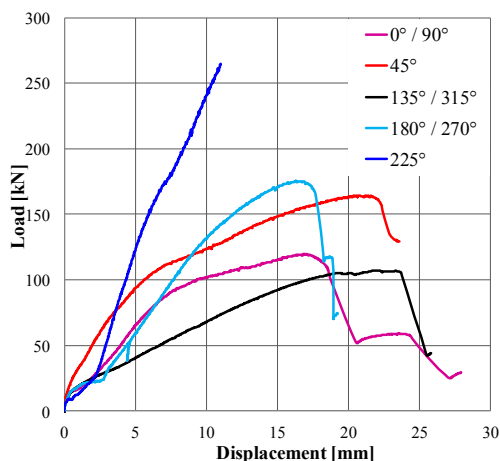


Figure 10: Experimental results in different load configurations, $F-v$ curves

In Figure 10 a comparison between the different mechanical behaviour of the specimens subjected to different external load has been performed. The load configuration 225° , equivalent to pure compression between the base of the connector and the CLT upper face, have not provided real specimen failure, due to the technical limitations of the testing machine maximum load.

Table 1: Experimental results in different load configurations

Angle [°]	N° of specimens	Resistance [kN]
$0^\circ/90^\circ$	6	128,95
45°	15	171,15
$135^\circ/315^\circ$	15	108,95
$180^\circ/270^\circ$	6	185,88
225°	3	289,66

The adopted setup and the measurement instrumentation used during the at failure tests are described in Figure 11.

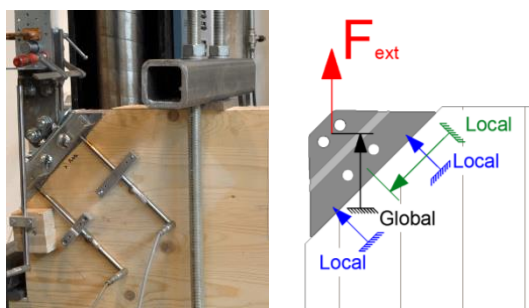


Figure 11: Setup adopted for $0^\circ/90^\circ$ load configuration

In the following, a series of pictures of the tested specimens are reported: it is possible, observing the details proposed in the figures, understand the different failure modes depending on the direction of the imposed external load.

Load configuration $0^\circ/90^\circ$, the failure was reached because of the rupture of the tensile screws (in the bottom part of the Figure 12). Failure mode: tension.



Figure 12: Specimens after the test in $0^\circ/90^\circ$ load configuration

Load configuration $180^\circ/270^\circ$, the failure was reached because of the rupture of the tensile screws (in the upper part of the Figure 13). It is also possible to see the expulsion of the head of the compressed screws (bottom part of Figure 13). Failure mode: combined tension and compression rupture of the screws.



Figure 13: Specimens after the test in $180^\circ/270^\circ$ load configuration

Load configuration 45° presents block tearing failure of the steel part. Load configuration $135^\circ/315^\circ$: as in Figure 13 it is possible to notice both tension (up) and compression (down) failure of screw.

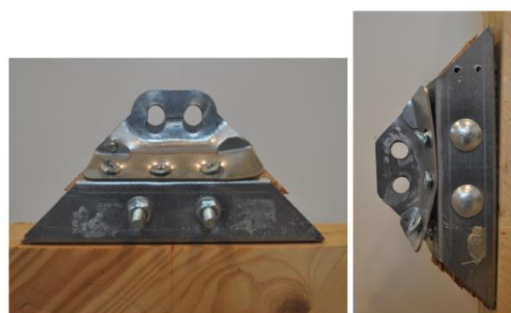


Figure 14: Specimens after the test in 45° (left) and $135^\circ/315^\circ$ (right) load configuration

Results obtained in 45° and $135^\circ/315^\circ$ configurations are in-depth analysed by [10] where are reported also mechanical parameters related to the post-elastic phase.

The different failure modes described above, referred to the different load configurations, are confirmed by the analytical calculations presented in section 4.2.

The specimens were tested in the different possible load configurations that the real connectors may undergo in a whole structure assembled with X-RAD as described in [11].

4 MECHANICAL CHARACTERIZATION

In order to define a complete model for the characterization of the X-RAD mechanical behaviour, different failure analytical models have been implemented. Those models permit, according to the static theorem, by analytical calculation, to define the failure equilibrium in different load configurations. Since the X-RAD is connected with screws that can act both in tension and in compression, it is possible to elaborate simply the "at failure" configuration taking into account the limit capacity of the screws. By way of example, in Figure 15 the "at failure equilibrium" describing two possible load configurations is presented.

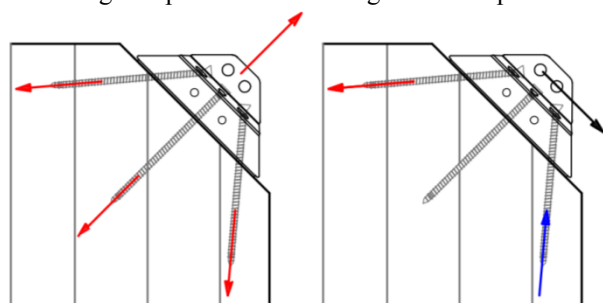


Figure 15: Example of at failure models, in "tension" and in "shear", red screws are in tension, blue in compression

Starting from the analytical failure models, that permit to calculate the ultimate capacity in the different load conditions, it was possible to define a "capacity domain". Two different capacity domains have been defined starting from experimental and analytical results, respectively are presented in Section 4.3.

4.1 CHARACTERIZATION OF MECHANICAL COMPONENTS

4.1.1 Fully threaded screws

Full threaded screws can be subjected by two different actions: tension [12], [13], [14] or compression. As regards screws subjected to tension, experimental outcomes show a steel tension failure mode. Failures due to screw head penetration were not observed since the head of the screw can not penetrate into the insert because the presence of external metal box and another additional metal element (see Figure 6). The calculations shown in paragraph 4.2. assume a mean tension resistance of the screws ($F_{VGS,T}$) equivalent to 42,0 kN derived from manufacturer test outcomes.

Full threaded screws subjected to compression tend to show extraction of the screw head from the top side of the metal box for external load configuration of Figure 15 right. This means that compression is governed by withdrawal resistance of screws from the LVL insert. The calculations shown in paragraph 4.2 assume an average withdrawal resistance $F_{VGS,C}$ equivalent to 34,5 kN. This value has been derived from the results of the tests presented in Section 3.1.

The standards and indications from the literature available to date do not provide values for the

calculation of the screws withdrawal resistance from the CLT panel in the X-RAD geometrical configuration. This because the variability in the panels stratigraphy and the double inclination of the screws are not parameters explicitly reported by the standards. Experimental tests show that, however, when using VGS $\Phi 11 \times 350$ screws for X-RAD connection, screw tension failure or compression failure is never observed in CLT panels. Thanks to the double inclination of the screws, splitting failure is not observed in most cases. In those few cases where CLT failure has been observed, splitting effects occurred due to the presence of load levels close to failure. For this reason, reinforcement with screws driven perpendicular to the panel is recommended, in those cases where the X-RAD is stressed with load values close to the failure domain boundary (Section 4.3).

4.1.2 Steel plates

The metal components of the X-RAD (external metal box and internal plate) consist of a 2,5 mm thick DX51D steel plate for the metal box and a 6 mm thick internal plate, Figure 6. These metal elements are characterised via several tests performed at the CNR-IVALSA Institute, where further tests are scheduled. The experimental campaign has shown a mean yield strength of 348 MPa, while the mean ultimate strength is equal to 429 MPa.

4.1.3 CLT Panels

The CLT resistance in respect to compression inclined to the grain, in the configuration shown in Figure 22, has been defined using the formulas given by Eurocode 5. CLT strength values have been derived from EN 338:2009 In this case characteristic values and not mean values have been considered because, as specified in paragraph 3.2, experimental values are not available yet. Assuming that the CLT panel is composed of C24 elements, the following values are derived: 21,0 MPa for compression parallel to the grain ($f_{c,0}$) and 2,5 MPa for compression perpendicular to the grain ($f_{c,90}$).

4.2 X-RAD CAPACITY AT FAILURE

The static theorem of limit analysis allows to calculate the lower limit (therefore a safety-oriented estimate) of the connection failure load. The equilibrium configurations analysed at the present section have been defined by observing failure mode shown by tests. The failure mechanisms involve the (tensile or compressed) VGS screws or the steel plates (block-tearing type of failure, [15]). The observation resulted in five analytical "at failure" mechanism that can be solved by simple equilibrium equations, in order to calculate the connection capacity.

4.2.1 Case $\alpha=0^\circ/90^\circ$

The limit configuration studied for "at failure" calculation is shown in Figure 16. This failure mechanism can be seen as the overlapping of the two cases seen below, where $R_{0\perp}$ is the load at $\alpha=45^\circ$. $R_{0//}$

instead is the at $\alpha=135^\circ$ load. Observation of the “at failure” samples shows rupture of the tensile screws.

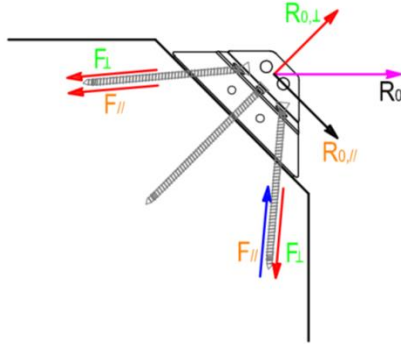


Figure 16: Limit configuration for $\alpha=0^\circ/90^\circ$

Simple equilibrium equations help calculate the resistance of the connection using the following formula:

$$R_0 = 2 \cdot F_{VGS,T} \cdot \sqrt{2} \cdot \left(\frac{1}{2+4 \cdot \sin(\alpha)} + \frac{1}{2 \cdot \cos(\alpha) + 2 \cdot \beta \cdot \cos(\alpha)} \right)^{-1} \quad (1)$$

where:

$$\beta = \frac{F_{VGS,C}}{F_{VGS,T}} = 0,821 \quad (2)$$

In the case under examination, formula (1) results in a capacity value $R_0 = 95,09$ kN.

4.2.2 Case $\alpha=45^\circ$

By observing the samples tested at failure it is possible to define, two different failure mechanisms: the first regards the tension failure of screws (Figure 17), the second is the block tearing failure of the metal box/internal plate system, failure occurs across the $\Phi 16$ bolt holes (Figure 18).

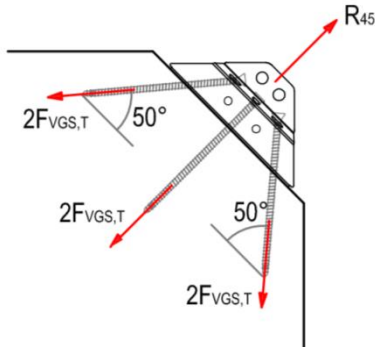


Figure 17: At failure equilibrium for $\alpha=45^\circ$

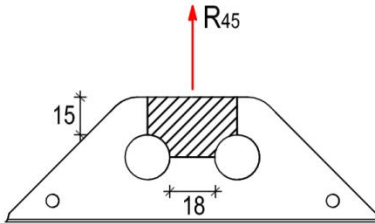


Figure 18: Block tearing mechanism

Solving simple equilibrium equations, it is possible to calculate the screws tension capacity by the following formula:

$$R_{45,VGS} = 2 \cdot F_{VGS,T} + 4 \cdot F_{VGS,T} \cdot \sin(\alpha) \quad (3)$$

According to the Eurocode 3 formula it is possible to calculate the block-tearing capacity

$$R_{45,EC3} = f_u \cdot A_{n,t} + \frac{1}{\sqrt{3}} \cdot f_y \cdot A_{n,v} \quad (4)$$

In this case, formula (3) provides a value of 212,69 kN while formula (4) provides a value equal to 151,24 kN. As confirmed by test results, the failure mode is governed by the weaker mechanism (block tearing) that provides a value $R_{45} = 151,24$ kN.

4.2.3 Case $\alpha=135^\circ/315^\circ$

As seen in the paragraph above, two possible failure modes have to be studied, Figure 19 and Figure 20.

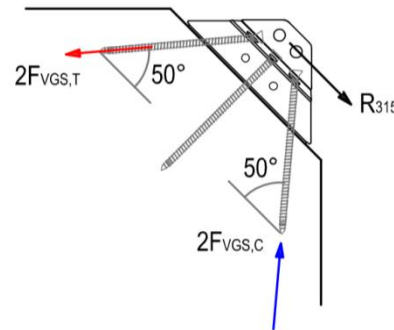


Figure 19: At failure equilibrium for $\alpha=135^\circ/315^\circ$

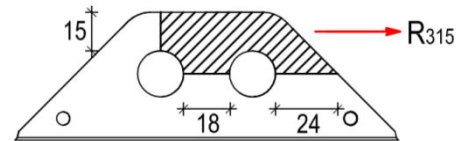


Figure 20: mechanism resistant to block tearing

Experimental outcomes show that failure occurs at the couple of tensile screws. Simple equilibrium equations permit to calculate the screws capacity as given by:

$$R_{315,VGS} = 2 \cdot F_{VGS,T} \cdot \cos(\alpha) + 2 \cdot F_{VGS,C} \cdot \cos(\alpha) \quad (5)$$

By applying the formula indicated in Eurocode 3-1-8, it is possible to calculate the block-tearing resistance

$$R_{315,EC3} = 0,5 \cdot f_u \cdot A_{n,t} + \frac{1}{\sqrt{3}} \cdot f_y \cdot A_{n,v} \quad (6)$$

Formula (5) provides a value of 98,35 kN while formula (6) provides a resistance value equal to 128,21 kN. The weaker mechanism (tension at the screws) is the real failure mechanism that provides a value $R_{315} = 98,35$ kN.

4.2.4 Case $\alpha=180^\circ/270^\circ$

The analyzed “at failure” limit configuration is shown in Figure 21.

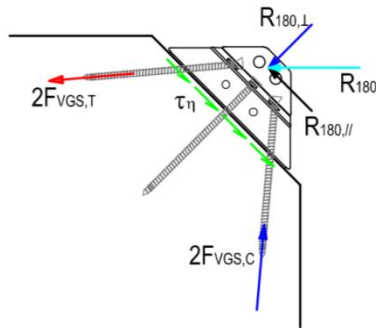


Figure 21: Limit configuration for $\alpha=180^\circ/270^\circ$

Simple equilibrium equations help calculate the tension loading the screws, using the following formula:

$$R_{180} = \sqrt{2} \cdot \frac{(2 \cdot F_{VGS,C} \cdot \cos(\alpha) + 2 \cdot F_{VGS,T} \cdot \cos(\alpha))}{1 - \mu} \quad (7)$$

where μ is the coefficient of friction for X-RAD-CLT contact, assumed to be 0,2. In the case under examination, formula (7) gives a resistance value $R_{180} = 173,85$ kN.

4.2.5 Case $\alpha=225^\circ$

Experimental tests have not provided real specimen failure, due to the technical limitations of the testing machine. The full thread screws resistance is to be integrated with the direct transfer of the X-RAD/CLT compression by contact force. The experimental tests have shown that, thanks to the connectors ductility, the failure displacement levels are such as to involve both resistance mechanisms.

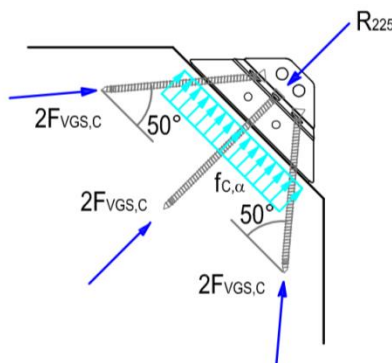


Figure 22: Limit configuration for $\alpha=225^\circ$

The compression between X-RAD-CLT load the CLT fibres at a 45° angle, regardless of the stratigraphic composition of the CLT panel. Using the Eurocode 5 formula it is possible to calculate the compression resistance of the CLT panel.

$$f_{c,\alpha} = \frac{f_{c,0}}{\frac{f_{c,0}}{k_{c,90} \cdot f_{c,0}} \sin^2(\alpha) + \cos^2(\alpha)} \quad (8)$$

By applying the resistance values indicated in paragraph 4.1.3, and assuming a coefficient $k_{c,90}=1,0$, a compression resistance at 45° value $f_{c,45}=4,5$ MPa is obtained. The X-RAD base dimensions are 90 x 273 mm, giving a C_{CLT} compression capacity equals 109,78 kN.

Simple equilibrium equations help calculate the capacity of the whole resistant mechanism.

$$R_{225} = 2 \cdot F_{VGS,C} + 4 \cdot F_{VGS,C} \cdot \sin(\alpha) + C_{CLT} \quad (9)$$

In the case under examination, formula (9) gives a resistance value $R_0 = 284,49$ kN.

4.3 X-RAD CAPACITY DOMAIN

Paragraph 3.2 represents the tests campaign carried out on the X-RAD; the tests were conducted in five different geometric configurations. In paragraph 4.2 the same configurations were analysed using simple analytical “at failure” mechanisms based on the limit calculation. These five analytical case studies are equivalent to the same number of load configurations characterized by different external load inclinations, Fig. 9. Observing the connection geometry and the reference system (Figure 9), thanks to the symmetry it is possible to extend the five geometric configurations to eight angles in the plane.

For this reason, eight resistance values have been defined; these values correspond to eight inclinations of the external force loading the connection. It is possible to obtain a plane figure of the “capacity domain” by connecting with segments the eight known points. The capacity domain defines the failure boundary of the connection. All points, representing possible external loads that falling inside the boundary are load states that the connection is capable of withstanding.

This capacity domain, scaled so as to meet the required safety levels, can be used to verify X-RAD connections (Chapter 5).

4.3.1 Experimental capacity domain

The “experimental capacity domain” is obtained by plotting on a plane the mean experimental resistance values derived considering the “at failure” capacity reached in the different load configuration tests described in Chapter 3.2.

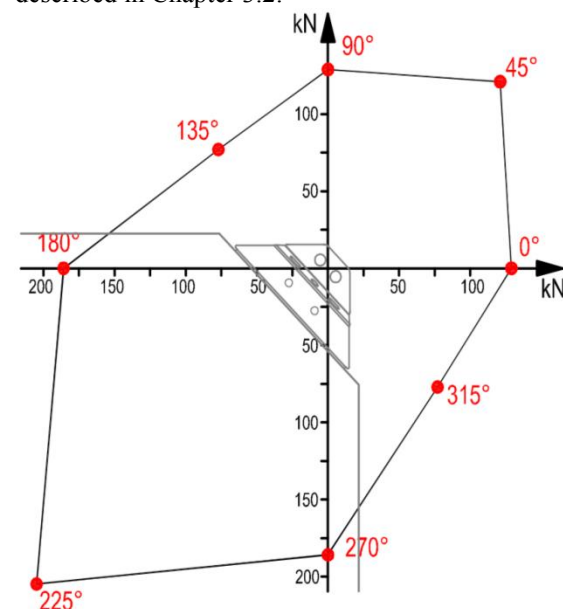


Figure 23: Experimental capacity domain

The domain is developed mainly on the diagonal with a 45°-225° inclination. This means that the connection shows greater resistance values when the single X-RAD is stressed by pure tension ($\alpha=45^\circ$) or by pure compression ($\alpha=225^\circ$) forces. The geometric configurations that envisage pure shear on the X-RAD ($\alpha=135^\circ/315^\circ$) show the lower resistance values. As shown in Figure 23, the higher resistance values are obtained when pure compression stresses ($\alpha=225^\circ$) are applied, where the resistance of the full thread screws is combined with the direct transfer of the X-RAD/CLT compression by contact force. Experimental tests have shown that, thanks to the connector ductility, the levels of failure displacement are such as to involve both resistance mechanisms. In this particular test configuration the limit capacity of the testing machine was reached: for this reason new tests have to be performed.

4.3.2 Analytical capacity domain

The analytical capacity domain, derived from the resistance values calculated in paragraph 4.2, has the same shape of the experimental domain and is shown in Figure 24. Therefore the same qualitative considerations given in the previous paragraph can be observed.

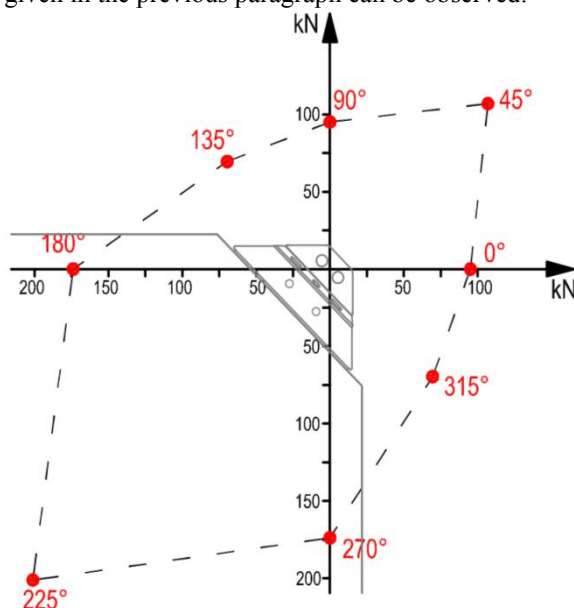


Figure 24: Analytical capacity domain

4.3.3 Comparison between experimental and analytical domain

The comparison between the analytical domain and the experimental one (Figure 25) one shows a good fitting. It is possible to affirm that the configurations 0°/90° and 135°/315° show the larger differences; this discrepancy is due to the fact that, in the real “at failure mechanism”, Figure 19, probably are involved also the central screws loaded at shear. In Section 4.2. all the equilibrium states were written not considering the shear contribution of the screws. A strut and tie model has been adopted but in configurations where, at large displacements, the central screws can exhibit a high shear resistance

(configurations 0°/90° and 135°/315°) this approximation probably is not a realistic hypothesis. More investigations have to be performed.

Table 2: Comparison between experimental and analytical resistances

Angle [°]	Experimental resistance [kN]	Analytical resistance [kN]	Δ [%]
0°	128,95	95,09	-26%
45°	171,15	151,24	-12%
90°	128,95	95,09	-26%
135°	108,95	98,35	-10%
180°	185,88	173,85	-6%
225°	289,66	284,49	-2%
270°	185,88	173,85	-6%
315°	108,95	107,35	-1%

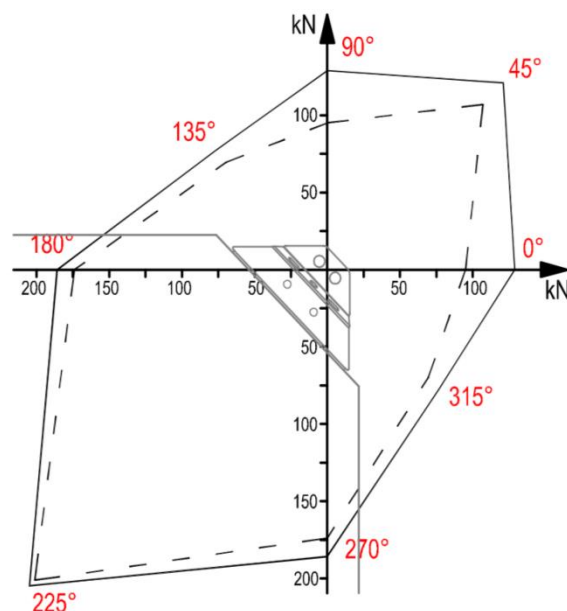


Figure 25: Comparison between experimental and analytical capacity domain

5 DISCUSSION

At the previous paragraph has been defined a capacity domain using the mean resistance values of the X-RAD connectors studied in different load configurations; it is possible in an analog way to define a capacity domain using the characteristic parameters derived from the tests, instead of the mean values.

The definition of the characteristic strength values of the connection allows to calculate the design values. According to the standards it is possible to achieve the design strengths starting from the characteristic values by means γ_M and K_{mod} coefficients.

Using the eight design strengths calculated in the different load configurations it is therefore possible to define a design capacity domain, which can be used to verify of the connection.

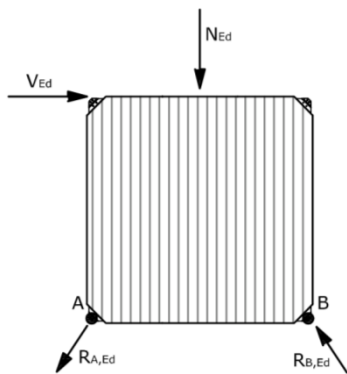


Figure 26: CLT panel loaded by generic external loads and resultant forces on X-RAD connectors

Figure 26 represents a generic panel connected to the foundation through two X-RAD and loaded by two generic external forces: an horizontal force V_{Ed} and a vertical force N_{Ed} . The external loads on X-RAD connectors are named $R_{A,Ed}$ and $R_{B,Ed}$.

In order to verify the X-RAD connection in a generic load configuration [16], such as that described by Figure 26, the following methods are proposed, both based on the capacity domains defined in the Chapter 4.3.

It is possible to perform a graphical verification by representing the external actions on the connector in the capacity domain: if the vector, representing of the X-RAD load, is inside the capacity domain area then the connection is verified (Figure 27).

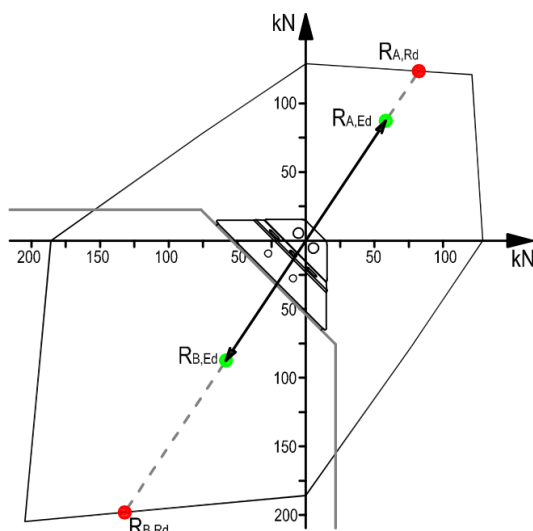


Figure 27: Proposed verification methods

Similarly, it is possible to perform an analytical verification [17] directly by the definition of resistance R_{Rd} connection; this is achieved by extending the R_{Ed} vector until it crosses the border of the capacity domain. The analytical verification is performed by calculating the parameter η by the use of formula 9.

$$\eta = \frac{R_{Ed}}{R_{Rd}} \quad (10)$$

The connector is verified if:

$$\eta \leq 1 \quad (11)$$

6 CONCLUSION

The paper analyze the mechanical behavior of the X-RAD connection elements: the connector is a point-to-point mechanical connection system, designed to be fixed with fully-threaded screws, to the corners of the CLT panels and intended to substitute both the hold downs and the shear angular brackets. The screws are installed at two different angles of inclination, so as to maximize the withdrawal strength by crossing more board layers.

Several experimental tests are presented and analysed: tests on screws and monotonic tests on different load configurations. The test outcome lead to the mechanical characterization of the connector. X-RAD has been studied also with an analytical approach: the different load configurations have been solved “at limit” condition by the use of equilibrium. The experimental and analytical approach permitted to define respectively the experimental and the analytical capacity domains.

The aforementioned strength domain permit the engineer to verify the connector in the different possible load direction acting on the connection system. Advanced FE non-linear models on the whole structure composed by CLT panel connected with the X-RAD have to be performed.

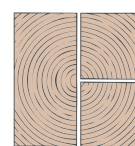
7 ACKNOWLEDGMENTS

The authors wish to thank G. H. Poh'siè, Matteo Izzi, Stefano Pacchioli, Ester Sinito, Francesca Paoloni and the staff of Mechanical Laboratory of CNR-IVALSA Mario Pinna and Diego Magnago. The tests presented in the paper were conducted within the framework of the research project X-REV, proposed and funded by Rothoblaas company and partially financed by the Autonomous Province of Bolzano.

REFERENCES

- [1] Brandner R., Flatscher G., Ringhofer A., Schickhofer G., Thiel A., (2016), Cross laminated timber (CLT): overview and development. European Journal of Wood and Wood Products, 10.1007/s00107-015-0999-5.
- [2] Loss C., Piazza M., Zandonini R., (2015), Connections for steel-timber hybrid prefabricated buildings. Part II: Innovative modular structures. Construction and Building Materials. doi:10.1016/j.conbuildmat.2015.12.001.
- [3] Nakashima S., Kitamori A., Komatsu K., Que Z., Isoda H., (2014), Development and evaluation of CLT shear wall using drift pinned joint. In: Proceeding of the 13th World Conference on Timber Engineering WCTE 2014, Quebec City, Canada.
- [4] Kraler A., Kögl J., Maderebner R., (2014), Sherpa-CLT-Connector For Cross Laminated Timber (CLT) Elements. In: Proceeding of the 13th World Conference on Timber Engineering WCTE 2014, Quebec City, Canada.

- [5] Popovski M., Pei S., van de Lindt J.W. and Karacabeyli E. (2014): Force modification factors for CLT structures for NBCC, Materials and Joints in Timber Structures, RILEM Book Series, 9:543-553, RILEM, Bagneux, France.
- [6] Gavric I., Fragiaco M., Popovski M. and Ceccotti A.: Behaviour of Cross-Laminated Timber Panels under Cyclic Loads. Materials and Joints in Timber Structures, RILEM Bookseries 9:689-702, 2014.
- [7] Polastri A. and Angeli A. (2014): An innovative connection system for CLT structures: experimental-numerical analysis, 13th WCTE, Quebec City, Canada.
- [8] European Organisation for Technical Assessment (EOTA) (2012), Rotho Blaas Self-tapping screws, European Technical Approval ETA-11/0030, Charlottenlund, Denmark.
- [9] European Organisation for Technical Assessment (EOTA) (2015), Rotho Blaas X-RAD, European Technical Approval ETA-15/0632, Vienna, Austria.
- [10] Polastri A., Brandner R., Casagrande D., (2016), Experimental analysis of a new connection system for CLT structures.. Structures and Architecture: Concepts, Applications and Challenges - Proceedings of the 3rd International Conference on Structures and Architecture, ICSA 2016
- [11] Polastri A., Angeli A., Dal Ri G., (2014), A new construction system for CLT structures. In: Proceeding of the 13th World Conference on Timber Engineering WCTE 2014, Quebec City, Canada.
- [12] Bejtka I., Blass H. J., (2002): Joints with inclined screws. Proceeding of the meeting 35 of the Working Commission W18-Timber Structures, CIB.Vancouver, Canada, paper CIB-W18/35-7-5.
- [13] Ringhofer A., Brandner R., Schickhofer G., (2013): Withdrawal resistance of self-tapping screws in unidirectional and orthogonal layered timber products. Materials and Structures. DOI:10.1617/s11527-013-0244-9.
- [14] Tomasi R, Crosatti A and Piazza M (2010) Theoretical and experimental analysis of timber-to-timber joints connected with inclined screws. Construction and Building Materials 24(9): 1560–1571
- [15] European Committee for Standardization, (2005), EN 1993-1-8:2005. Eurocode 3 - Design of steel structures - Part 1-8: Design of joints. CEN, Brussels, Belgium.
- [16] Pozza L., Scotta R., Trutalli D., Polastri A., Smith I., (2016), Experimentally based q-factor estimation of CLT walls. Proceedings of the Institution of Civil Engineers: Structures and Buildings, doi: 10.1680/jstbu.15.00009
- [17] European Committee for Standardization, (2014), EN 1995-1-1:2004+A2:2014. Eurocode 5 - Design of timber structures, Part 1-1, General - Common rules and rules for buildings. CEN, Brussels, Belgium.



EXPERIMENTAL CAMPAIGN FOR THE MECHANICAL CHARACTERIZATION OF CONNECTION SYSTEMS IN THE SEISMIC DESIGN OF TIMBER BUILDINGS

Daniele Casagrande¹, Andrea Polastri², Tiziano Sartori³, Cristiano Loss⁴, Manuela Chiodega⁵

ABSTRACT: The seismic behaviour of timber buildings is strongly related to the energy dissipation capacity of connections. According to Standard, since timber is characterized by a brittle failure when subjected to tensile or bending actions, the dissipative zones shall be located in joints and connections, whereas timber members themselves shall be regarded as behaving elastically. In order to ensure the global structural ductility, connections and joints shall be able to deform plastically at the associated ductility level without a significant reduction of their resistance under cyclic loads. The paper deals with an experimental campaign for the mechanical characterization of timber connection systems, commonly adopted in Europe, in the seismic design of timber buildings. The main objective was to find out the capacity, the stiffness and the ductility of the tested connections and to investigate their loss of capacity under cyclic loads. The obtained results were analysed in order to understand if the current provisions, reported in Standard for the different typology of traditional connectors, can be adopted in case of connection systems used for seismic purposes, such as hold-down or angle brackets. Their interaction with other structural parts was then investigated testing six full-scale timber walls, subjected to monotonic and cyclic loads. The tests were carried out at the Laboratory of Materials and Structural Testing of the Trento University (Italy).

KEYWORDS: experimental tests, seismic, connections, mechanical devices

1. INTRODUCTION

In last years, an important role in the construction market of Mediterranean Area has been achieved by timber buildings. Countries in this area, differently from Northern European ones, are characterized by a low tradition in the construction of timber buildings and, at the same time, by a high seismic hazard. For this reason, particular attention must be paid in the design of earthquake-resistant timber buildings [1].

The tradition approach in seismic engineering is based on the seismic energy dissipation, which should be achieved in specific zones of the buildings. These are designed in order to be able to deform plastically at an appropriate ductility ratio without a significant reduction of their resistance under repeated cyclic loads.

Since timber is to be considered as a brittle material when subjected to tensile or bending loads, the energy dissipation is to be achieved in mechanical joints and connections by means of the metal fasteners plasticization and the embedment of timber at the

interface with the fasteners. In section 8 of European Standard EN 1998-1 [2] some provisions are provided in order to ensure a correct design of timber buildings and hence a suitable ductility and energy dissipation capacity.

It is explicitly required that *“In order to ensure that the given values of the behaviour factor may be used, the dissipative zones, specified in the capacity design rules for each structural type, shall be able to deform plastically for at least three fully reversed cycles at a static ductility ratio reported in Table 8.3, (equal to 4 and 6 for a medium and ductility class respectively) without more than a 20% reduction of their resistance between the first and third cycles envelope curve”*. In addition, simplified provisions, based on the check of the ratio between the fastener diameter and the timber element thickness, are reported to ensure the previous requirement. Furthermore, the non-dissipative connections and timber elements need to be designed according to the capacity design approach ([3],[4],[5]).

2. OBJECTIVE

The work presented in this paper deals with the experimental investigation of some mechanical connection systems, which nowadays are commonly adopted in seismic areas.

The main objective was to find out the capacity, the stiffness and the ductility of the tested connections and to investigate their loss of capacity under cyclic loads, in

¹ Daniele Casagrande, University of Trento – Italy
daniele.casagrande@unitn.it

² Andrea Polastri, CNR Ivalsa – Italy
andrea.polastri@cnr.ivalsa.it

³ Tiziano Sartori, ReWiS Engineering – Italy,
tiziano.sartori@rewis.it

⁴ Cristiano Loss, University of Trento – Italy,
cristiano.loss@unitn.it

⁵ Manuela Chiodega Prudent Engineer, Rothoblaas srl – Italy
manuela.chiodega@rothoblaas.com

order to understand if they are, or not, in accordance with the current provisions reported in Standard. In most cases, in fact, technical documents of these products (European Technical Approval) are simply related to the strength properties. No specific reference regarding their stiffness or ductility is available. However, a correct design of timber buildings cannot be performed without the knowledge of these parameters.

Stiffness is, in fact, the key-parameter in the linear structural analysis [6], especially when numerical modelling ([7], [8], [9], [10], [11]) is used to predict the dynamic properties of the buildings (i.e. natural frequencies), the distribution of horizontal forces between structural elements (i.e. shear walls) as well as the inter-storey drifts. On the contrary, the ductility and the strength-reduction under cyclic loads become the fundamental parameters in those connections designed in order to dissipate the seismic energy. Their capacity to ensure a suitable plastic deformation is, in fact, strongly related to the seismic reduction factor.

Six full-scale timber walls were then tested under monotonic and cyclic loads. Both Cross-laminated Timber (CLT) and Light-Timber Frame (LTF) walls were investigated. The tested walls were assembled with the connection systems investigated in the previous part of the research campaign in order to determine a relation between the local mechanical properties of connections/mechanical devices and the global behaviour of the walls.

3. THE SEISMIC-REV PROJECT

All experimental tests were carried out at the Laboratory of Materials and Structural Testing of the Trento University (Italy) under the Seismic X-REV project, within a scientific partnership between the Timber Research Group of the University of Trento, the CNR IVALLSA Institute and the Rothoblaas Company.

The experimental campaign was conceptually divided into three different phases. Firstly, 40 tests were carried out on timber-to-timber, steel-to-timber and sheathing-to-timber connections. Secondly, hold-downs and angle brackets, typically used to anchor timber walls to the foundation were investigated: an amount of 21 tests were performed. Lastly, 6 full-scale timber walls were tested. The same mechanical devices tested in previous phases were used to anchor the walls to the setup steel basement.

The tests were carried out according to the testing protocols provided by the European Standards. During the monotonic tests, a displacement control was adopted with a constant rate of 0.05 mm/s up to the failure condition of the specimen. On the contrary, for the cyclic loading tests, different rates were used depending on the cycle amplitude.

The mechanical parameters of the tested specimens were obtained from the force vs displacement curves of monotonic tests, according to the European Standard EN 12512 [12]. These are: the maximum load F_{max} , the displacement corresponding to the ultimate load v_u , the displacement corresponding to the maximum load v_{max} ,

the elastic stiffness K_{ser} , the yield displacement v_y and the static ductility μ_s .

For cyclic tests the strength reduction between the first and the third cycle at a certain displacement was evaluated. In European Standard for seismic design of buildings [1], in fact, it is required that a mechanical connection in dissipative zones shall be able to deform plastically for at least three fully reversed cycles at a static ductility ratio equal to 4 and 6, without more than a 20% reduction of their resistance between the first and third cycles envelope backbone curve, for high ductility and medium ductility classes respectively. It is important to highlight that this provision can be directly adopted in case of connections (nails, screws, dowels, bolts) and not in the case of mechanical devices (hold-downs, angle brackets).

In case of mechanical devices it is necessary to take into account that the steel-to-timber connection is to be regarded as a dissipative zone, whereas the other components (such as plates or anchoring bolts) should be designed with an adequate over-strength.

Connectors are meant the metallic fasteners used to connect two timber elements or a steel plate or device with a timber element (Figure 1). Since they are made of steel, a ductile behaviour is expected with the formation of plastic hinges able to deform plastically under cyclic loads without a significant strength reduction.

Connection is the term used to describe the connectors and the two elements connected (timber elements and steel plates). Depending on the geometrical and mechanical properties of the connectors and the connected elements, different behaviours may be achieved. Connection system (or mechanical device) is the term used to describe the entirety of the device, including all connectors and other parts.

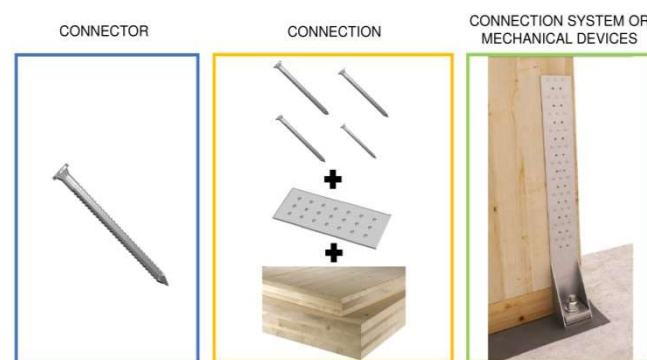


Figure 1: Connector, connection and mechanical device

4. EXPERIMENTAL TESTS ON CONNECTIONS

In this section the tests on timber-to-timber and timber-to-steel connections are described. In all tests the direction of load acting on connectors was parallel to the glulam element grain. Monotonic (M) and Cyclic (C) were carried out (Figure 2, 3, 4 and Table 1, 2, 3).

Two types of timber-to-timber connections were tested. The first one is represented by a sheathing-to-framing connection made of two 15 mm thick OSB/3 panels, a 160x80 mm solid wood vertical stud and 14 fasteners (7 for each panel). 2.8x80 mm ring nails, 4.5x45 HBS and 5x50mm LBS screws were tested with a spacing of 50 mm. These tests were designed in accordance with the results reported in [7].

Table 1: tests on sheathing-to-framing connections

Test ID	#	Fasteners [mm]	Spacing [mm]	Incl.
OSB 2.8X80_M	1	14 ring nails 2.8x80	50	90°
OSB 2.8X80_C	2	14 ring nails 2.8x80	50	90°
OSB 4.0X45_M	1	4.0x45 14 HBS screws	50	90°
OSB 2.8X80_C	2	14 HBS screws 4.0x45	50	90°
OSB 5.0X50_M	1	14 LBS screws 4.0x45	50	90°

The second type of tested connection is made with two glulam elements connected by vertical and/or 45° inclined screws. 160 mm length HBS screws with a diameter of 6, 8 and 10 mm were used in case of “vertical screw” tests, whereas 9x280 VGZ fully-threaded screws were adopted in the case of “45° screws”.

Table 2: tests on screws timber-to-timber connections

Test ID	#	Screws (mm)	Spacing (mm)	Incl.
HBS_6x160_M	2	6x160 - 5 HBS	90	90°
HBS_6x160_C	2	6x160 - 5 HBS	90	90°
HBS_8x160_M	1	8x160 - 3 HBS	140	90°
HBS_8x160_C	2	8x160 - 3 HBS	140	90°
HBS_10x160_M	1	10x160 - 3 HBS	140	90°
HBS_10x160_C	2	10x160 - 3 HBS	140	90°
VGZ_9x280_M	1	9x280 - 2 VGZ	-	+/-45°
VGZ_9x280_C	2	9x280 - 2 VGZ	-	+/-45°
VGZ_9x280_T_M	1	9x280 - 2 VGZ	-	+/+45°

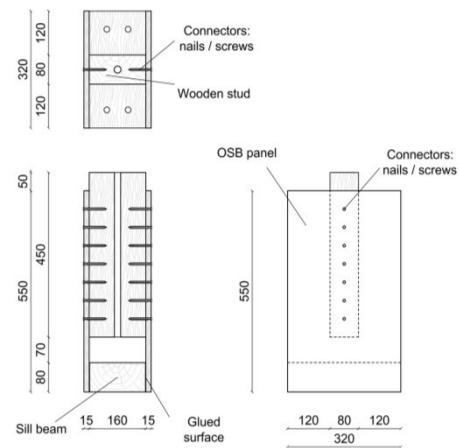


Figure 2: geometrical properties of specimens for sheathing-to-framing connection tests

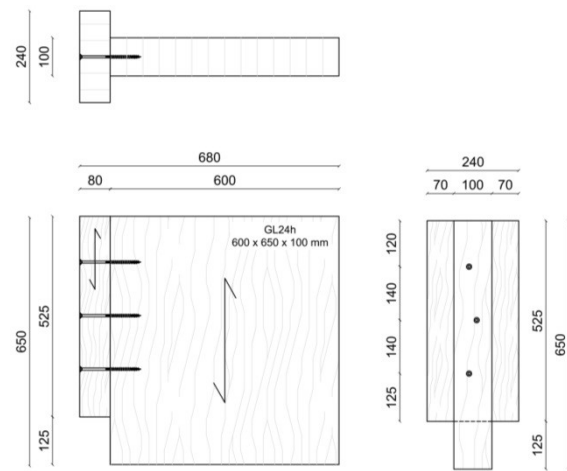


Figure 3: geometrical properties of specimens for screwed timber-to-timber connection tests

The timber-to-steel connections were composed of a glulam element and a steel plate with different thickness (1.5, 3 and 4 mm) whereas the fasteners were 4x60 mm Anker Nails and 5x50 mm LBS screws.

Table 3: tests on timber-to-steel connections

Test ID	#	Fasteners	Plate thickness
A4x60_1.5_M	1	4x60 mm 8 Anker nails	1.5 mm
A4x60_3_M	1	4x60 mm 8 Anker nails	3 mm
A4x60_3_C	2	4x60 mm 8 Anker nails	3 mm
A4x60_6_C	1	4x60 mm 8 Anker nails	6 mm
LBS5x50_1.5_M	1	5x50 mm 8 LBS screws	1.5 mm
LBS5x50_3_M	1	5x50 mm 8 LBS screws	3 mm
LBS5x50_3_C	2	5x50 mm 8 LBS screws	3 mm
LBS5x50_6_C	1	5x50 mm 8 LBS screws	6 mm

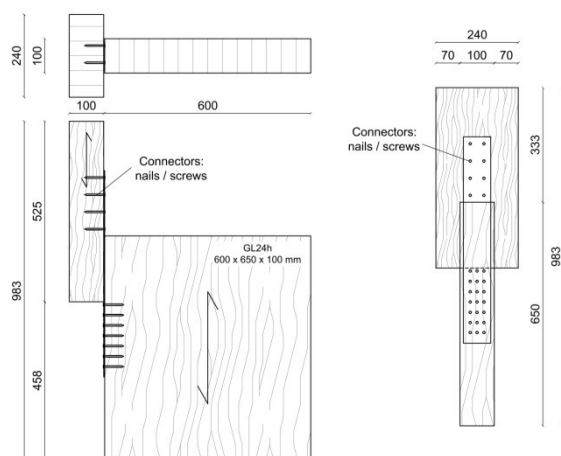


Figure 4: geometrical properties of specimens for steel-to-timber connection tests

The setup of all connection tests was composed of two vertical HEM 120 steel profiles connected by a UPN 40 profile placed on the steel base reaction frame (Figure 5). The setup of all connection tests was made with the aim of reproducing a vertical roller (using polyzene, steel profiles and steel plates, see Figure 5)

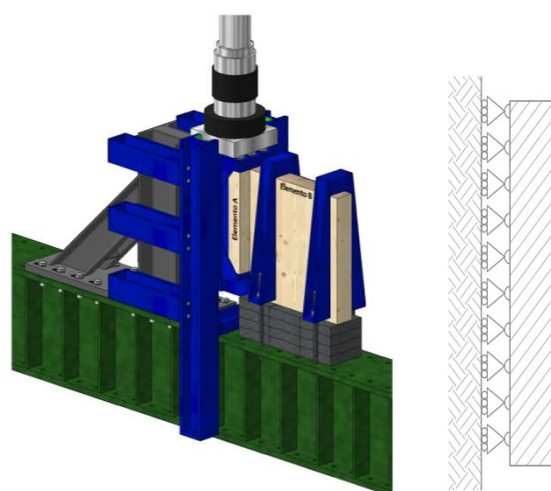


Figure 5: test set-up for timber-to-timber connections tests (left) and set-up schematization

5. EXPERIMENTAL TESTS ON MECHANICAL DEVICES

The mechanical behaviour of angle-brackets and hold-down devices were tested under monotonic (M) and cyclic loads (C). Hold-down devices were subjected to a tensile load only, whereas angle brackets were tested under shear (S) or, tensile (T) loads, see Figure 6 and 7. In this project was in fact studied the capacity of angle bracket devices to bear tensile loads which usually are absorbed by hold downs.

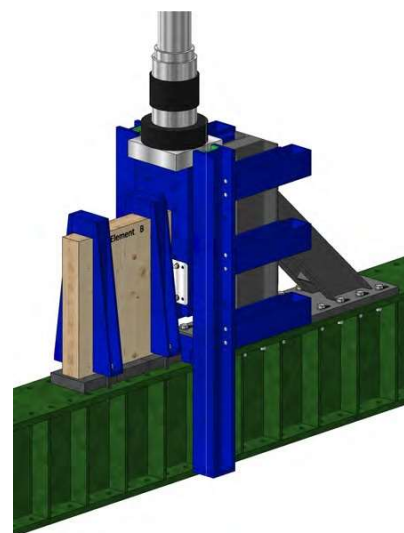


Figure 6: shear test on TCF 200 angle bracket

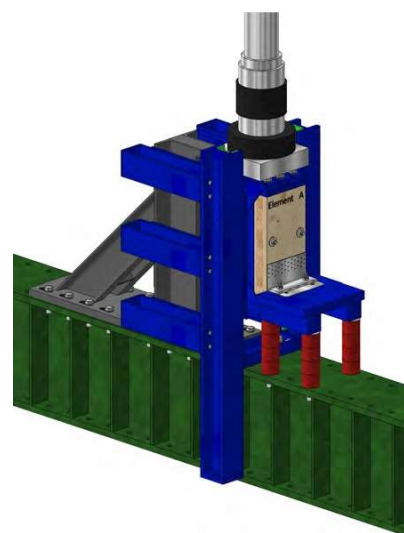


Figure 7: tensile test on TCN 240 angle bracket

Hold-downs were connected to the CLT specimen by means of 4x60 mm Anker nails with the aim of simulating a wall tensile anchoring to the foundation. The same typology of nails was adopted for angle brackets.

Three hold-down devices were tested, namely WHT 340, WHT 440 WHT 620, characterized by 20, 30 and 55 nails, respectively. An additional test was performed with WHT 620, using a partial fixing with 33 fasteners (differently from the previous tests not all the holes of the hold-down were nailed).

Angle brackets TCF 200 and TTN 200 were tested under shear load for CLT-to-CLT and CLT-to-steel connection respectively. The angle bracket TCN 240 was, on the contrary, tested under a tensile load (Figure 6). All the angle brackets were connected by means of Anker 4x60 nails.

These tests were designed in accordance with the results reported in [14]. The same set-up of connections specimens was adopted for the tests reported in Table 4.

Table 4: tests on mechanical devices

Test ID	#	Devices	Load	Nails
TCF200_M	1	TCF200	Shear	30
TCF200_C	2	TCF200	Shear	30
TTF200_M	1	TTF200	Shear	30
TTF200_C	2	TTF200	Shear	30
TCN240_M	1	TCN240	Tensile	36
TCN240_C	2	TCN240	Tensile	36
WHT340_M	1	WHT340	Tensile	20
WHT340_C	2	WHT340	Tensile	20
WHT440_M	1	WHT440	Tensile	30
WHT620_M	1	WHT620	Tensile	55
WHT620_P_M	1	WHT620	Tensile	33
WHT620_P_C	2	WHT620	Tensile	33

6. EXPERIMENTAL TESTS ON FULL-SCALE WALLS

In order to investigate the interaction between the local mechanical behaviour (Section 4 and Section 5) with the global behaviour of timber shear walls, 6 full-scale tests (CLT and LTF) were performed (Table 5). The relationship between the connection ductility and wall ductility was analysed depending on the mechanism failure achieved.

The walls were subjected simultaneously to a horizontal force and a uniform vertical load, equal to 20 kN/m, representing the seismic force and the gravitational load respectively. The walls were tested with the reaction frame in Figure 8.



Figure 8: shear wall test set-up

All the tested walls were 2.5 m long and 2.5 m high. The Light Timber Frame (LTF) walls, sheathed with OSB panels, were 190 mm thick whereas the Cross-Laminated Timber (CLT) walls were composed of 3 layers with a total thick of 100 mm.

The timber frame of the LTF walls was made of solid timber members. The lateral vertical studs had a section of 100x160 mm. The top and the bottom plate section

was of 60x160 mm. The five vertical studs were placed with a constant spacing (Figure 9).

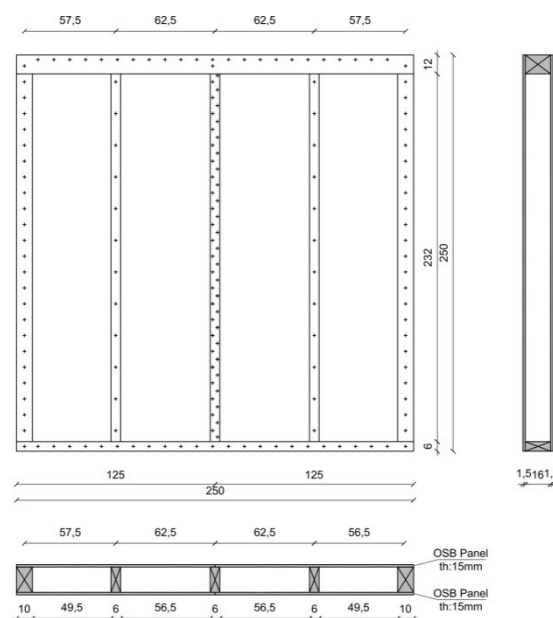


Figure 9: LTF shear wall

The OSB panels had dimensions of 1250x2500 mm and were 15 mm thick. Two panels for each side were used to sheath the wall. The sheathing OSB panels were connected to the timber frame with 2.8x80 mm nails and a spacing of 100 mm on the edge of the panels and of 200 mm on the stud along the centre of the panel. The anchoring against tensile loads was made with WHT 620 hold downs (with partial fixing – 33 Anker 4x60 nails) for LTF walls and the two first CLT walls. Two TCN 200 were used to prevent the sliding of the walls.

The last 2 tests on CLT walls were carried out adopting 4 TCN 240 angle brackets with proper washers; no hold down connectors were used; the tensile anchoring was made with the angle brackets positioned at the corners of the wall (Figure 10).



Figure 10: Detail of anchoring devices for CLT_TITAN_M and CLT_TITAN_M tests

Table 5: tests on full scale walls

Test ID	#	Hold-Down (at each corner)	Angle brackets
LTF_M	1	WHT 620 Part.	2 TCF 200
LTF_C	1	WHT 620 Part.	2 TCF 200
CLT_M	1	WHT 620 Part.	2 TCF 200
CLT_C	1	WHT 620 Part.	2 TCF 200
CLT_TITAN_M	1	TCN 200	2 TCN 200
CLT_TITAN_C	1	TCN 200	2 TCN 200

A load cell (LC) was used to measure the force applied by the hydraulic jack. The top wall horizontal displacement, the wall rigid sliding and the uplift of the wall corners were measured by means of Linear Variable Displacement Transducers (LVDTs) whereas the diagonal deformation of the wall was monitored by two wire potentiometers (WP), see Figure 11.

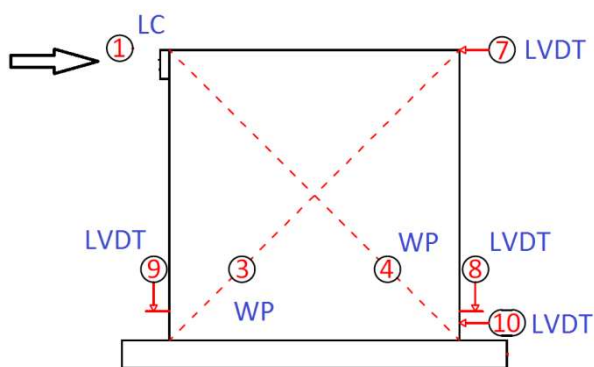


Figure 11: shear wall test measuring set-up

7. TEST RESULTS

For each specimen the maximum load F_{max} , the displacement corresponding to the ultimate load v_u , the displacement corresponding to the maximum load v_{max} , the elastic stiffness K_{ser} , the yield displacement v_y , the static ductility μ were obtained from monotonic tests. The ductility class (DC) at the third cycle for a displacement of $4 v_y$ and $6 v_y$ (when these were reached) was analysed for connections and mechanical devices from cyclic tests. When the strength degradation resulted lower than 20% for a displacement of $4 v_y$, the connection, or the mechanical device, was considered as dissipative zone in a medium ductility class (M). On the contrary, when the strength degradation resulted lower than 20% for a displacement of $6 v_y$, the connection or the mechanical device was considered as dissipative zone in a high ductility class (H). In case that the ultimate displacement was lower than $4 v_y$ or the two previous provisions were not satisfied, the connection was not assumed as a dissipative zone (L).

7.1 CONNECTION TESTS

The results of the sheathing-to-framing (Table 6), timber-to-timber (Table 7) and steel-to-timber (Table 8) connections are reported dividing the experimental values of F_{max} and K_{ser} by the number of connectors.

Table 6: sheathing-to-framing connection results

Test ID	F_{max} [kN]	K_{ser} [N/mm]	v_y [mm]	v_u [mm]	μ [-]	DC [-]
OSB 2.8X80	1.36	550	1.28	27.51	21.5	H
OSB 4.0X45	1.67	500	1.60	21.7	13.6	M
OSB 5.0X50	2.2	916	0.80	21.2	26.5	-

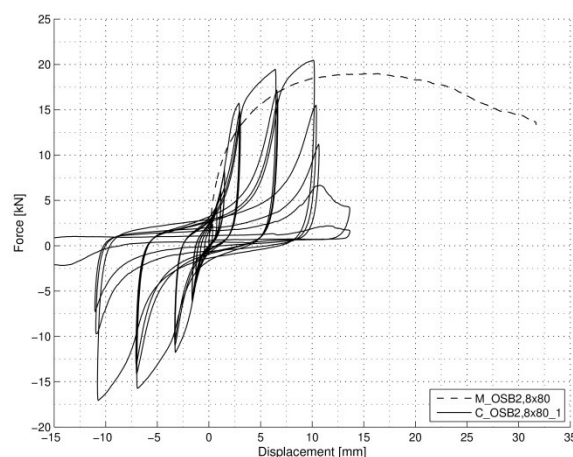


Figure 12: Force vs displacement curves for monotonic and cyclic load tests for OSB 2.8x80 specimens

All specimens showed a significant ductility capacity under monotonic loads. OSB 5x50 and OSB 4x45 tests were characterized by the same ultimate displacement but the former was characterized by a much higher stiffness.

However, it is important to highlight that in the case of screws ($d=4.0$ mm and 5.0 mm) a larger wood element is required in order to satisfy the edge distance prescriptions according to Standards [15]. 2.8×80 ring nails (Figure 12) and 4.0×45 HBS screws are characterized by similar strength and stiffness. However, nails showed a much higher ductility and satisfy the prescriptions for a HDC design approach whereas HBS 4.0×45 can be used only for a MDC design approach.

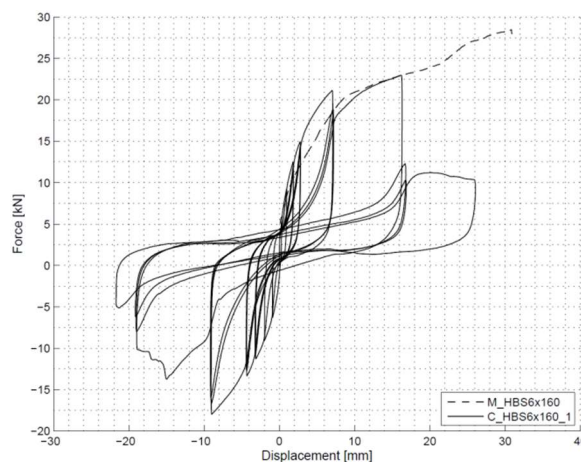


Figure 13: Force vs displacement curves for monotonic and cyclic load tests for HBS 6x60 timber-to-timber specimens

Table 7: timber-to-timber connection

Test ID	F_{max}	K_{ser}	v_y	v_u	μ	DC
	[kN]	[N/mm]	[mm]	[mm]	[-]	[-]
HBS 6x160 M 1	5.6	753	3.8	30	7.9	L
HBS 6x160 M 2	7.2	750	5.2	29.6	5.7	L
HBS 8x160 M	6.2	1716	1.6	30	18.8	H
HBS 10x160 M	8.8	1150	2.8	30	10.7	H
VGZ 9x280 M 1	18.17	14365	1	2.8	2.8	L
VGZ 9x280 M T	26.32	20929	1.2	5.0	4.33	-

As expected, a higher ductility was obtained in case of screws under a shear load (HBS screws) than 45° inclined screws. However, 45° inclined screws showed larger stiffness and strength. 8 and 10 diameter HBS screws are in accordance with HDC requirements. Despite their small diameter and their high static ductility, 6 diameter screws showed a brittle failure under cyclic loads (Figure 13). The main reason is due to the mechanical properties of the steel: to ensure a sufficient strength in the screwing phase, the yield strength of steel has to be particularly high. However a significantly decrease of oligo-cycle fatigue was observed. As a result, the capacity of connectors under oligo-cycle loads should be verified by means of specific tests when they are intended to be used as dissipative connections.

Table 8: steel-to-timber connection results

Test ID	F_{max}	K_{ser}	v_y	v_u	μ	DC
	[kN]	[N/mm]	[mm]	[mm]	[-]	[-]
A4x60 1.5	3.04	678	3.49	15.81	4.53	-
A4x60 3	3.49	853	2.46	16.23	6.60	H
A4x60 6	-	-	-	-	-	H
LBS5x50 1.5	4.75	325	12.02	30	2.50	-
LBS5x50 3	3.25	1043	1.93	10.34	5.36	H
LBS5x50 6	-	-	-	-	-	H

All connections can be considered as dissipative zones according to a HDC approach. In case of a steel plate with a thickness of 3 mm, LBS 5x50 screws showed a higher stiffness and strength but a lower ductility than Anker nails 4.0x60 (Figure 14). Because of a significant rope-effect, LBS screws tested with a steel plate with a thickness of 1.5 mm were characterized by a higher strength but with a significantly lower stiffness and ductility than the steel plate test with a thickness of 3 mm.

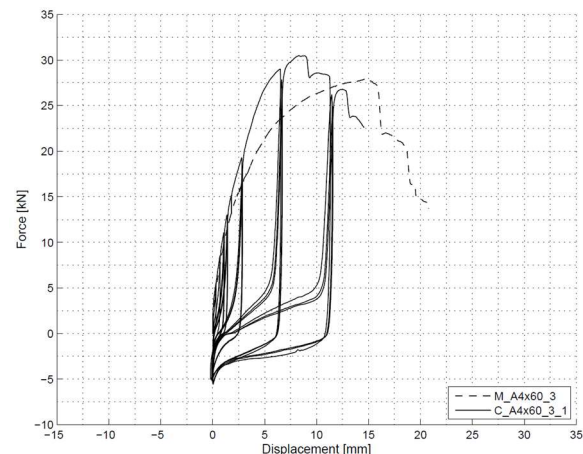


Figure 14: Force vs displacement curves for monotonic and cyclic tests for Anker nails 4.0x60 3 mm thick steel plate specimens

7.2 MECHANICAL DEVICES TESTS

Low and medium values of ductility were obtained for all mechanical devices with the exception of TCN 240 angle bracket under a tensile load (Table 9). This angle bracket showed significant values of strength as well as stiffness, becoming a valid alternative to traditional hold-down devices (Figure 15).

Table 9: mechanical devices results

Test ID	F_{max}	K_{ser}	v_y	v_u	μ
	[kN]	[N/mm]	[mm]	[mm]	[-]
TCF 200	41.03	8479	4.23	7.40	1.75
TTF 200	70.04	8945	6.45	26.07	4.04
TCN 240 (Tensile)	93.80	28455	2.30	18.40	8.00
WHT340	60.19	5705	8.92	21.2	2.37
WHT440	78.14	6609	9.28	28.47	3.07
WHT620*	107.32	13247	6.38	20.7	3.24
WHT620 P	100.08	9967	7.94	30.00	3.78

The partial fixing (see Section 5) of WHT 620 hold-down did not cause a significant reduction of strength with an increasing of ductility. However, the failure mechanism of WHT620 was characterized by the brittle tensile breakage of the steel plate. As a result, in seismic regions the partial fixing is recommended.

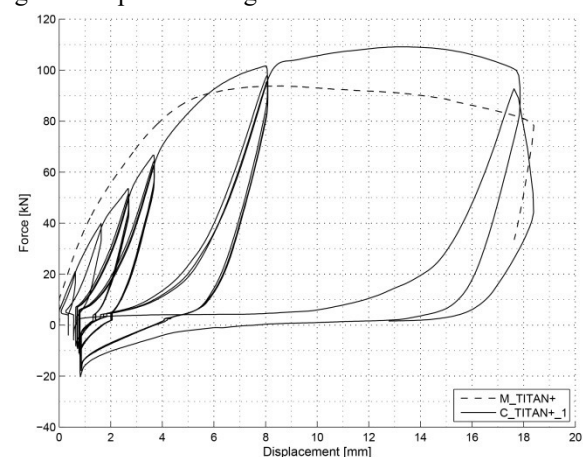


Figure 15: Force vs displacement curves for monotonic and cyclic tensile load tests for TCN 240 angle brackets

The partial fixing (see Section 5) of WHT 620 hold-down did not cause a significant reduction of strength with an increasing of ductility. However, the failure mechanism of WHT620 was characterized by the brittle tensile breakage of the steel plate. As a result, in seismic regions the partial fixing is recommended.

7.3 WALL TESTS

CLT walls showed higher values of strength and stiffness but lower values of ductility than LTF wall (Table 10). In CLT walls the mechanism failure was associated with hold-down failure (Figure 16) whereas in LTF with sheathing-to-framing connection failure.

Table 10: wall tests results

Test ID	F_{max}	K_{ser}	v_y	v_u	μ
	[kN]	[N/mm]	[mm]	[mm]	[-]
LTF	93.9	3454	18.9	71.89	3.80
CLT	138.4	5796	19.46	37.15	1.91
CLT TITAN	149.3	9445	13.5	33.30	2.53

Therefore, since sheathing-to-framing connection which, as previously reported, is characterized by a higher static ductility than hold-down devices, a higher ductility of the LTF wall than the CLT walls was observed. The use of TCN 200 as hold-down device show a significant increasing of stiffness as well as of ductility of the CLT wall.

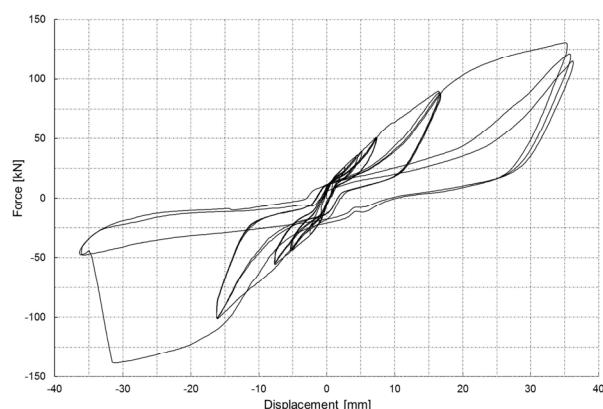


Figure 16: Force vs displacement curves for CLT wall's cyclic test

8. CONCLUSIONS

In this paper, an experimental campaign for the mechanical characterization of connection systems commonly adopted in Europe in the seismic design of timber buildings was presented. Different results were obtained in terms of stiffness, strength, ductility and oligo-cyclic capacity of connectors and connection systems largely adopted in the seismic design of timber-frame as well as CLT buildings, in accordance with Eurocode 8

From the tests on 6 mm diameter screws under a lateral load, it was highlighted how the oligo-cycle fatigue capacity was not achieved despite the ratio between the screw diameter and the timber element thickness was in

accordance with the Standard prescription. As a result, oligo-cycle fatigue load tests should be performed on fasteners in order to ensure a sufficient energy dissipation under cyclic loads. Tensile tests on TCN 240 showed how this kind of angle brackets can be adopted as an excellent alternative to hold-down devices in timber shear walls. Lastly, a partial fixing of the WHT 620 Hold-down device should be preferred in order to achieve a higher ductility when hold-down devices are assumed as dissipative connections as in case of CLT walls.

9. ACKNOWLEDGMENT

The presented research was developed within the X-REV research project funding by the Province of Bolzano (Italy) and Rothoblaas Company. A special thank also goes to the staff of the Laboratory of Materials and Structural Testing of the University of Trento.

10. REFERENCES

- [1] Piazza, M., Zanon P. and Loss C. (2015). Timber structures. In The state of Earthquake Engineering Research in Italy: the ReLUIS-DPC 2010-2013 Project, edited by G. Manfredi and M. Dolce, 143-172 Napoli (Italy): Doppiavoce. DOI: 10.14599/r101304.
- [2] European Committee for Standardization (CEN) (2013): Eurocode 8 - design of structures for earthquake resistance, part 1: General rules, seismic actions and rules, CEN Brussels, Belgium.
- [3] Casagrande D., Sartori T., Tomasi R., (2014) Capacity design approach for multi-storey timber-frame buildings. In: Proceedings of the international network on timber engineering research (INTER), Bath, UK
- [4] Pozza L., Scotta R., Trutalli D., Polastri A., Smith I. (2016), Experimentally based q-factor estimation of CLT walls, Proceedings of the Institution of Civil Engineers: Structures and Buildings, doi: 10.1680/jstbu.15.00009
- [5] Gavric, I., Fragiaco, M., Ceccotti, A., "Cyclic behaviour of typical metal connectors for cross-laminated (CLT) structures", 2015, "Materials and Structures/Materiaux et Constructions, 48,6,1841,1857,10.1617/s11527-014-0278-7
- [6] Polastri A., Pozza L., Loss C., Smith I., (2016), Numerical analyses of high- and medium- rise CLT buildings braced with cores and additional shear walls. Structures and Architecture: Concepts, Applications and Challenges - Proceedings of the 3rd International Conference on Structures and Architecture, ICSA 2016
- [7] Casagrande D., Rossi S., Sartori T., Tomasi R., (2015) Proposal of an analytical procedure and a simplified numerical model for elastic response of single-storey timber shear -walls. In: Proceedings of the Institution of Civil Engineers: Construction Materials

- [8] Rossi S., Casagrande D., Piazza M., Tomasi R., (2015) Seismic elastic analysis of light timber-frame multi-storey buildings: Proposal of an iterative approach. In: Proceedings of the Institution of Civil Engineers: Construction Materials
- [9] Ceccotti A., Sandhaas C., Okabe M., Yasumura M., Minowa C. and Kawai, N. (2013): SOFIE project – 3D shaking table test on a seven-storey full-scale cross-laminated timber building. *Earthquake EngStruct. Dyn.*,42: 2003-2021.
- [10] Popovski, M. and Gavric, I. (2015). Performance of a 2-Story CLT House Subjected to Lateral Loads. *J. Struct. Eng.*, 10.1061/(ASCE)ST.1943-541X.0001315, E4015006.
- [11] Fragiaco, Massimo; Dujic, Bruno; Sustersic, Iztok (2011) Elastic and ductile design of multi-storey crosslam massive wooden buildings under seismic actions. *Engineering Structures*, Vol. 33 (11), p. 3043-3053. ISSN 0141-0296. eISSN 1873-7323
- [12] European Committee for Standardization (CEN) (2006) EN 12512 - Timber structures – Test methods – cyclic testing of joints made with mechanical fasteners. Brussels, Belgium
- [13] Sartori T. and Tomasi R., Experimental investigation on sheathing-to-framing connections in wood shear walls in *Engineering Structures*, v. 56, (2013), p. 2197-2205
- [14] Tomasi R. and Sartori T., (2013) Mechanical behaviour of connections between wood framed shear walls and foundations under monotonic and cyclic load. *Constr Build Mater* 44:682–690
- [15] European Committee for Standardization (CEN) (2009) EN 1995 - Eurocode 5 - design of timber structures, Part 1-1, General - Common rules and rules for buildings. Brussels, Belgium.

SYSTEM SOLUTIONS FOR POINT-SUPPORTED WOODEN FLAT SLABS

Philipp Zingerle¹, Roland Maderebner², Michael Flach³

ABSTRACT: The challenge with point-supported flat slabs is the stress concentration at the supporting points. The small strength of the wood perpendicular to the grain should not reduce the load carrying capacity of the CLT –Panels. Therefore, there are some existing state of the art methods of reinforcement with self-tapping screws, which open up the possibilities to increase the resistance of transverse pressure and rolling shear. These improvements are important, but not sufficient for a breakthrough of flat slabs in wood. Additional solutions have to be combined with these methods. As a result a building systems of economic interest for multi-storeyed buildings in a wood adequate flat slab building method should be offered. A promising way to achieve the objectives provides the concept “SPIDER Connector” which is applied for patent by the University of Innsbruck. Initial results show a local increase of the stiffness and improve the load carrying capacity in the transition area between plate and support. Extensive studies are planned in course of a research project that should check a sufficient capacity and serviceability of the system.

KEYWORDS: cross-laminated-timber, point-supported flat slab, multi-story wooden buildings, reinforcement, connection system

1 INTRODUCTION

The rapid development in the use of plane elements such as cross-laminated-timber (CLT) since the 1990s opens entirely new areas of application for wooden constructions. Large scaled plate- and wall structures can now be carried out, similar to concrete constructions. Today one-way CLT slabs are frequently used instead of classic wooden beam constructions. The wooden slabs are mostly carried by continuous supports like walls or beams. Point-supported wooden slabs are only very sporadic and limited to small column grids, otherwise the loads in the introduction points are getting to high. Due to the unfavorable ratio of stiffness to mass with wooden slabs compared to concrete slabs there is a frequently higher appearance of undesirable slab-vibrations.

In architectural concepts of building plans a flat ceiling with the widest possible grid of columns is often required. Therefore conventional wooden solutions become complicated and inefficient.

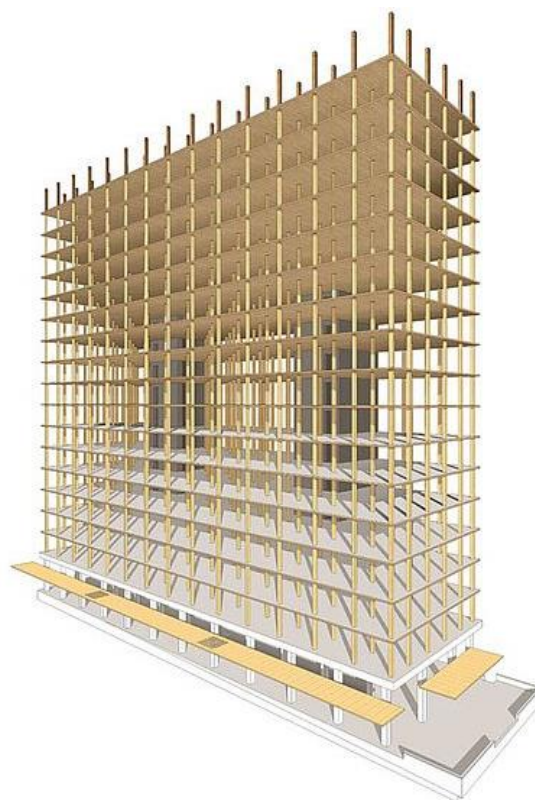


Figure 1: Load-bearing structure of the point supported student residence in Vancouver [1]

¹ Philipp Zingerle, University of Innsbruck, Austria,
philipp.zingerle@uibk.ac.at

² Roland Maderebner, University of Innsbruck, Austria,
roland.maderebner@uibk.ac.at

³ Michael Flach, University of Innsbruck, Austria,
michael.flach@uibk.ac.at

At the moment a worldwide competition in the matter of multistoried buildings in wood is taking place. In Vancouver a 18 stories residential home for students (Figure 1) is arising and in Vienna the so called HoHo (wooden skyscraper) with 24 stories is right before its realization. A study in London even deals with the feasibility of a 300 m „skyscraper“ in wood. This trend indicates that wooden constructions are no longer confined to single-family homes, but that in future larger buildings are built with structural elements in wood. To intensify the use of wood as a building material with the largest CO₂ - reduction potential, further solutions, which can substitute energy-intensive building materials, must be offered [2].

2 STATE OF SCIENTIFIC KNOWLEDGE

As Cross Laminated Timber (CLT) is arranged of orthogonally and glued together wooden board plies it theoretically has two main structural directions. Currently CLT is available on the market in widths of 1,25 m to 3,50 m and (almost) unlimited length. For these reasons, usually a dominant load transfer direction is present and can be calculated on dimensional panel strips. The transverse layers in this case practically act as "distance" for longitudinal layers - and must, however, transmit the resulting shear forces.

Suitable models according to the Eurocode 5 for dimensioning CLT with normal and bending loads are the shear force analogy, the orthotropic plate and the girder grid [14]. Figure 2 shows a simplification of the distribution of normal-, bending- and shear stresses in both main bearing directions.

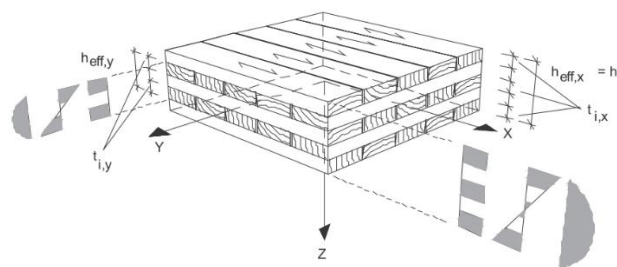


Figure 2: stress distribution in the longitudinal and transvers cross section [3]

The arising stresses must be compared with the corresponding strengths. Particular attention must be paid to the rolling shear, since the rolling shear strength compared to the strength in direction of the grain is small [4]. In Figure 3 the rolling shear failure of the cross layers is displayed.



$f_{R,k}$ rolling shear capacity, characteristic value
 $f_{v,k}$ shear capacity, characteristic value

Figure 3: rolling shear failure [5]

characteristic properties of a single layer of CLT			N/mm ²
plates	shear	$f_{v,k}$	2,3
	rolling shear	$f_{r,k}$	0,7

Figure 4: shear and rolling shear properties [15]

The characteristic values for shear in grain direction and rolling shear according to ÖNORM EN 1995-1-1 Eurocode 5 is displayed in Figure 4.

Several works show that stress interactions that result from a multi-axial load transfer (plate bearing effect) can affect the rolling shear properties positively and allow an increase in the strength [4,5,6,7]. More load carrying capacity is generated through a 2D - load transfer [8,9].

As an additional problem location of point supported / loaded CLT plates, the compressive strength perpendicular to the grain must be mentioned. Despite an increased strength of CLT compared to glulam (GLT) and solid wood [10,11] the resistance perpendicular to the grain is far from sufficient to transmit the column loads of several floors through the plate without damage. Also reinforcing measures with full-thread screws are not efficient enough.

The Swiss scientists Boccadoro, Frangi and Zöllig 2013 presented first studies on the feasibility of flat slabs made out of wood [12]. Therefore an attempt was made to enable a 4-storey model house in wood construction without beams. This research group has dealt primarily with the use of beech veneer woods in the highest stress areas of load application.

Figure 5 shows the test setup of a combined spruce-beech plywood plate.



Figure 5: test setup ETH Zürich [13]

As preliminary result from the investigations it was clear: „ ... due to the large cutting forces that occur in the joints, the high forces can not be transmitted economically with the help of conventional rod-shaped connecting means ... Even with slotted plates and dowels the effort would be excessively high. Therefore new connection systems based on these requirements have to be explored." As it is apparent from these quotations of Zöllig, no satisfactory solutions have been developed at the ETH Zurich despite these investigations.

Anyway, the participation of a total of three partners from industry expressed “the strong interest in this design principle” by the construction industry [12].

In addition to research and studies in Switzerland, 2011 Mestek already wrote his dissertation at the TU Munich about the possibilities of shear reinforcement in point supported CLT plates using fully threaded, inclined screws [5]. Thereby a simple static dimensioning concept has already been developed. At a critical section the shear verification for both supporting directions (x- and y-direction) has to be done. The rolling shear strength of the middle layers is of dimensioning relevance in this concept. The point support creates increased lateral stresses at this section. Further reinforcement and additional increase in the transverse compressive stress generated by the screwed-in 45 ° fully-tapped screws, which are designed as tie rods on a framework model. In this concept, the rolling shear strength may be increased by a maximum of 20% Figure 6.

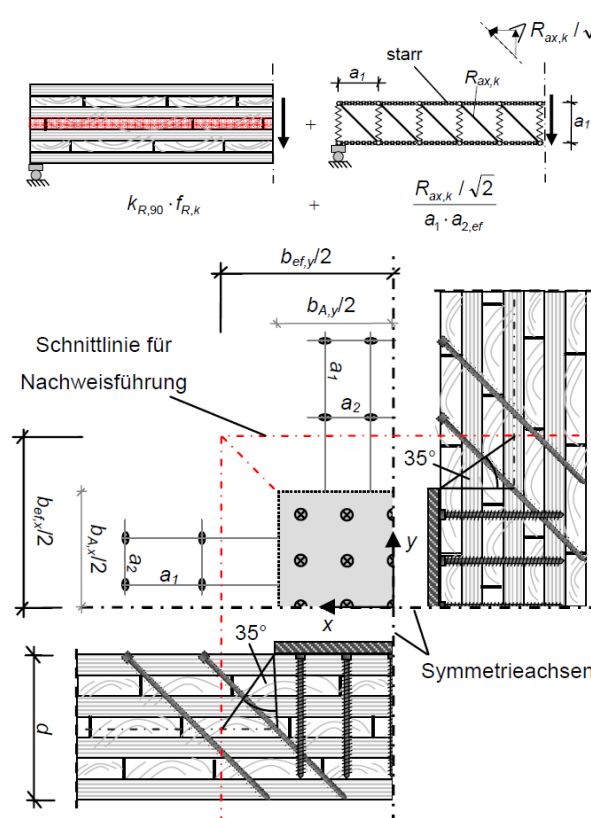


Figure 6: verification of shear at the critical section [12]

3 REQUIREMENTS

Based on the existing scientific work the subject point supporting of flat slabs of wood was picked up at the University of Innsbruck in concept developments. Ideas for reinforcement of the high loaded areas emerged associated with modular construction systems [13]. A requirement profile for this connection means is shown in Figure. 6

Requirements: Connection System for point supported flat slabs		
ULS	SLS	benefit
support grid (5 - 6 m)	limitation of deflection	construction without beams (volume - costs)
min. 3 wooden floors (4-storey building)	limitation of floor vibrations	system solution with easy calculation
assembling loads	sound insulation between the floors	flexibility
vertical load bearing system		easy to mount / assemble
ductile / plastic behavior		adjustable height for common tolerances
resistance against fire		

Figure 7: requirements for the connection system

For the load carrying capacity of a prefabricated flat slab there are two points of special interest. On one hand the point of load introduction between column and plate and

on the other hand the joint between the different plates. To create performance specifications a 4-story residential building with a free span between the columns of min. 5 m was chosen. For horizontal loads walls or staircase-cores can be used as stiffening members. For the Connection-System just the vertical loads are taken under account. Also special loads during the assembling and the resistance against fire are to consider. In case of a collapse of the system plastic failure with advanced notice is aspired. For reaching the limits of serviceability (SLS) – deflection and floor vibrations – stiffness and mass are the main factors of influence. Beside local stiffness mainly the stiffness and mass of the whole floor-system is important. Beside the mechanical properties, raising requirements for sound insulation also have to be fulfilled.

The main advantages of the system with point supported flat slabs is the high flexibility in the floor plan and a simple adaption for future requirements. Many architects and builder also decide to use this method because of the smaller use of construction volume. Due to the no longer necessary beams, the volume and the overall costs can be reduced. Often esthetical requirements of a flat ceiling is desired, and also the more easy way of installation is an advantage.

Economic efficiency calculations were carried out to compare the flat slab system with a plate and beam system. Although it is necessary to use thicker plates for the flat slab, the construction volume can be reduced appreciable. If this construction method is used for a building with 10 floors, and following the standards for ceiling heights, one additional floor is possible within the same height of the building.

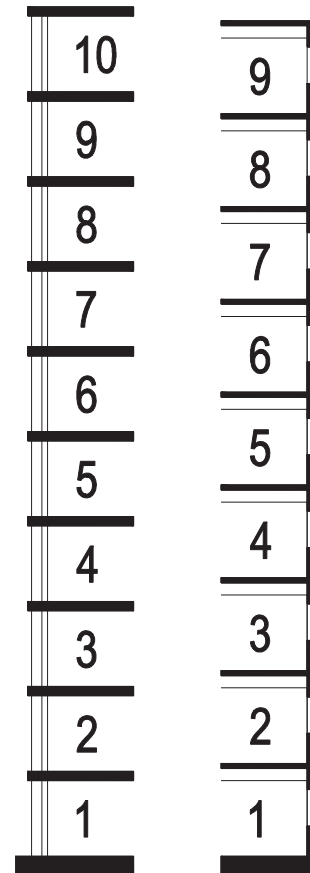


Figure 8: comparison of flat slab with beam construction

4 STRUCTURAL SYSTEM

In the first step, the load bearing structure is simple. CLT Plates with dimensions of 2,5 m width can be hoisted at the columns. Therefore, the columns have to be spread during the assembling process. The so-called belt-strip as main load-bearing system runs continuously between the columns. For reaching the requirements of 5 m of free span, a secondary load-bearing system of 2,5 m width has to be hang in between the two main plates. The main load bearing direction of the so-called field-strip is orthogonal to the belt-strip. A big challenge is to find a solution for the transition between the two plates. Therefore the joint is situated at a place where the bending moment has just small values. Figure 9 shows how the different plates could be assembled to a flat slab.



Figure 9: concept of assembly and construction

At the places with red circles in Figure 9 (right) the load introduction into the CLT plate is critical. There the

“SPIDER Connector” can be mounted for reinforcement of the CLT plate. Figure 10 and Figure 11 show a detailed concept of the system.

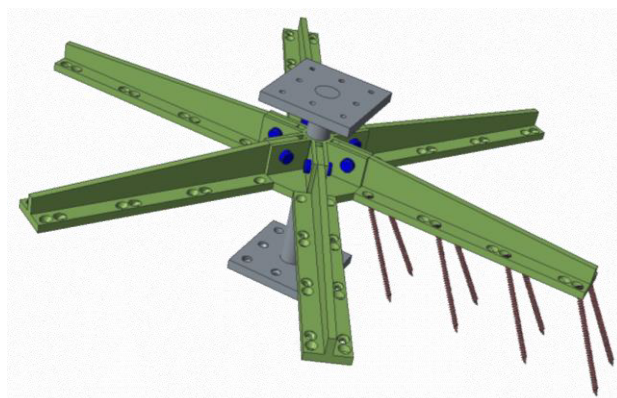
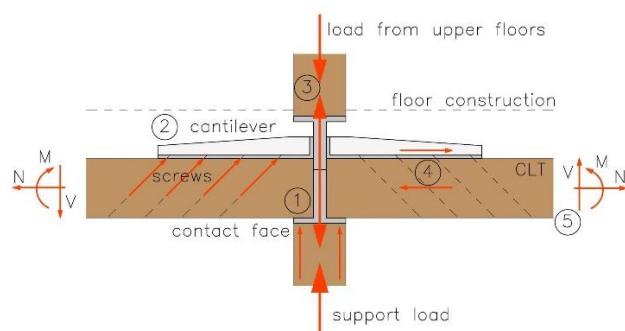


Figure 10: 3D Model of the SPIDER Connector [15]



- (1) Contact face at the column head
- (2) Overhead suspension of the slab with connection-elements
- (3) Load pass through the plate with compression member
- (4) Local shear reinforcement
- (5) Continuous joint of the CLT elements

Figure 11: Concept of the SPIDER Connector

For reducing compression perpendicular to the grain the contact face just has to resist the loads during the assembling process. After mounting of the inclined screws the main load is running across the cantilever arms of the connector. The inclined screws also increase the resistance of rolling shear [5]. Steel parts penetrate through the CLT plate for carrying the loads from the upper floors.

5 FIRST TESTS AND RESULTS

This construction method of “activation of many reserves” in and around the connecting point of the column, as well as an additional activation of wooden volume, the load carrying capacity is significantly increased. Based on the initial results of preliminary tests

at 5-layered CLT with a thickness of 160 mm (Figure 12) the potential of this concept is rated as very high.

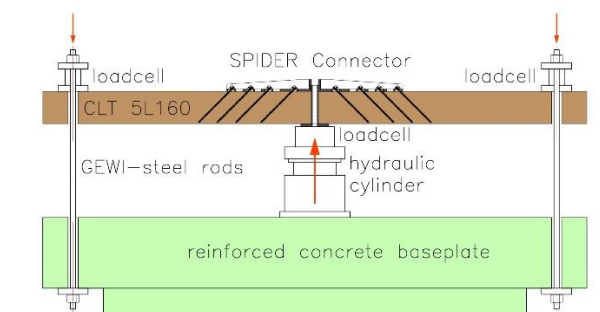


Figure 12: test setup

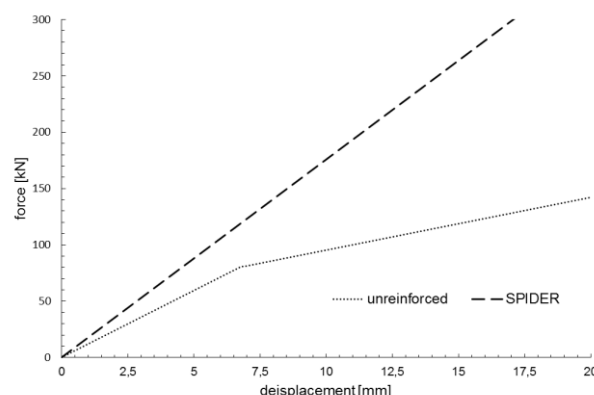


Figure 13: evaluation of the preliminary tests

In Figure 13, the local increase in stiffness of the plate tests with SPIDER reinforcement by approximately 50% in the linear elastic range can be seen. Furthermore almost twice the load can be transmitted at the displacement of 10 mm in the middle of the plate. The first tests were carried out with a maximum of 300 kN in the center of a square plate of 2,4 m. The behavior of the CLT plate with Reinforcement-System shows just elastic deformations. No failure or cracks were detected at this stage.

So far studies found out, that it is absolutely necessary to coordinate the different levels of stiffness and to use the full capacity for the design of the connection. This is necessary because of the interaction between contact, suspension, compression member and shear reinforcement. Further investigation about the increasing of stiffness and floor vibrations have to be carried out during a FFG project.

ACKNOWLEDGEMENT

The authors would like to thank the company ROTHOBLAAS for being part of the FFG Bridge Project no. 5973065.

REFERENCES

- [1] Acton Ostry Architects Inc., online: <http://www.actonostry.ca/project/brock-commons-phase-1-vancouver/> [Zugriff am 26.04.2016]
- [2] Timber Construction Europe; Aufruf zur Recourcenwende, Holz: Baustoff mit dem größten CO2-Reduktionspotenzial, online: <http://www.timber-construction.eu;> [Zugriff am 26.04.2016]
- [3] ETA 06/0138; European Technical Approval; KLH solid wood slabs; Wien; 2012
- [4] Kreuzinger, H., Scholz A.; Nachweis in Grenzzuständen der Tragfähigkeit bei Platten und Scheiben aus Holz und Holzwerkstoffen unter Spannungskombinationen
Bauforschung, Frauenhofer IRB Verlag, München, 1999.
- [5] Mestek, P.; Punktgestützte Flächentragwerke aus Brettsperrholz (BSP) – Schubbemessung unter Berücksichtigung von Schubverstärkungen, München, 2011
- [6] Czaderski, Ch., Steiger, R., et al.; Versuche und Berechnungen an allseitig gelagerten 3-schichtigen Brettsperrholzplatten. Holz als Roh- und Werkstoff 65: S. 383-402, Zürich, 2007
- [7] Hochreiner, G., Füssl J.; Eberhardsteiner J., Aicher S.; CLT Plates under concentrated Loading – Experimental Identification of Crack Modes and Corresponding Failure Mechanisms, RILEM Stuttgart; 2014
- [8] Bogensperger, T., Silly, G.; Zweiachsige Lastabtragung von Brettsperrholzplatten; Bautechnik 91; Berlin 2014
- [9] Bogensberger, T., Jöbstl, R., Concentrated load introduction in CLT elements perpendicular to plane; CIB World Congress; 2015
- [10] Ciampitti, A.; Untersuchungen ausgewählter Einflussparameter auf die Querdruckkenngrößen von Brettsperrholz, Masterarbeit TU Graz, 2013
- [11] Halili Y.; Versuchstechnische Ermittlung von Querdruckkenngrößen für Brettsperrholz, Masterarbeit TU Graz, 2008
- [12] Boccadoro L.; Frangi A.; Flachdecken aus Holz, Reliable timber and innovative wood products for structures - Structural elements of wood and wood products made of beech, Zürich, 2013
- [13] Prighel, P.; Durchstanzverstärkungen für die Brettsperrholz-Bauweise, Modellierung eines Systemverbinders, Innsbruck, 2014.
- [14] ÖNORM EN 1995-1-1; Eurocode 5: Bemessung und Konstruktion von Holzbauten - Teil 1-1: Allgemeines – Allgemeine Regeln für den Hochbau, Austrian Standard Institute, Wien 2015
- [15] Maderebner R.; Erfindungsmeldung Spider Connector, Universität Innsbruck, 2013

- | | | |
|-----------|--|-------------------|
| 01 | Experimental analysis of flanking transmission of different connection systems for clt panels
ACOUSTICS IN WOODEN BUILDING _ <i>Monday, 22 August 1:30pm - 3:00pm</i> | pag. 07_14 |
| <hr/> | | |
| 02 | Clt buildings laterally braced with core and perimeter walls
SYSTEM LEVEL STRUCTURAL DESIGN OF HYBRID STRUCTURES _ <i>Monday, 22 August 1:30pm - 3:00pm</i> | pag. 17_26 |
| <hr/> | | |
| 03 | Structural analysis of clt multi-storey buildings assembled with the innovative x-rad connection system:
case-study of a tall-building
TALL BUILDINGS - CASE STUDIES _ <i>Tuesday, 23 August 10:30am - 12:00pm</i> | pag. 29_38 |
| <hr/> | | |
| 04 | Mechanical characterization of an innovative connection system for clt structures
JOINTS IN TIMBER STRUCTURES _ <i>Tuesday, 23 August 1:30pm - 3:00pm</i> | pag. 41_49 |
| <hr/> | | |
| 05 | Experimental campaign for the mechanical characterization of connection systems
in the seismic design of timber buildings
SEISMIC DESIGN AND BEHAVIOR OF INNOVATIVE TIMBER SYSTEMS _ <i>Thursday, 25 August 10:30am - 12:00pm</i> | pag. 53_61 |
| <hr/> | | |
| 06 | System solutions for point-supported wooden flat slabs
SUSTAINABLE MODULAR BUILDING SYSTEMS IN WOOD _ <i>Thursday, 25 August 10:30am - 12:00pm</i> | pag. 63_68 |

your
perfect partner
to design and build
with **wood**



Discover all our products and services
visit our website!

www.rothoblaas.com



Rotho Blaas srl - I - 39040 Cortaccia (BZ) - Via Dell'Adige 2/1
Tel. +39 0471 81 84 00 - Fax +39 0471 81 84 84
info@rothoblaas.com - www.rothoblaas.com

